VDa

[redacted]

CENTRAL RESEARCH LIBRARY
DOCUMENT COLLECTION

OAK RIDGE NATIONAL LABORATORY LIBRARY
3 4456 0023207 7

ORNL-1678
Progress
8a

Inv
55

HOMOGENEOUS REACTOR PROJECT

QUARTERLY PROGRESS REPORT

FOR PERIOD ENDING JANUARY 31, 1954

CENTRAL RESEARCH LIBRARY
DOCUMENT COLLECTION

LIBRARY LOAN COPY

DO NOT TRANSFER TO ANOTHER PERSON

If you wish someone else to see this document, send in name with document and the library will arrange a loan.

OAK RIDGE NATIONAL LABORATORY
OPERATED BY
CARBIDE AND CARBON CHEMICALS COMPANY
A DIVISION OF UNION CARBIDE AND CARBON CORPORATION

UCC

POST OFFICE BOX P
OAK RIDGE, TENNESSEE

RESTRICTED DATA

This document contains Restricted Data as defined in the Atomic Energy Act of 1946. Its transmittal or the disclosure of its contents in any manner to an unauthorized person is prohibited.

[redacted]

[redacted]

ORNL-1678

This document consists of 116 pages.
Copy 8 of 211 copies. Series A.

DECLASSIFIED

CLASSIFICATION CHANGED TO:
BY A TID-1148
BY: R. Morrison 7/22/57

Contract No. W-7405-eng-26

HOMOGENEOUS REACTOR PROJECT

QUARTERLY PROGRESS REPORT

For Period Ending January 31, 1954

Project Director – J. A. Swartout
Engineering – J. A. Lane
Chemistry – C. H. Secoy
Corrosion – E. G. Bohlmann
Chemical Technology – F. R. Bruce
Metallurgy – E. C. Miller

Compiled by W. E. Thompson

DATE ISSUED

MAR 31 1954

OAK RIDGE NATIONAL LABORATORY
Operated by
CARBIDE AND CARBON CHEMICALS COMPANY
A Division of Union Carbide and Carbon Corporation
Post Office Box P
Oak Ridge, Tennessee

[redacted]

OAK RIDGE NATIONAL LABORATORY LIBRARY
3 4456 0023207 7

[redacted]

INTERNAL DISTRIBUTION

1. C. E. Center
2. Biology Library
3. Health Physics Library
4. Metallurgy Library
5-6. Reactor Experimental Engineering Library
7-9. Central Research Library
10-16. Laboratory Records Dept.
17. Laboratory Records, ORNL R.C.
18-19. ANP Reports Office
20. R. E. Aven
21. S. E. Beall
22. R. G. Berggren
23. E. P. Blizard
24. E. G. Bohlmann
25. G. E. Boyd
26. W. M. Breazeale (Consultant)
27. R. C. Briant
28. R. B. Briggs
29. F. R. Bruce
30. A. D. Callihan
31. D. W. Cardwell
32. G. H. Cartledge
33. G. H. Clewett
34. T. E. Cole
35. D. D. Cowen
36. F. L. Culler
37. J. S. Culver
38. L. B. Emlet (K-25)
39. J. L. English
40. D. E. Ferguson
41. W. R. Gall
42. J. P. Gill
43. C. B. Graham
44. J. C. Griess
45. W. O. Harms
46. C. S. Harrill
47. P. N. Haubenreich
48. C. G. Heisig
49. A. Hollaender
50. A. S. Householder
51. G. R. Jenkins (C&CCC, South Charleston)
52. G. H. Jenks
53. R. W. Johnson
54. C. P. Keim
55. M. T. Kelley
56. E. M. King
57. A. S. Kitzes
58. J. A. Lane
59. C. E. Larson
60. S. C. Lind
61. R. S. Livingston
62. R. N. Lyon
63. W. L. Marshall
64. H. F. McDuffie
65. J. R. McWherter
66. E. C. Miller
67. K. Z. Morgan
68. E. J. Murphy
69. J. P. Murray (Y-12)
70. H. F. Poppendiek
71. L. R. Quarles
72. P. M. Reyling
73. W. L. Ross
74. J. P. Sanders
75. H. C. Savage
76. C. H. Secoy
77. C. L. Segaser
78. E. D. Shipley
79. A. H. Snell
80. I. Spiewak
81. C. D. Susano
82. J. A. Swartout
83. E. H. Taylor
84. D. G. Thomas
85. W. E. Thompson
86. [illegible] Tobias
87. S. [illegible]isner
88. W. [illegible] Walker
89. A. M. [illegible]einberg
90. T. A. W[illegible]on
91. E. P. Wig[illegible]r (consultant)
92. C. E. Winte[illegible]
93. F. C. Vonder[illegible]ge
94. F. C. Zapp
95. P. C. Zmola
96. G. C. Williams
97. J. C. Wilson

[redacted]

[redacted]

EXTERNAL DISTRIBUTION

[redacted]. AF Plant Representative, Burbank
[redacted] AF Plant Representative, Seattle
10[redacted] AF Plant Representative, Wood-Ridge
10[redacted] ANP Project Office, Fort Worth
102-112. [redacted]gonne National Laboratory
113. [redacted]ned Forces Special Weapons Project (Sandia)
114. A[redacted]ed Forces Special Weapons Project, Washington
115-119. A[redacted]c Energy Commission, Washington
120. Ba[redacted]e Memorial Institute
121-123. Broo[redacted]ven National Laboratory
124. Burea[redacted]f Ships
125-126. Califo[redacted] Research and Development Company
127-132. Carbide[redacted]d Carbon Chemicals Company (Y-12 Plant)
133. Chicago [redacted]tent Group
134. Chief of [redacted]al Research
135. Commonwe[redacted]n Edison Company
136. Department [redacted]he Navy – Op-362
137. Detroit Edis[redacted]Company
138-142. duPont Compa[redacted] Augusta
143. duPont Compa[redacted] Wilmington
144. Foster Wheeler [redacted]oration
145-147. General Electric [redacted]npany (ANPP)
148-151. General Electric C[redacted]pany, Richland
152. Hanford Operations [redacted]ice
153. Iowa State College [redacted]
154-157. Knolls Atomic Power [redacted]oratory
158-159. Los Alamos Scientific [redacted]oratory
160. Massachusetts Institute o[redacted]echnology (Kaufmann)
161. Monsanto Chemical Compa[redacted]
162. Mound Laboratory
163. National Advisory Committee[redacted]r Aeronautics, Cleveland
164. National Advisory Committee [redacted] Aeronautics, Washington
165. Naval Research Laboratory
166-167. New York Operations Office
168-169. North American Aviation, Inc.
170. Nuclear Development Associates, [redacted]
171. Patent Branch, Washington
172-178. Phillips Petroleum Company
179. Powerplant Laboratory (WADC)
180. Pratt and Whitney Aircraft Division (F[redacted]Project)
181. Rand Corporation
182. San Francisco Operations Office
183. Sylvania Electric Products, Inc.
184. USAF Headquarters
185. U. S. Naval Radiological Defense Laboratory[redacted]
186-187. University of California Radiation Laboratory, [redacted]rkeley
188-189. University of California Radiation Laboratory, [redacted]ermore
190. Walter Kidde Nuclear Laboratories, Inc.
191-196. Westinghouse Electric Corporation
197-211. Technical Information Service, Oak Ridge.

[redacted]

[redacted]

Reports previously issued in this series are as follows:

ORNL-527	Date Issued, December 28, 1949
ORNL-630	Period Ending February 28, 1950
ORNL-730	Feasibility Report – Date Issued, July 6, 1950
ORNL-826	Period Ending August 31, 1950
ORNL-925	Period Ending November 30, 1950
ORNL-990	Period Ending February 28, 1951
ORNL-1057	Period Ending May 15, 1951
ORNL-1121	Period Ending August 15, 1951
ORNL-1221	Period Ending November 15, 1951
ORNL-1280	Period Ending March 15, 1952
ORNL-1318	Period Ending July 1, 1952
ORNL-1424	Period Ending October 1, 1952
ORNL-1478	Period Ending January 1, 1953
ORNL-1554	Period Ending March 31, 1953
ORNL-1605	Period Ending July 31, 1953
ORNL-1658	Period Ending October 31, 1953

[redacted]

[redacted]

SUMMARY

PART I

HOMOGENEOUS REACTOR EXPERIMENT

During this quarter the experimental program of the HRE was completed, and planning was begun for dismantling the reactor in preparation for the installation of a second experimental reactor to be called the Homogeneous Reactor Test (HRT). The HRE was operated at power levels as high as 1600 kw over a period of more than 1000 hr between November 15, 1953 and January 31, 1954; the quarter was climaxed by a highly successful experiment with dissolved copper as an internal recombiner for the decomposition gases, hydrogen and oxygen. Power levels as high as 1350 kw were attained without measurable gas production.

The only difficulty experienced was the failure of a high-pressure, remote, liquid-level-indicating device. This highly radioactive instrument (50 r/hr) was repaired by erecting a temporary shield through which it was possible to drill into the instrument and to weld the hole closed afterwards.

The core-concentration effect described in the previous progress report was found to impose a limitation to the region of stable reactor operation in terms of maximum power for a particular temperature, pressure, and fuel inventory. This instability, apparently unique to rotating-core systems with low-pressure gas recombination, is discussed.

The generalized corrosion rate of the reactor stainless steel was approximately 7 mpy over this operating period, during which time the reactor was operated mainly at power levels above 500 kw and temperatures above 220°C. This apparent increase in the rate of corrosion over the 1 to 3 mpy previously reported is not related to the copper additions but appears to be due to operation in the corrosion-sensitive temperature region near a 225°C average core temperature. The corrosion rates observed in the HRE agree with those observed with solutions of the same concentration under similar conditions in out-of-pile dynamic-corrosion tests.

PART II

BOILING REACTOR RESEARCH

The steam bubbles formed in a boiling homogeneous reactor will rise or slip through the reacting solution at a rate which is a function of several variables including the pressure on the boiling system and the ratio of steam volume to liquid volume. If the so-called "slip velocity" is high, the bubble holdup in a boiling reactor will be low and the fuel inventory for a reasonable power density will not be excessive. If, on the other hand, the slip velocity is low, natural or forced convection of the liquid through the reactor will be required to move the bubbles rapidly from the reactor core to a point where the two phases can be separated.

Slip-velocity and natural-convection studies have been continued during the quarter, and a negotiation for a short-term contract with an industrial concern for tests on commercial steam separators has been completed. In addition, a small investigation of separator pumps was initiated.

PART III

GENERAL HOMOGENEOUS REACTOR STUDIES

Homogeneous Reactor Design

The Homogeneous Test Reactor is being designed to replace the HRE. It is to be a 5-Mw, two-region reactor, fueled with highly enriched uranium, moderated and reflected with D_2O, and operated at 300°C and 2000 psia. The fuel solution will be circulated through a 32-in.-dia zirconium core tank centered in a 56-in.-ID pressure vessel which contains the D_2O reflector. Copper sulfate will be added to the fuel solution to recombine the D_2 and O_2 produced in the reactor. Flowsheet information, design data, and progress on some of the equipment studies are contained in this report.

A study of large aqueous homogeneous reactors for producing central station power has been completed and published as ORNL-1642. A summary of the section on Th-U^{233} fueled reactors was presented in the last report. Some of the results of the study of the uranium-plutonium fueled reactors are discussed in this report.

Engineering Development

An alternate model to the straight-through-flow core now being fabricated of zirconium has been tested. This model simplifies construction of the reactor. A full-scale experimental model of the

[redacted]

gas separator has been built and has undergone initial testing with water. Flow rates varied from 4600 to 5900 gpm, and the pressure drop observed at the rated 5000 gpm is about 2.5 psi.

Present plans for the TBR and HRT include a high-pressure catalytic recombiner for burning the radiolytic gas formed in the core. A small test loop, which will give operating experience on a high-pressure recombiner, is under construction and will operate at pressures from 1000 to 2000 psi.

Contract negotiations have been started for the large reactor components – the main fuel-circulating pump, the large gas circulators for recombiner systems, and the main fuel and gas condenser heat exchangers. Negotiations are also in progress for heat-exchanger development and automatic tube-joint welding.

A development contract for a 20,000-gpm centrifugal pump has been active for approximately two years. Difficulties encountered with the bearing-testing equipment have been overcome and successful operation has been attained.

Construction, instrumentation, and pump electrical supply of the 4000-gpm loop are essentially complete. Pressure testing and component testing will be required before actual operation can begin.

Contract negotiations to fabricate and test the small components – small gas circulators for recombiner systems, models 150C and 400A Westinghouse pumps, and 500-gpm fuel-circulating pump – have been started with two manufacturers.

The pulsafeeder pump loop successfully pumped thoria slurry for an accumulated 63 hr. The pump was started each morning after the slurry was allowed to settle overnight.

Pressed cyclindrial pellets, which included a number of ceramic variations, are being tested for abrasion against each other and against samples of brass, stainless steel, and zirconium by fluidizing various beds of pellets with water. Initial abrasion rates are large, and tests are being continued to determine whether these rates will continue.

Reactor Analysis

Critical conditions for the proposed HRT have been calculated for several mixtures of H_2O and D_2O moderator in the core and for three blankets – heavy water, ThO_2 slurries, and low-enrichment uranyl sulfate solutions.

Initially, interest was expressed in a reactor with a 24-in. core diameter, ¼-in. zirconium-alloy core tank, and a 12-in. heavy-water reflector. Calculations for this configuration were made for various H_2O-D_2O mixtures by use of the usual two-group method.

The minimum critical concentration occurs for a volume fraction of H_2O in the H_2O-D_2O mixture of about 55% and is about 19% lower than the critical concentration for pure H_2O moderator. In this particular case, the reactor was not critical as a thermal reactor with pure D_2O moderator.

At lower uranium concentrations (larger reactors) no advantage accrues from the mixing of H_2O with D_2O, and hence pure D_2O moderator was selected. The core diameter was increased to 32 in., bringing the critical fuel concentration down to about 10 g of uranium per kilogram of D_2O with a 12-in. D_2O reflector.

Some preliminary results on the rate of formation of decomposition gases have been obtained from the water boiler experiment conducted last August. Immediately following an addition of reactivity, there is a decrease in reactivity, primarily due to the formation of decomposition gases, since at least 10% of the decomposition products of water appear in the vapor phase within 0.1 sec. In all cases the measured rate of decrease in reactivity immediately after the addition of reactivity by withdrawal of the absorber rod was greater than five times that which can be attributed to core temperature rise. As the gas bubbles leave the core, reactivity effects due to increase in core temperature become relatively more important.

From the known steady-state rates of formation of gases within the water boiler, the maximum reactivity effect due to gas formation was calculated. In the above runs the observed rate of reactivity decrease was below the maximum rate obtained by assuming immediate formation of gas saturated with water vapor, except for one run. The data reveal no trend in initial rate of reactivity decrease with core temperature or power level.

Controls and Instrumentation

Instrumentation provided for the test-model in-pile loop has been operating quite satisfactorily for the past three months and is providing almost perfect control. A difference of several degrees has been observed between the pressurizer temper-

[redacted]

ature and the temperature equivalent to the measured pressurizer steam pressure when the system is operated with water. This difference has been constant for a number of runs and appears to be a summation of the tolerances of all temperature- and pressure-measuring components, plus some intangible effects due to location of thermocouples.

The sealing bellows is one of the most vulnerable spots in high-pressure valve design. An interview with a representative of Breeze Corporations, Inc., Union, N. J., disclosed that that company has been supplying the Navy with welded diaphragm bellows of type 347 stainless steel which has been operating at 2500 psi and about 300°F. This bellows is heliarc welded by machines and leak tested by the mass spectrograph.

The present HRE pressurizer level controller is being redesigned for improved operation at 2000 psi and 300°C. A buoyant member consisting of solid titanium is being considered. This body would weigh approximately 50% more than a hollow stainless steel member of adequate wall thickness but should be relatively immune to pressure and temperature effects.

Occasional troubles with the liquid-level controller of the HRE pressurizer have pointed out the need for a secondary system of level indication to check the accuracy of the primary measuring system. The practicality of an ultrasonic system for this purpose has been investigated. Quartz piezoelectric transducers clamped to a water-filled tank were energized with damped pulses of 5 Mc/sec frequency. The pulses and echoes from inserted metallic surfaces and from the surface of the water were observed on an oscilloscope connected to an amplifier. The tests were repeated with solutions containing $2\frac{1}{2}$ to 40 g of uranyl sulfate per liter.

The method bears some promise as a means of providing visual indication of level but would not be suitable for recording or controlling. As in radar, spurious echoes are present which can hardly be screened out electronically and must be evaluated visually by observation of an oscilloscope.

Measurements made in uranyl sulfate solutions indicated that attenuation of the sound waves varied markedly with concentration. Thus, determination of concentration might be obtained by measuring the attenuation in the solution. One method would be to measure the log slope of attenuation vs frequency, which should be independent of amplifier and apparatus errors.

Corrosion

The studies in the temperature range from 200 to 225°C have now been extended to 0.02 M UO_2SO_4 solution containing 0.005 M H_2SO_4. As in the case of the 0.17 M UO_2SO_4 solution under similar conditions, the iron and chromium oxide coating formed is not so protective as that formed in the temperature range from 250 to 300°C. Thus, corrosion of the austenitic stainless steels continues at an appreciably higher rate at these intermediate temperatures. However, this rate is quite time- and concentration-dependent, and indications are that at 0.02 M UO_2SO_4 the ultimate rate at low velocity is less than 1 mpy. Preliminary results from examination of the films formed at the two temperatures indicate that the oxide is hydrated at 225°C and anhydrous at 250°C.

Molybdate, phosphate, pertechnetate, and silicate have been investigated as inhibitors in 0.17 M UO_2SO_4 at 250°C. No significant effects were observed.

Operation of the titanium loop with 0.02 M UO_2SO_4 solution containing 0.005 M H_2SO_4 at 300°C did not show appreciable attack on the titanium. However, a small amount of the uranium was precipitated as a mixed titanium-uranium oxide not identifiable with any known compound by x-ray or electron diffraction. The same compound was precipitated when the loop was run with 0.02 M UO_2SO_4 with no added H_2SO_4 at 250°C. Addition of 0.005 M H_2SO_4 in a subsequent run prevented the precipitation at that temperature, and another run is now in progress at 300°C with 0.01 M H_2SO_4 to determine whether this amount of excess acid will do the same at the higher temperature.

Design of the in-pile loop equipment is largely complete. Construction is progressing satisfactorily, although some delays are probable as a result partially of changes necessitated by development experience and partially of vendors' failures to meet stated delivery dates.

Static studies on the stability of Graphitar pump-bearing material indicate some question regarding the stability of this material in uranyl sulfate solution. The results, however, do not seem consistent with the successful use of bearings made of this material in the 100A pumps used in the out-of-pile test loops.

[redacted]

Tests of the loop-package design indicate that it is satisfactory with respect to flow, temperature, and pressure control. Some problems have arisen with regard to correlation of the results obtained with the coupons in the in-pile loops with results obtained in the 100A test loops. These problems are believed to be related to such variables as surface-to-volume ratio and operational history of the loop and presumably can be resolved in subsequent runs.

Metallurgy

Examination of welded austenitic stainless steel specimens exposed in dynamic-corrosion tests showed no appreciable preferential attack on either weld or base metal at moderately high temperatures (250 to 300°C) and low concentrations of uranium as uranyl sulfate (5 to 15 g of uranium per liter). A preferential attack was observed on samples in higher concentration solutions (300 g of uranium per liter) and lower temperatures (150 to 175°C). This attack manifested itself as an intergranular corrosion penetration in the sensitized portions of susceptible austenitic stainless steels and in the ferrite microconstituent in predominantly austenitic stainless steels, in which the ferrite occurred as elongated stringers.

Selective oxidization, by pretreatment in moist hydrogen, developed films on austenitic stainless steels, which provided an improved corrosion resistance.

The impact testing program on zirconium alloys, exposed for extended periods of time to dynamic loop corrosion testing environments, has not indicated any increased brittleness susceptibility or other detrimental chemical or mechanical effects within the limits of the tests thus far conducted.

Aqueous Solution and Radiation Chemistry

Examination of one stainless steel out-of-pile bomb (H-16) has shown the presence of Fe_2O_3 on the walls of the bomb in both the solution and vapor phases, the Fe_2O_3 crystallites in the vapor phase being larger than those in the solution. No evidence of pit or void type of corrosion has been found in the two in-pile stainless steel bombs (H-2 and H-11) that have been examined. The uranium-titanium compound previously found in the all-titanium loop has been also found in an out-of-pile titanium bomb (H-15) in addition to the rutile phase of TiO_2.

Examination of two out-of-pile bombs (H-15 and H-16) has shown that the vapor phase of both stainless steel and titanium bombs can be corroded significantly, and therefore conclusive corrosion data on the solution phase alone cannot be obtained from pressure data without modifying the technique. Metallographic studies show that the metal used in some of the bombs (H-16 and H-15) has abnormal physical structure and therefore is not suitable for use in conclusive tests.

The solution analyses that have been carried out to date show inconsistencies. It is believed to be necessary both to alter the experimental methods of carrying out the tests and to improve the reliability of the existing experimental techniques of analysis before precise material balances on the various constituents of the solutions can be calculated.

Blanket Systems

Thorium Oxide Chemistry. Development of an aqueous thorium oxide slurry for use in the blanket of a thermal power breeder has continued. Effort has been concentrated on methods of preparing the slurry oxide from the oxalate, formate, and oxycarbonate.

Decomposing thorium oxalate by heating first at 375 to 400°C, then at 475 to 500°C, and finally at 575 to 600°C was efficacious in producing an oxide of less than 0.1 μ average size, with excellent slurry properties, and only slightly abrasive in laboratory testing. Calcining oxalate at 650°C reduced the nitrate content of the oxide product to less than 10 ppm. The addition of a washing step after a low burning period (200 to 350°C) followed by calcination at 600°C also gave oxide products containing less than 10 ppm nitrate.

Pure thorium oxide of small particle size (100 to 1000 Å) has been prepared by the pyrohydrolysis of oxalate in water at 250°C. Calcination of the recovered solids either at 250, 500, or 585°C permitted the oxides to be dispersed as aqueous slurries containing thorium in excess of 1000 g/liter.

Thorium formate was hydrolyzed completely to the hydrous oxide by steam distillation.

Thorium oxycarbonate prepared either by eluting thorium from an ion-exchange column with ammonium carbonate or by the metathesis of the hydroxide with carbonate was decomposed at 500°C

[redacted]

to yield oxide products containing less than 50 ppm of nitrate.

Engineering Tests. The results of four runs completed during the quarter ending January 31, 1954, in which thorium oxide slurries were circulated at 250°C, confirmed earlier observations; the components most severely attacked were the pump and flow restrictor. This had been anticipated because of the pump design and the high velocities (40 to 80 fps) through the flow-restricting orifices. The remainder of the circulating system (straight runs of pipe, ells, tees, and reducers), exposed to velocities of the order of 20 fps, was unattacked by the slurry.

Two loops described in the previous report were in operation using Ames oxide that had been passed through 100-mesh screen, with the actual size of the particles being 100 to 200 Å. The ThO_2 slurries were circulated without difficulty, and concentrations have essentially been constant. With the slurry containing 1000 g of thorium oxide per liter, a slightly smaller impeller was used to prevent overloading the motor because of the density of the fluid. In all runs the Graphitar bearings were continually lubricated with water by condensing steam from the pressurizer; the back bearing showed essentially no wear. The front bearing, however, did show some wear, 0.005 to 0.012 in. across the diameter, after 800 hr of operation. Apparently, the stream of water through the back of the pump was not sufficient to keep the front bearing flushed of solids at all times. In recent runs with some titanium components, normally abraded areas have become coated with a thin, shiny, adherent, abrasion-resistant metallic film. The nature of this film, referred to as "chrome plate," and the conditions under which it is formed are under study at the present time.

Chemical Processing

The optimum temperature for operation of a CaF_2 column to give complete removal of rare-earth fission products and lowest fluoride contamination of the treated fuel is about 40°C, based on data obtained under flow conditions expected in a full-scale process. It has not been found possible to lower the fluoride contamination of CaF_2-treated fuel solution below 55 ppm other than by evaporating the solution to dryness and heating the solid UO_2SO_4 to 300°C. Since preliminary data on the corrosion of zirconium by dilute uranyl sulfate solution containing fluoride indicate that 50 ppm of fluoride probably accelerates corrosion, the CaF_2 process does not look attractive, at present, for a two-region thermal breeder using a zirconium core tank.

Of alternate inorganic adsorbents tested, only titanite appears to be attractive; however, in its natural form this mineral removes significant amounts of uranium from solution in addition to rare earths.

The most promising alternate method for rare-earth removal is the precipitation of an insoluble sulfate such as $CaSO_4$, $BaSO_4$, or $Th(SO_4)_2$ at elevated temperature. In batch tests, precipitation of $CaSO_4$ at 270°C from a solution saturated with $CaSO_4$ at 40°C has consistently removed 65 to 70% of Eu^{155}-traced mixed rare earths from dilute uranyl sulfate solution. In column tests as much as 97% of the rare earths were removed by this same method.

Preliminary solubility data for a mixture of rare-earth sulfates, approximating the mixture obtained from fission, indicate that the total solubility of these rare-earth sulfates in dilute uranyl sulfate at 300°C may not be greater than 0.2 g/liter. This concentration is low enough that the neutron poison of these elements may be kept at an acceptable level by filtering off the insoluble rare-earth sulfates; however, the addition of an insoluble sulfate such as $CaSO_4$ to effect additional removal may be desirable.

[redacted]

[redacted]

CONTENTS

SUMMARY v

PART I. HOMOGENEOUS REACTOR EXPERIMENT

HOMOGENEOUS REACTOR EXPERIMENT 3

Reactor Operations 3
Corrosion 4
Internal Recombination Experiments in the HRE 4
Analysis of "Walk-Away" Phenomenon 7
Example of walk-away 8
Discussion of core concentration effect on stability 9

PART II. BOILING REACTOR RESEARCH

BOILING REACTOR RESEARCH 15

Steam Removal from Boiling Reactors 15
Slip velocity 15
Forced convection 15
Commercial separators 17
Separator pumps 17

PART III. GENERAL HOMOGENEOUS REACTOR STUDIES

HOMOGENEOUS REACTOR DESIGN 21

Homogeneous Test Reactor 21
Flowsheet and general design considerations 21
Reactor vessel 21
Pumps 27
Main heat exchanger 27
Gas separator 27
Valves 28
Steam system 28
Aqueous Homogeneous Reactors for Central Station Power 29
Basis for power study 29
Fuel processing 29
Cost of power 30

ENGINEERING DEVELOPMENT 33

Core and Gas Separator Development 33
Alternate HRT core 33
Gas separators 33
High-Pressure Catalytic Recombiner Test 34
Test of Thoria Pellets in Fluidized Bed 37
Large Reactor Components 37
Main fuel and gas condenser heat exchangers 37
Heat exchanger development 37
Automatic tube-joint welding 37
Worthington Corporation pump development 37

[redacted]

[redacted]

Small Reactor Components 38
Small gas circulators for recombiner systems 38
Model 150C and 400A Westinghouse pumps 38
500-gpm fuel circulating pump 38
Status of the 4000-gpm loop 38
HRE-type pulsafeeder as a slurry pump 38

REACTOR ANALYSIS 40
Criticality Calculations for HRT 40
Mixed H_2O-D_2O moderator 40
Small D_2O reactors 41
Water Boiler Kinetics Experiment 42

CONTROLS AND INSTRUMENTATION 46
In-Pile Corrosion-Loop Experiments 46
Homogeneous Reactor Test Instrumentation 46
Control-valve program 46
Valve-test loop 46
Pressurizer-level controller 46
Waterproofing of instrumentation 46
Ultrasonic Liquid-Level Indicator 47
Recombiner and Entrainment-Separator Loops 47
Axial-Flow Gas-Separator Loop 47
Salt Loop 47
Thermal Conductivity Electrical Analogue 47

CORROSION 48
Dynamic-Corrosion Tests 48
Pump loop operation and maintenance 48
HRE mockup 49
Westinghouse model 100A pumps 49
Loop test results 50
General corrosion rates 50
Effect of condition of the loop on corrosion of stainless steel 50
Effect of additives on corrosion of stainless steel 59
Corrosion of stainless steel by 0.02 *M* uranyl sulfate at 200 and 225°C 59
Titanium loop operation 60
In-pile loop experiments 60
Small-scale dynamic-corrosion program 63
In-Pile Loop 63
Complete installation 63
Loop package 67
Static Corrosion Studies 69
Corrosion by decontamination solutions 69
Other studies 73

METALLURGY 74
Corrosion of Welded Austenitic Stainless Steel Specimens 74
Properties of Titanium and Zirconium Alloys 75
Commercial titanium 75

[redacted]

[redacted]

Zirconium-tin-iron-chromium-nickel-carbon (Zircalloy II) 76
Selective Oxidation of Austenitic Stainless Steels 79

AQUEOUS SOLUTION AND RADIATION CHEMISTRY 81

Homogeneous Reactor Solutions Under Irradiation 81
Microscopic examination of bombs 81
New irradiations 81
Solution analyses 81
Conclusions 84
Future plans 84

BLANKET SYSTEMS 85

Thorium Oxide Chemistry 85
Preparation of thorium oxide from thorium oxalate 85
Thermal decomposition 85
Pyrohydrolysis 87
Hydrolytic decomposition of thorium formate 88
Preparation of thorium oxide from the carbonate 89
Engineering Tests 90
Thorium oxide slurry tests 90
Thorium hydroxide studies 94
Alternate materials of construction 96
Homogeneity of circulating slurries 97
Abrasion tests 98

CHEMICAL PROCESSING 100

Calcium Fluoride Process 100
Optimum temperature for CaF_2 adsorption 100
Alternate Methods of Removing Rare Earths 100
Precipitation of $CaSO_4$ at elevated temperature 100
Solubility of rare-earth sulfates in a simulated fuel solution 101
Alternate rare-earth adsorbents 101
Summary of Chemical Process Development by the Vitro Corporation of America 102
Calcium fluoride process 102
Adsorption tests with titanate 102

[redacted]

Part I

HOMOGENEOUS REACTOR EXPERIMENT

HRP QUARTERLY PROGRESS REPORT

HOMOGENEOUS REACTOR EXPERIMENT

S. E. Beall, Section Chief

S. Visner, Experimental Physics Group Leader

E. L. Compere, Reactor Chemistry Consultant[1]

J. J. Hairston J. W. Hill, Jr.
Operations Group Leaders

D. M. Eissenberg S. I. Kaplan
V. K. Paré P. M. Wood
Reactor Engineers

T. E. Haynes J. A. Watts J. D. Jones
A. L. Johnson G. H. Johnstone W. B. Krick
R. Smith, Jr.
Technicians

REACTOR OPERATIONS

Failure of the remote level indicator on the fuel pressure reservoir (Fig. 1) necessitated a two-week shutdown of the HRE early in November. The performance of the indicator prior to failure led to the conclusion that the sealed float chamber had stuck in a downward position, and this was verified by radiographic examination of the indicator parts. Furthermore, the radiographic films indicated that one of the two supporting arms was bent; this distortion had caused sufficient misalignment of the float to account for the sticking. Although the radiation level in the vicinity of this instrument was in the neighborhood of 50 r/hr, it was possible to install a lead shield, and, by drilling a small hole in the float chamber and straightening the bent arm with a push rod inserted through the drilled hole, the instrument could be repaired. After the rod had been straightened the drilled hole was closed and seal welded. No further difficulty has been experienced with the instrument.

Operations were resumed, and the reactor was maintained at approximately 1 Mw for nearly 100 hr before it was shut down. Difficulty was experienced in stabilizing the reactor at high power levels and temperatures because of a tendency of the circulating fuel solution to become more concentrated at high gas (hydrogen and oxygen) flows. (See "Analyses of 'Walk-Away' Phenomenon" below.)

A run was made to demonstrate the effectiveness of the copper ion as a homogeneous catalyst for the internal recombination of the decomposition gases hydrogen and oxygen. At the start of the run, a sufficient amount of copper sulfate was added to the uranyl sulfate fuel solution to recombine 10% of the total decomposition gas with the reactor operating at 1000 kw, 250°C, and 1000 psi. After approximately 50 Mwhr of operation, during which data were collected at various temperatures and power levels, the quantity of copper was raised to 25% of that required for total recombination at 1 Mw. A third addition, which raised the copper content to 75% was made after another 40 Mwhr of operation, during which the reactor was operated at a power as high as 1500 kw for several hours. Finally, sufficient copper was added for complete recombination at 1500 kw, 250°C, and 1000 psi, and there was a very successful demonstration of total recombination at these conditions. The data collected on the performance of the copper and the results are discussed in detail in the section "Internal Recombination Experiments."

Early in January, the leakage of steam through a high-pressure valve from the fuel pressurizer made it impossible to maintain the reactor pressure at 1000 psi. During this period of difficulty, additional data for copper were collected at pressures down to 750 psi, which is the lowest pressure at which the reactor can be maintained in a stable condition if the temperature is above 200°C. The troublesome valve was originally installed in order to permit bleeding off accumulated hydrogen and oxygen gas from the top of the fuel pressurizer and thus to prevent an explosive mixture from forming at that

[1]On loan from Chemistry Division.

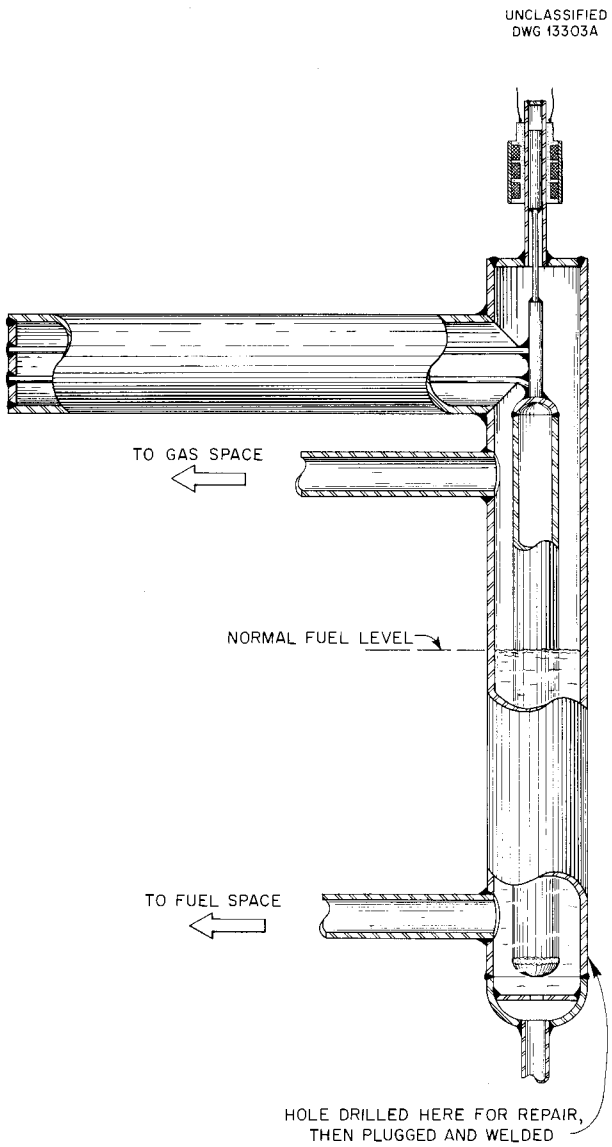

Fig. 1. Pressurizer-Level Indicator.

point. Actually, since no gas accumulation had been observed in the pressurizer during several hundred hours of operation, there was some question as to the need of the valve, especially with the homogeneous copper catalyst. It was decided to stop the leakage by freezing the line leading to the valve and to observe whether explosive gases accumulated. After 50 Mwhr of operation with the line frozen, there was no indication that any decomposition gases had accumulated in the pressurizer space, and normal experimental operations were continued. The collection of the copper ion recombination data was completed on January 21, 1954. A final high-power run was made from January 24 to February 1, at which time reactor operations were terminated in preparation for disassembling the reactor.

Corrosion

A generalized corrosion rate as indicated by the nickel content of the fuel solution has been followed throughout this period of operation. The results shown in Fig. 2 indicate an average rate of approximately 7 mpy with a possible error of ±30%. It may be recognized that this rate is considerably higher than the 3 mpy quoted previously for high-power operation at 200°C, and it should be noted that the rate of 7 mpy is for high-power operation at temperatures considerably above 200°C. There is no evidence at present that the addition of copper has affected either the chemical or corrosion characteristics of the HRE. These findings are consistent with the findings reported in the corrosion section of this report which were based on specimens exposed in out-of-pile circulating loops. The loop data indicate a maximum corrosion rate of approximately 9 mpy in the case of 40 g of uranium per kilogram of solution at 225°C, which is the average HRE solution temperature when the core outlet temperature is 240°C. Temperatures above 250°C result in much lower corrosion rates and have been specified for any future reactor operation.

INTERNAL RECOMBINATION EXPERIMENTS IN THE HRE[2]

The HRE experiments with dissolved copper have demonstrated conclusively that the decomposition gases, hydrogen and oxygen, can be completely recombined internally in aqueous homogeneous systems. Copper ion was added as copper sulfate on four occasions, gradually increasing the copper concentration to 10, 25, 75, and 150% of the estimated concentration necessary for complete recombination in a static system at 250°C, 1000 psi total pressure, and with a uniform power density of 20 kw/liter. Since the HRE is neither static nor of uniform power density, it was expected that the results would be somewhat different from those of the static-bomb experiments.

The effectiveness of the copper as an internal recombiner in the HRE was measured by comparing

[2] In the planning and analysis of these experiments, the HRE Group is being assisted by P. N. Haubenreich, H. F. McDuffie, and C. H. Secoy.

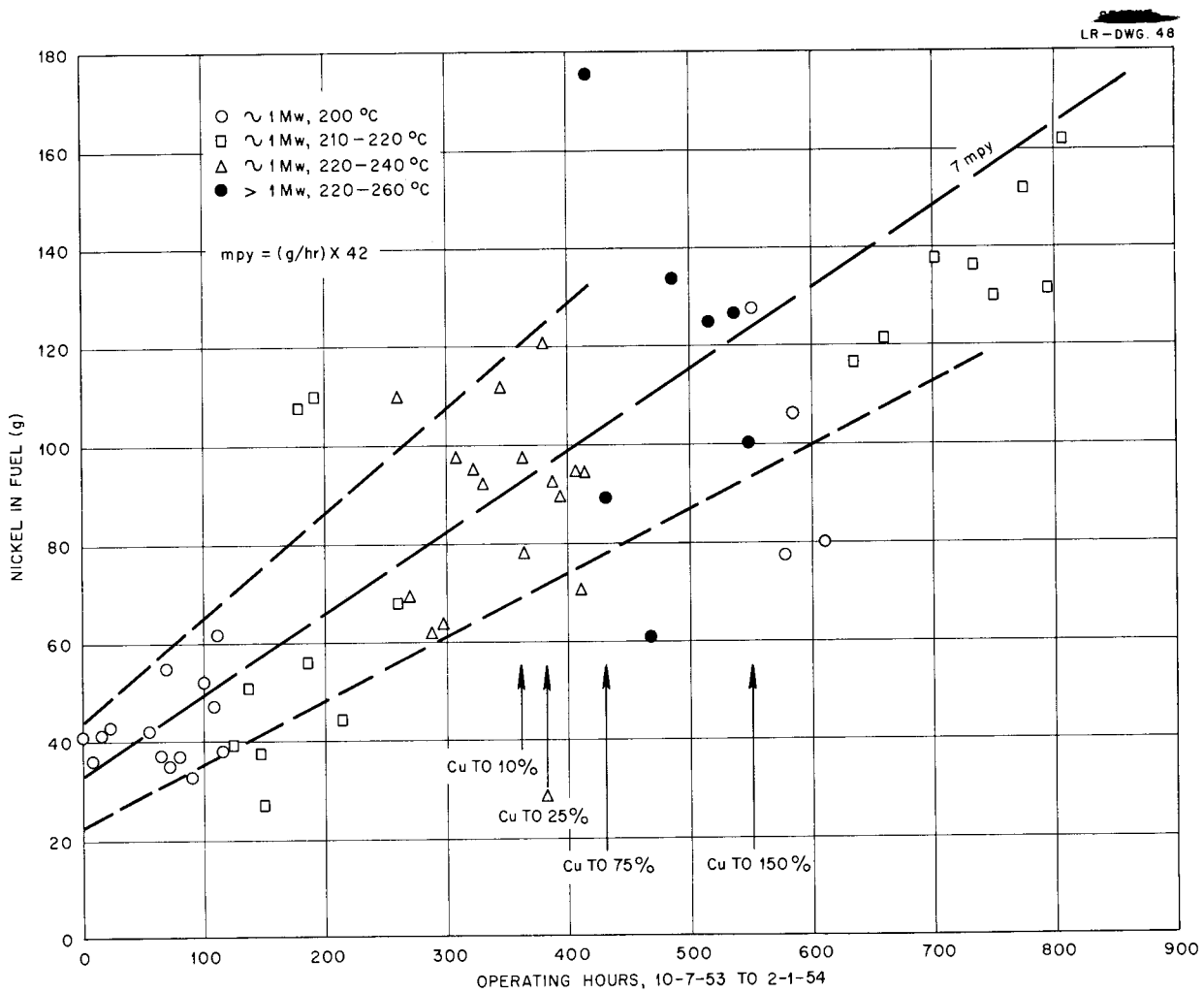

Fig. 2. Generalized Corrosion Rate of HRE Circulating System.

the rate of heat production from gas recombination in the external recombiner system with the rate previously measured when no copper was used. Measurements were taken for each copper addition at temperatures from 210 to 260°C, at pressures from 765 to 1200 psi, and at powers as high as 1600 kw. Figure 3 shows typical data for the 75% copper level compared with the reference line determined without added copper. The lines at each temperature are generally parallel to the reference line and can be extrapolated to the reactor power at which no gas reaches the external recombination system. Several such "zero gas" points are plotted on Fig. 4 against the temperature variable.

The effectiveness of the copper depends on the temperature and the partial pressure of hydrogen gas. Thus, for a given total pressure, the maximum effectiveness should be obtained at the temperature for which the product of the rate constant and the hydrogen pressure is a maximum. The solid line (actual data) in Fig. 4 indicates a maximum effectiveness at about 245°C, whereas in a static core with a uniform power density (indicated by the broken "one-region" line) the maximum would be expected near 260°C.

The "two-region" line on Fig. 4 agrees more closely with the experimental data than does the "one-region" line. This line is based on the assumption of a relatively stagnant region in the

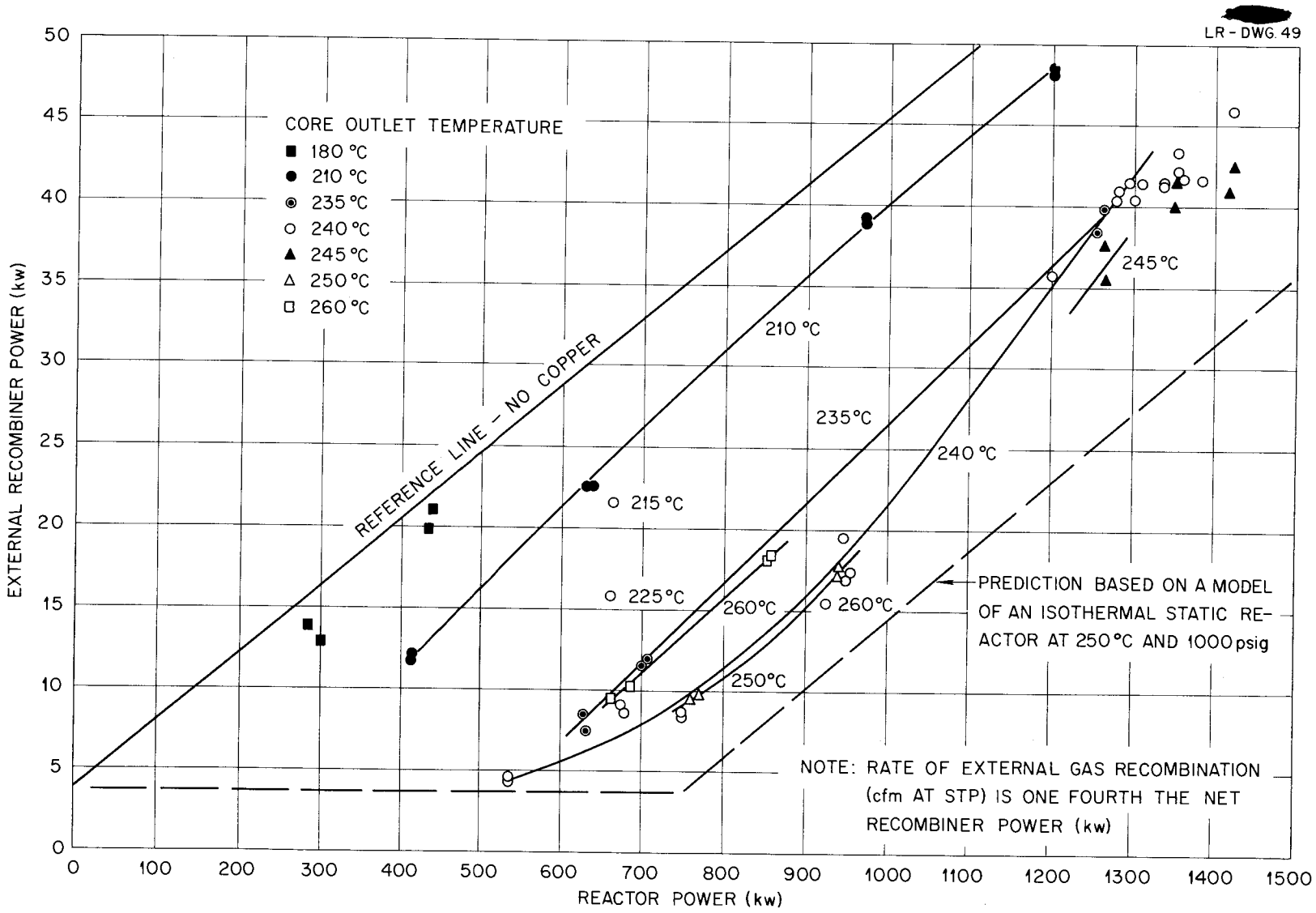

Fig. 3. HRE Copper Recombination Studies. Fuel Pressure, 1000 psig; 0.03 *M* Cu^{++} (75%).

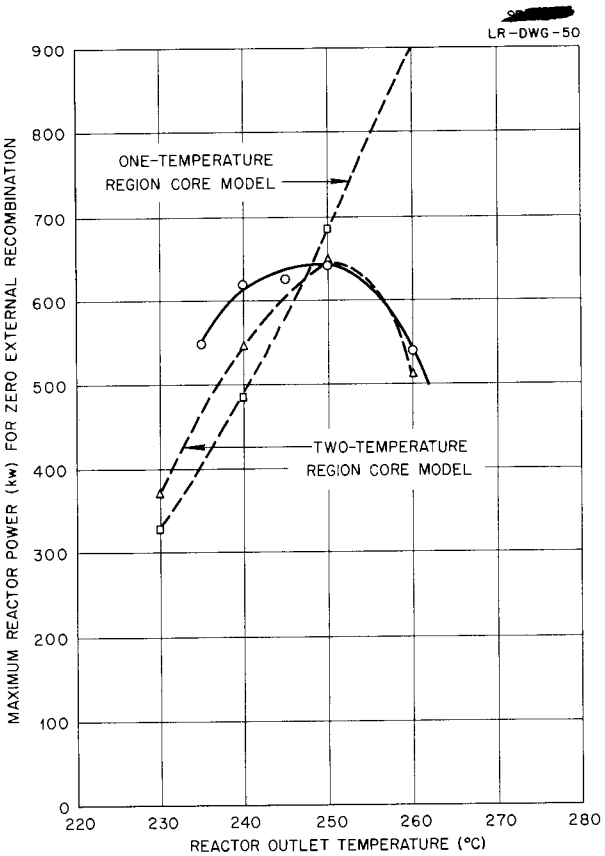

Fig. 4. Effect of Temperature on Internal Gas Recombination. Fuel pressure, 1000 psig; 0.03 *M* Cu^{++} (75%).

reactor sphere, existing as a hollow cylinder and coaxial with the gas vortex, in which the temperature is higher than that of the core outlet by an amount roughly proportional to the square root of the reactor power. The existence of such a "hot spot" was indicated in a study by Spiewak and Bradfute[3] during early developmental work on the HRE core and has recently been suggested by the results of analyses of the operational instabilities described in the section "Analysis of 'Walk-Away' Phenomenon." These independent indications of a high-temperature donut within the HRE core are being investigated further. At present the situation may be summarized as follows:

1. Copper ion is a highly effective internal recombination catalyst in an operating homogeneous reactor.

2. The data for a given total pressure always show a temperature for maximum effectiveness several degrees centigrade lower than would have been predicted from static-bomb data. It appears that the explanation for this difference may be associated with a "hot spot," within the core, operating at a temperature higher than the average.

ANALYSIS OF "WALK-AWAY" PHENOMENON

Operation of the HRE during the past quarter has disclosed possible operating conditions which are unstable because of the interrelation, in this reactor, between power, temperature, and fuel concentration in the core.

It has been known for some time that there is an increase in the operating temperature of the HRE with power level. The basis for this behavior, as described in a previous report,[4] is that the fuel concentration in the core is enhanced, with respect to that in the low-pressure system, by the removal of water from the core by decomposition as radiolytic gas and accompanying steam. In this process there is a net transfer of uranium from the low- to the high-pressure system. More recently, it has been shown that this increase in temperature, which is accompanied by an increase in the rate of steam removal, leads to a further increase in concentration and temperature. When the resulting rate of increase of reactivity with temperature from the concentration effect exceeds the negative temperature coefficient of reactivity, the core temperature and power steadily increase at a relatively slow rate, a phenomenon which has been termed a "walk-away."

The rise in temperature can proceed, unless stopped by the operator, to such a point that the let-down system becomes overloaded with gas. At this time, all the uranium solution being pumped into the high-pressure system by the pulsafeeder accumulates there, with only water being removed. By reducing the reactivity and the power extraction, it has always been possible to return the reactor to the region of stable operation; however, in some cases the fuel outlet temperature from the core reached a temperature of 282°C, 3 deg below the boiling point.

[3] I. Spiewak and J. O. Bradfute, *Effect of Density Difference on Flow in the HRE Core*, ORNL CF-51-10-165 (Oct. 17, 1951).

[4] S. E. Beall *et al.*, *HRP Quar. Prog. Rep. July 31, 1953*, ORNL-1605, p 5.

Example of Walk-Away

The behavior of the reactor during a walk-away is illustrated in Fig. 5. In the case given the reactor had been operating stably at 1000 kw, 1000 psig, and at a core outlet temperature of 220°C; in an attempt to raise the reactor temperature, 0.7 kg of water was evaporated from the fuel. Under these conditions, a 2°C rise in temperature based on low-power experience was anticipated. However, as will be shown later, the value of the reactivity controls, including fuel concentration, is enhanced when the reactor is operating at high power, and the resulting rise in temperature was sufficient in this case to bring the reactor into an unstable operating region. The temperature continued to rise at a rate of 3°C/min, and when the temperature reached 246°C it was necessary to considerably dilute the fuel. The increase in the fuel level in the pressurizer was caused by the generation of gas and steam in the core at a rate exceeding the capacity of the let-down system. The subsequent rise in fuel pressure is attributed to the compression of the steam in the pressurizer.

Further exploration of the behavior of the reactor has revealed that the walk-away phenomenon is a function of both the initial operating temperature and the power level.

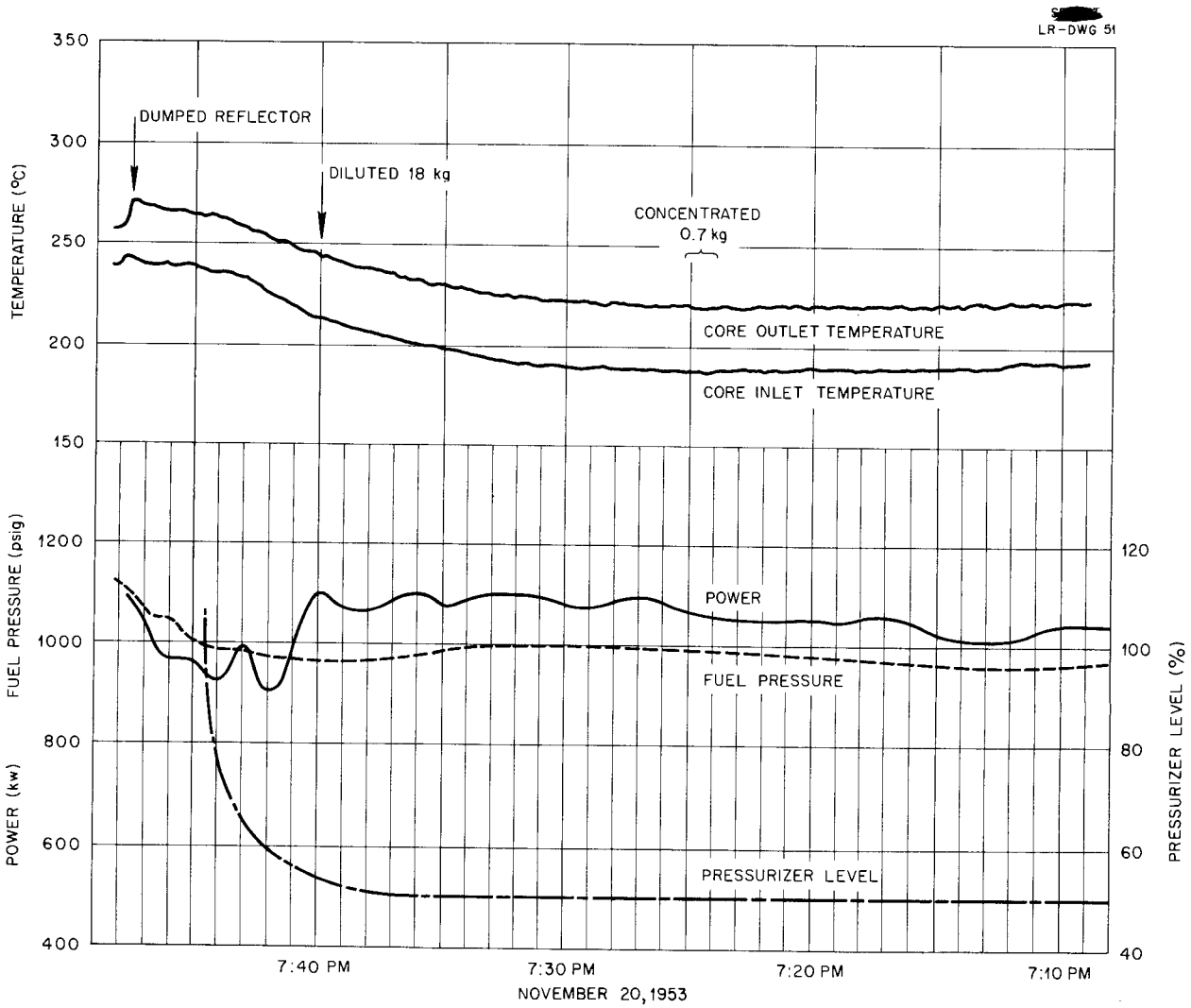

Fig. 5. Behavior of HRE During "Walk-Away," Nov. 20, 1953.

Discussion of Core Concentration Effect on Stability

As was shown in a previous progress report,[4] the enhancement of the core concentration, C_H, with respect to its value at low power, C_0, is given by

$$\frac{C_H}{C_0} = \frac{1}{1 - \dfrac{g}{f\left(1 + \dfrac{M_H}{M_L}\right)}} ,$$

where M_H and M_L are the mass of solution in the high- and low-pressure systems, respectively, and f is the rate of circulation between the two systems, that is, the pulsafeeder pumping rate. The quantity g is the rate at which water is removed from the core and has two components: radiolytic gas which is proportional only to the power and associated steam which is directly proportional to the power, the absolute temperature, and the steam density and inversely proportional to the gas pressure. The gas pressure is the difference between the total pressure and the steam pressure. The equilibrium concentration is approached asymptotically with a time constant of the order of 7 min. For a given power level and constant total pressure, the water-removal rate depends on temperature only. This is shown in Table 1, with the corresponding values of C_H/C_0 for the stated conditions.

The enhancement of core concentration with temperature is even more pronounced than indicated by Table 1 when an increase in power output with the steam temperature is permitted, as when the position of the steam throttle valve is fixed. Thus, the power withdrawal is proportional to the steam pressure which is determined by the reactor temperature and power level. However, the concentration effect, as calculated above by assuming the maximum core temperature to be that measured at the outlet, is not sufficient to account for the reactor performance described in Fig. 5. As is shown in Table 1, the effect is strongly temperature dependent and may be influenced by the complex temperature pattern of the core.

TABLE 1. ENHANCEMENT OF FUEL CONCENTRATION FROM GAS GENERATION

Basis: power = 1000 kw
pulsafeeder flow = 1 gpm
U^{235} inventory = 3.79 kg
fuel pressure = 1000 psig

	VORTEX TEMPERATURE (°C)					
	200	220	240	250	260	270
g (kg/min)	0.23	0.29	0.42	0.54	0.77	1.34
C_H/C_0	1.030	1.038	1.056	1.072	1.108	1.200

There is evidence, supported by mixing experiments,[3] that a relatively stagnant region exists in the core surrounding the vortex and that the effective temperature of this region at 1000-kw power level is 15 to 20°C hotter than the outlet temperature of the fuel solution. This hot spot can account for the increase in the rate of steam removal accompanying the decomposition gas. As far as affecting the enhancement of core concentration is concerned, the thickness of the hotter region need only be sufficient to saturate all the radiolytic gas passing through to the vortex.

Essentially, the effect of the hot region can be included in the previous treatment by assigning to the temperature of the steam accompanying the radiolytic gas a value which is higher than the core outlet temperature by 20°C for each 1000 kw of reactor power. For example, in Table 1 the temperature given is that for the steam, and the core outlet temperature is therefore lower by 20°C. It is to be noted that the rate of water removal from the core for a given fuel outlet temperature is then no longer strictly proportional to the power level because the temperature of the hot region is dependent on the power. The enhancement of the core concentration calculated by taking into account the hot region and the power variation with reactor temperature is shown in Fig. 6. For comparison, the curve for constant power is also shown.

It is possible to predict whether stable operation is attained for a particular set of reactor conditions by comparing the rate of enhancement in concentration with temperature with the variation of critical concentration with temperature. Operation can be stable only if the rate of change of critical concentration with temperature is greater. Such an analysis is presented in Fig. 7 for the case in which the steam-outlet valve has been set to deliver 1000 kw when the reactor outlet temperature is 250°C. The solid curve shows the actual

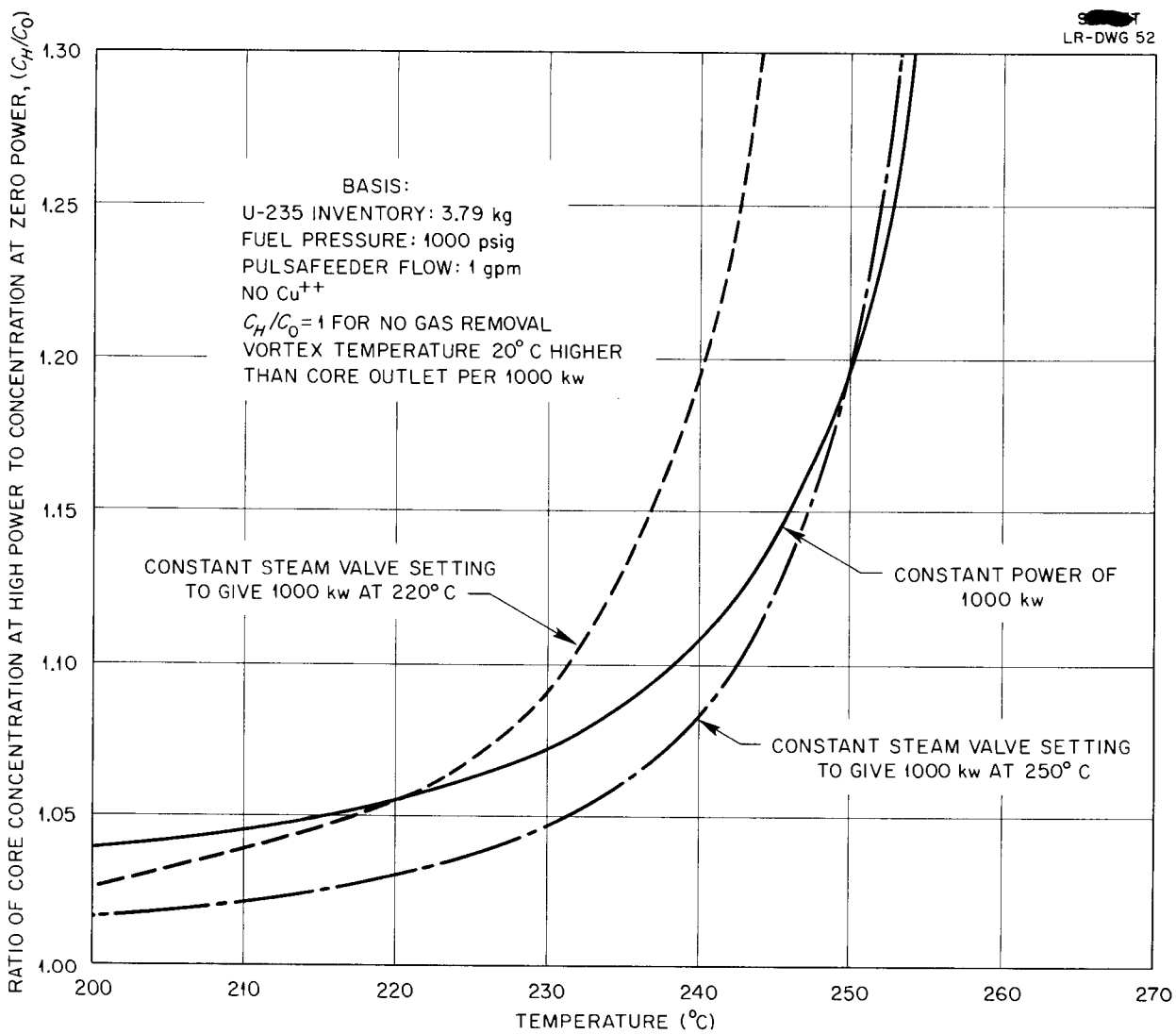

Fig. 6. Enhancement of Fuel Concentration in Core as Result of Removal of Gas and Steam.

fuel concentration in the core for any outlet temperature; the reactor power will increase with temperature since the setting of the steam valve is constant. The lower broken curve indicates the variation of core concentration with temperature in the vicinity of the operating point of 216°C and 650 kw, which, from this analysis, should be stable. The upper broken curve is associated with 240°C and 900 kw, which should be unstable. This condition of marginal stability is determined by graphical methods.

The strong dependence of the concentration effect on temperature at appreciable reactor power serves to enhance the effect of the reactivity controls in the reactor. Thus if the reactivity is quickly increased, a rise in temperature of the same magnitude as that obtained at very low power is immediately achieved; however, this is followed by a gradual increase in core concentration and an additional increase in temperature. This effect is illustrated in Fig. 7 for a case in which the reactor temperature can rise from 216°C to 240°C by the removal of 5 kg of condensate. At low power where gas production is negligible, 10 kg of condensate must be removed to bring about this temperature rise.

A theoretical curve shown in Fig. 8 defines the maximum power at which the HRE can be operated

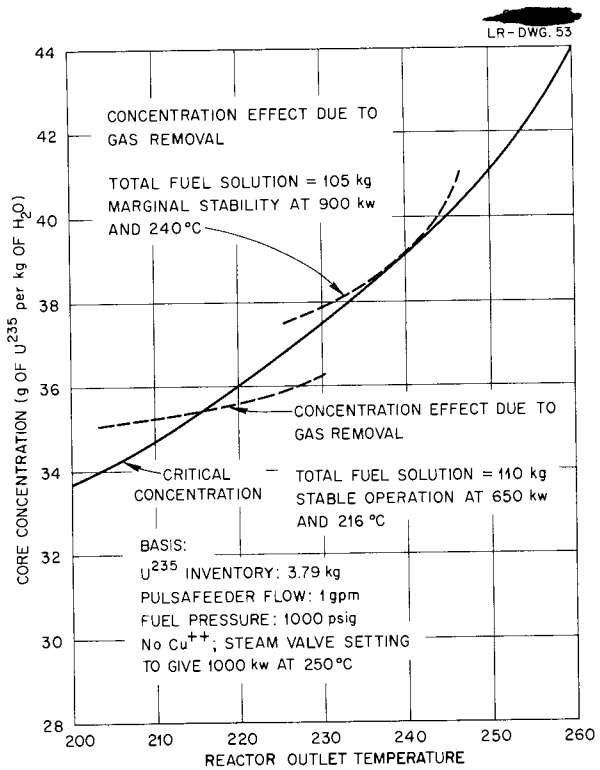

Fig. 7. Analysis of HRE Stability in Terms of Fuel Concentration Effect in Core.

stably for any temperature with the given fuel inventory and without any homogeneous catalyst for gas recombination. Below this curve, the HRE has operated stably but all attempts to take the reactor above the curve have led to walk-aways. Also shown is a curve relating the temperature to the power level for the maximum capacity of the let-down system at 1000 psig fuel pressure and a

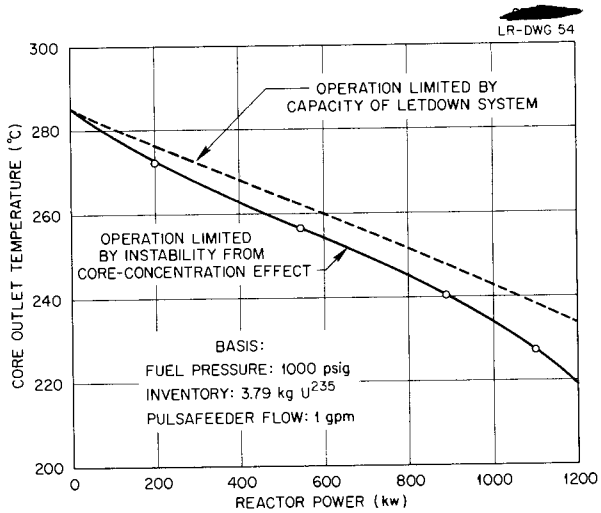

Fig. 8. Maximum Power for Stable Operation of HRE. No Cu^{++} as recombination catalyst.

pulsafeeder flow of 1 gpm. The basis for this curve is flow data obtained at 250 and 20°C during the preoperational testing.

In conclusion, it should be pointed out that the unstable condition discussed has not seriously limited reactor operation. It has necessitated more caution in making reactivity increases at high powers and temperatures. Furthermore, it is important to note that the effect is significant only with respect to reactor systems with rotational flow in the core and gaseous let-down instead of internal or high-pressure recombination. By adding copper ion for internal recombination of the decomposition gases, it has been possible to increase the permissible reactor power more than 50% above the design power of 1000 kw.

Part II

BOILING REACTOR RESEARCH

BOILING REACTOR RESEARCH

R. N. Lyon, Section Chief

STEAM REMOVAL FROM BOILING REACTORS

R. J. Goldstein H. A. MacColl
C. G. Lawson M. Richardson
P. C. Zmola

Slip Velocity

Applications to which boiling homogeneous reactors might be suited cover a wide range of reactor sizes and pressures. For this reason, in addition to experiments with specific geometries and pressures, it is of interest to determine the relationship between these parameters and the gross hydrodynamic behavior of this two-phase system. Work reported in previous quarterly reports has been directed in large measure to investigating the effect of size, which is perhaps the less straightforward scaling parameter since it involves the general hydrodynamic flow pattern in the core and the variables which influence it. Work involving possible core configurations has been continued, with particular attention being devoted to the influence of diameter and the relative velocity of vapor to liquid.

In addition, work is proceeding on two pressure systems. The first is a 4-in.-dia natural-vapor-rise apparatus which will be capable of operating up to 1500 psia. The relation between power density and mean fluid density will be obtained as a function of pressure by taking a radiogram of the apparatus under operating conditions to determine the boiling height. This apparatus is in the construction stage. The second system, which is in the preliminary design stage, is a natural-circulation apparatus generally similar to the 1.25 × 4 in. natural-circulation system which has been described previously[1] and which was used to obtain the information reported below on slip velocities. It is planned to investigate the influence of test-section height and diameter on the relationship between power density and mean fluid density over a range of pressures up to 2400 psi.

During the past quarter, the slip-velocity measurements reported previously[2] have been extended to 0.5 and 2.0 atm absolute. The results are shown in Fig. 9. The slip velocities are given by the difference between the plotted vapor and liquid velocities. At a given power the slip velocities decrease strongly with increasing system pressure in the range of 0.5 to 2.0 atm, and it is not possible to extrapolate the results to even moderate pressures. Therefore it will be necessary to operate a similar system at higher pressures to obtain the desired data.

In a qualitative way, volume boiling by utilizing electrical-resistance heating simulates nuclear power production since a decrease in density results in decreased electrical power. With this correspondence in mind, the influence of pressure on power fluctuations was investigated. Since the line voltage remains essentially constant, a trace record of the current was made with a Brush oscillograph at approximately 1 and 2 atm absolute. Sections of these traces are shown in Fig. 10. The amplitude of the fluctuations dropped from about 5% at atmospheric pressure to 3% at 2 atm.

It was previously reported[2] that for systems in which slip velocity governs, the power density varies inversely with the diameter for a given vapor fraction. This was based on results obtained from a number of natural-rise systems, the largest being the 69-in.-dia air-water apparatus. In order to test the influence of diameter, an "egg crate" of 8-in.-square cells was installed in the tank. However, the results obtained were the same as those obtained without the "egg crate," within the limits of experimental error. This seems to indicate that other parameters such as the height-to-diameter ratio or a friction factor need to be included in the correlating expression. Further experiments with both the 69-in.-dia and the 24-in.-dia air-water equipment are planned.

Forced Convection

If the slip velocity is low, natural or forced convection is required and some mechanical method of phase separation may be necessary.

[1] R. V. Bailey *et al.*, *HRP Quar. Prog. Rep. July 31, 1953*, ORNL-1505, p 24-25.

[2] R. V. Bailey *et al.*, *HRP Quar. Prog. Rep. Oct. 31, 1953*, ORNL-1658, p 15.

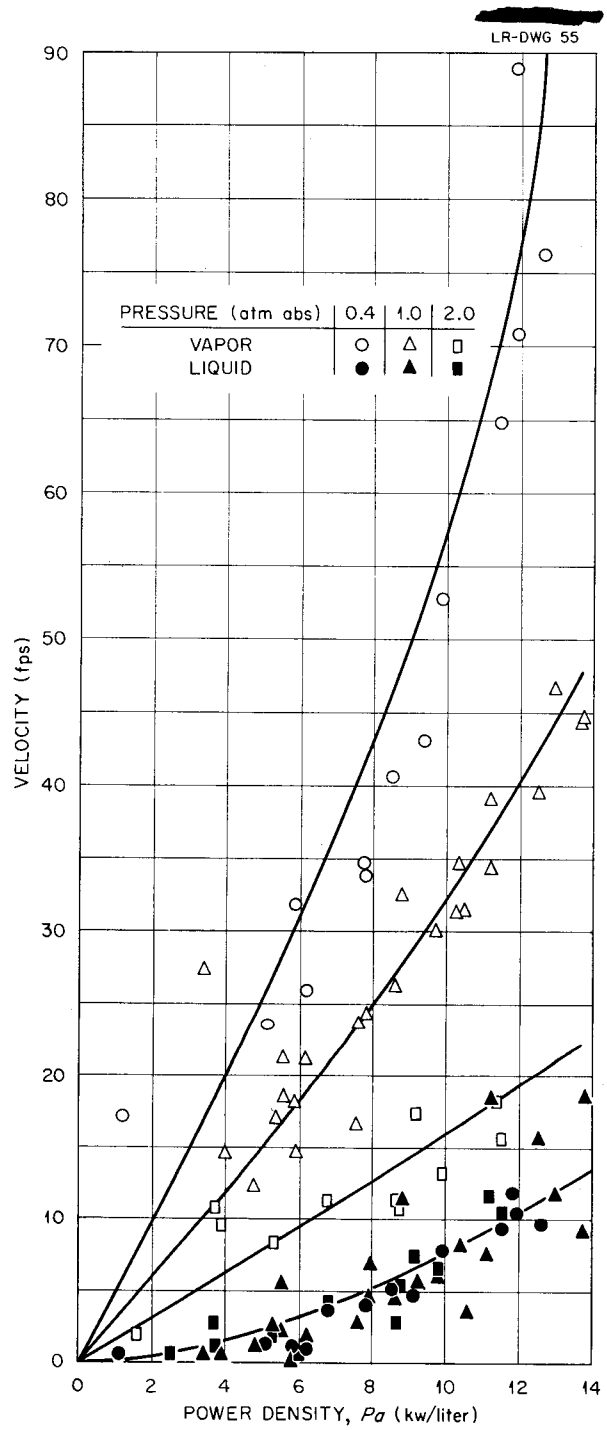

Fig. 9. Influence of Total Pressure on Average Vapor and Liquid Velocities at Exit of 1.25 × 4 in. Natural Circulation Apparatus.

During the past quarter consideration was given to the related problems of convection and separation.

In Fig. 11 the flow rate required in the downcomer per kilowatt of reactor power in a circulating boiling reactor is indicated vs reactor pressure for a number of void fractions at the top of the riser. It was assumed in making this plot that there is negligible slip.

For purposes of comparison, Fig. 12 shows the temperature drop in the circulating liquid of a nonboiling reactor which would correspond to the heat removed in the steam from a boiling reactor with the same circulation rate. It is seen that for reasonable void fraction at the outlet the required circulation rate would be somewhat higher in a boiling reactor with no slip than in currently contemplated nonboiling reactors. It should be

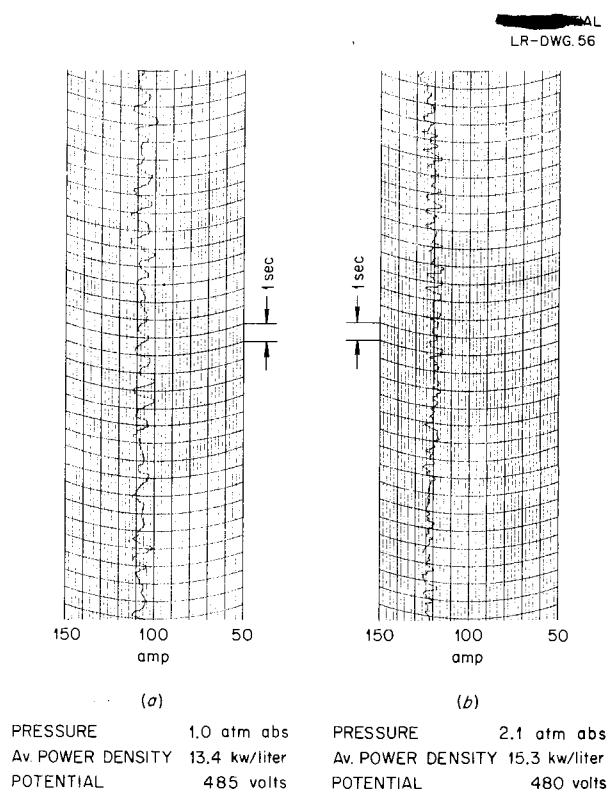

Fig. 10. Influence of Pressure on Power Fluctuations. Sections of Brush oscillograph recording taken at approximately 1 and 2 atm in 1.25 × 4 in. circulating system.

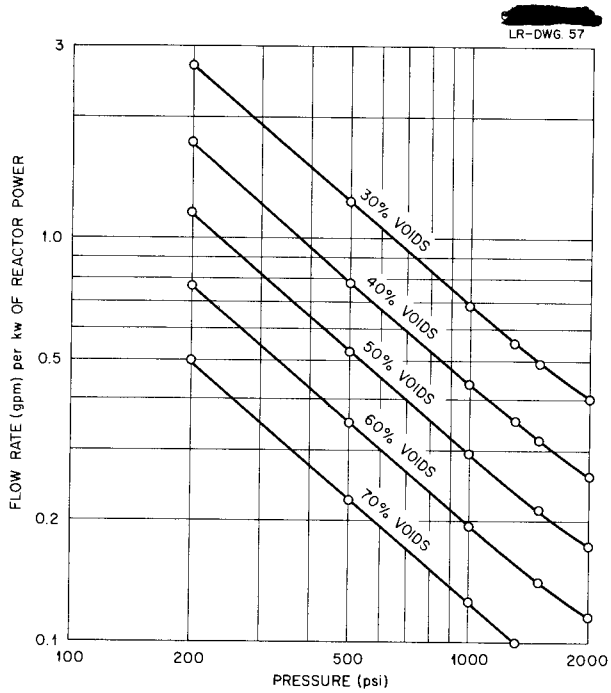

Fig. 11. Gallons of Liquid per Minute for Each Kilowatt of Reactor Power.

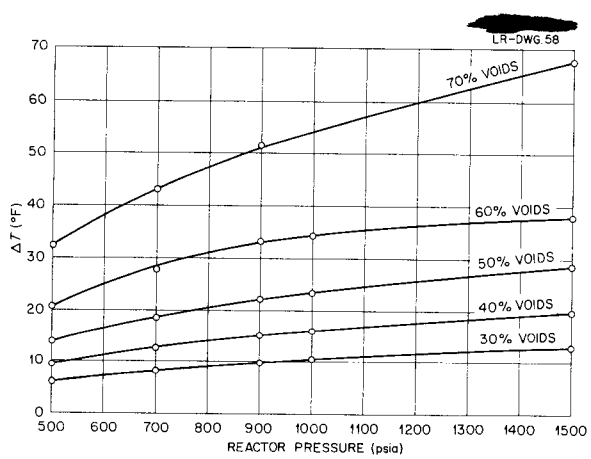

Fig. 12. Temperature Drop Required to Remove Equal Power from Circulating Liquid and from Condensing Steam vs Reactor Pressure. Parameter is void fraction leaving core.

borne in mind, however, that the pressure drop through a heat exchanger is reduced or eliminated and that the difference in densities in the downcomer and riser will supply some of the pumping energy – the proportion depends on the effective diameters of downcomer and riser, the height of the riser, and the pressure drop in the steam separator.

Commercial Separators

A subcontract has been arranged with the Babcock and Wilcox Company for a survey of commercial separation practice and to obtain data on the behavior of their separators for removing entrained vapor from a stream of liquid in the range of void fractions beyond that of present practice. These data will enable an evaluation to be made of the pressure drop around the system and will provide the basis for a more realistic picture of a practical boiling reactor.

Separator Pumps

Since the power required for a pressure change at low velocities along a flowing system is equal to

$$\int_{p_1}^{p_2} F \, dp \quad ,$$

where F is volume flow rate and p is pressure, a small increase in separated-liquid pressure should be obtainable from a correspondingly small decrease in separated-steam pressure. For example, in a high-pressure system with 50% voids leaving the riser, a pressure rise of slightly more than 5 psi in the recirculated liquid is thermodynamically possible if the energy from a pressure drop of 5 psi in the steam is fully used.

The best way of utilizing this principle is believed to be some type of centrifugal separator with no moving parts. In such a device, however, the liquid would have to flow at high velocities with minimum friction and maximum pressure recovery.

A vapor-liquid separator roughly similar to one designed by Foster Wheeler Corporation[3] was set up and tested with air and water at room temperature. Flow rates of up to 50 gpm of water and 50 scfm of air could be maintained in this apparatus.

The air and water mixture entered the separator through a rectangular nozzle and expanded from about 15 psig down to atmospheric pressure. This expansion greatly accelerated the mixture, which then proceeded through a 10-in.-dia semicircular

[3] R. A. Lorenzini, *Heat Engineering* 27, 94 (1952).

path where much of the gas was removed as a result of the centrifugal action. The liquid then entered a small angle, straight wall, rectangular diffuser through a narrow opening. The water that did not enter the diffuser, due to difference in size of entrance and to the water layer necessary to ensure absence of gas in the diffuser, was removed through a drain.

The preliminary experiments showed several inherent disadvantages in the system. Either because the gas phase was not completely separated by the time the mixture reached the diffuser entrance or because air from the liquid-gas interface was drawn into the diffuser, a large amount of gas left with the liquid. When the diffuser-entrance area was reduced to prevent gas in the diffuser, large amounts of liquid spilled over. An appreciable loss of total head apparently took place during the formation of a new boundary layer at the free surface where it entered the diffuser. In addition, the high velocity and relatively large surface area in the circular part of the apparatus caused a high head loss where the mixture was at maximum velocity. As a result of both these effects, the over-all pressure drop in the separator was excessive, and further development of this type of separator has, at least temporarily, been abandoned.

A different liquid-vapor separator has been designed and a model will be tested during the coming quarter. In the new model the mixture enters the separator through a central pipe, being discharged in a sheet approximately tangent to the pipe wall through a slot running the length of the pipe. A large coaxial cylinder surrounds this inlet pipe and a vortex is expected to be set up in the annulus between the two. The gas phase is separated from the liquid by the centrifugal action and is taken off at the top of the apparatus. (Some of the gas and perhaps some of the liquid may have to be removed at the bottom to stabilize the vortex.) The liquid, the velocity of which is expected to decrease as it moves toward the outer perimeter, will be removed at the bottom through the space between two coaxial cones (bases upward) with guide vanes for halting the rotation.

This latter design has several important advantages over the first separator. Since the velocity at the wall is low, the skin friction loss should not be so great. The carryover of gas in the liquid should be much smaller because of the extra rotation and the absence of a liquid-gas interface near the exit. In addition the velocity at the exit where a new boundary layer is formed is low and therefore a smooth transition is expected.

Part III

GENERAL HOMOGENEOUS REACTOR STUDIES

HOMOGENEOUS REACTOR DESIGN

R. B. Briggs, Section Chief

R. E. Aven
R. H. Chapman
R. D. Cheverton
W. L. DeRieux
W. R. Gall
P. N. Haubenreich
T. H. Mauney
J. R. McWherter
J. P. Sanders
C. L. Segaser
W. Terry
T. H. Thomas
F. C. Zapp

HOMOGENEOUS TEST REACTOR

Flowsheet and General Design Considerations

A homogeneous test reactor (HRT) is being designed to replace the HRE. The design is to utilize the best information now available regarding operating conditions and equipment to provide a reliable experimental reactor for investigating general operational problems of aqueous homogeneous reactors and for testing fuels and concepts which are being considered for large power and production reactors.

The present HRT flowsheet is shown in Fig. 13. It combines features of both the HRE flowsheet and the ISHR flowsheet presented in ORNL-1605.[1] The HRT will be a 5-Mw, two-region reactor fueled with highly enriched uranium, moderated and reflected with D_2O, and operated at 300°C and 2000 psia. A uranyl sulfate solution containing 10 g of uranium per kilogram of D_2O will be circulated through a 32-in.-dia core tank, a gas separator, and a shell-and-tube heat exchanger at a rate of 400 gpm by a canned rotor pump. Copper sulfate will be added to the solution as a homogeneous catalyst to recombine D_2 and O_2 produced in the reactor, so only that gas which is required to strip the fission-product gases will be removed in the separator and let down to the low-pressure system.

The reactor core will be centered in a 56-in.-ID pressure vessel, leaving a 12-in.-thick reflector or blanket. Initially the reactor will be operated with a D_2O reflector; however, the system will be designed so that a uranyl sulfate solution blanket can be substituted in order to investigate the production of plutonium low in Pu^{240} content. A thorium fuel can be used in the blanket in an investigation of breeder problems. It is assumed that the core and reflector circulating systems will be similar, and they will be interconnected through the pressurizers so that there will be no large pressure differences between the core and the reflector.

Low-pressure systems for core and blanket will be similar to the low-pressure fuel system of the HRE. Provision will be made for changing the uranium concentration, for recombining D_2 and O_2 in an amount equivalent to that produced when the the reactor is operated at a power of 1 Mw without copper in the solution, and for storage of solutions and fission-product gases.

General design data are presented in Table 2.

The arrangement of equipment and the design of the reactor cells are in the conceptual stage. Since ease of maintenance is to be a primary consideration, the cell compartments will be designed so that they can be flooded for major maintenance operations. Complete sealing of the cells will be required in order to prevent escape of radioactive materials in the event of a major leak. Consideration is being given to underground construction of the shield with the top at ground level.

A tentative schedule calls for completion of the HRT design by July 1, 1954. Procurement of components will begin as soon as firm designs are available.

Reactor Vessel

One of the latest conceptions of the reactor vessel is shown in Fig. 14. A 32-in.-dia, ¼-in.-thick zirconium core tank is centered in the pressure vessel and supported by the inlet and exit nozzles. Because of the large size of the core tank and because the reactor system is to operate at a pressure of 2000 psi, it appears necessary to eliminate large openings and to assemble the core and pressure vessel together. While it will not be possible to remove the core tank at will, the critical joints between zirconium nozzles and stainless steel connecting piping are made on the outer side of the pressure vessel where they will be accessible. Mechanical seals are provided to

[1] R. B. Briggs *et al.*, *HRP Quar. Prog. Rep. July 31, 1953*, ORNL-1605, p 32.

TABLE 2. TENTATIVE HRT DESIGN DATA

General Data

Nominal power level	5000 kw
Fuel solution	UO_2SO_4 in D_2O
Core diameter	32 in.
Core material	Zirconium
Core thickness	¼ in.
Core volume	290 liters
Core specific power	17.3 kw/liter
Reflector solution	D_2O
Reflector thickness	12 in.
Reflector vessel material	Stainless-steel-clad carbon steel
Operating pressure	2000 psia
Operating temperoture	300° C (572° F)
Fuel circulating rate	400 gpm
Maximum fuel velocity	20 fps at 250°C

Core Fluid

Fuel solution	UO_2SO_4 in D_2O
Uranium concentration	~10 g per kilogram of D_2O
Uranium enrichment	93.5% U^{235}
Heat capacity (av from 493 to 572°F)	1.24 Btu/lb/°F
Density at 300°C	50.60 lb/cu ft
Thermal conductivity at 500°F	0.35 Btu/hr/ft^2/°F/ft
Viscosity at 300°C (572°F)	0.24 lb/ft/hr
Viscosity at 500°F	0.29 lb/ft/hr
G for water decomposition	(1.67 molecules of D_2)/100 ev
Rate of formation of D_2	0.00179 lb-mole/sec
Rate of formation of O_2	0.00089 lb-mole/sec
Vapor pressure of D_2O over fuel solution at 300°C	~1246 psi
Compressibility of D_2O vapor at 300°C	0.702
Heat of recombination of D_2 and O_2	11,300 Btu/min (199 kw)
Heat of vaporization of D_2O at 300°C	602.7 Btu/lb
	12,000 Btu/lb-mole
Gas dissolved in fuel solution leaving core at 2000 psia and 300°C: D_2	0.10 mole/liter
O_2	0.05 mole/liter
Volume of gas generated (D_2 and O_2): at 2000 psia and 300°C	0.0148 cfs
at STP	0.963 cfs
$CuSO_4$ Concentration (recombination catalyst)	0.0058 g-mole/liter
Per cent of gas recombined in core at 2000 psia and 300°C	80 to 100

Reflector Fluid

Reflector fluid	D_2O
Heat capacity (2000 psia): at 256°C	1.16 Btu/lb/°F
at 300°C	1.33 Btu/lb/°F
Density (2000 psia): at 256°C	0.876 g/cc
	54.7 lb/cu ft
at 300°C	0.798 g/cc
	49.8 lb/cu ft
Viscosity (2000 psia): at 256°C	0.285 lb/ft/hr
at 300°C	0.242 lb/ft/hr
G for D_2O decomposition	(1.0 molecule of D_2)/200 ev
Heat removed from reflector	<500 kw

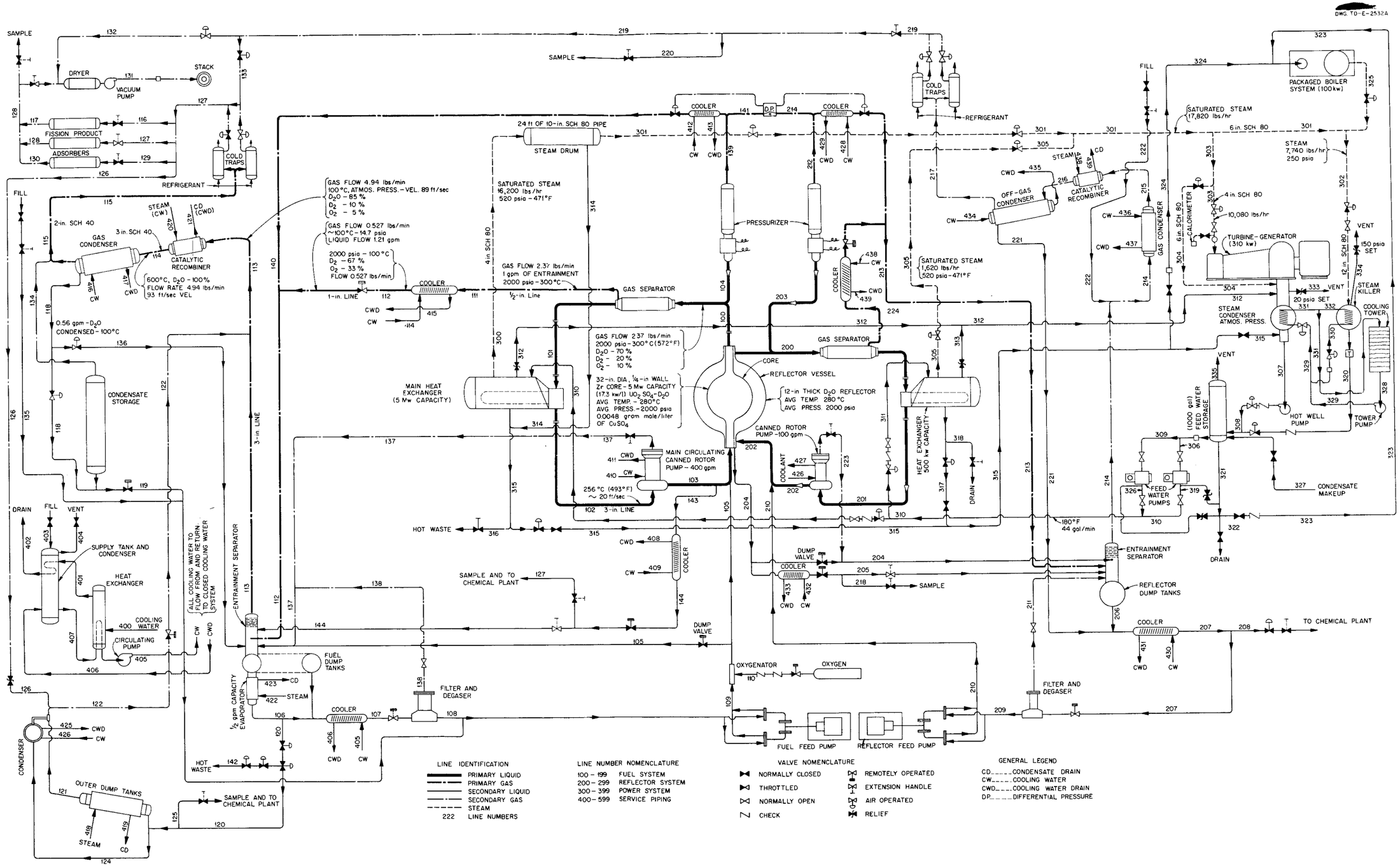

Fig. 13. HRT Flowsheet.

prevent mixing of the core and blanket materials. An expansion joint appears necessary to prevent undue stressing of the core tank caused by differences in expansion of the various metals. If the conical and spherical portions of the core vessel have the same thickness, the conical portion determines the allowable pressure difference between core and blanket. By using ¼ in. as the thickness for both portions, the vessel will withstand an internal pressure of 225 psi before the

UNCLASSIFIED
DWG 23175

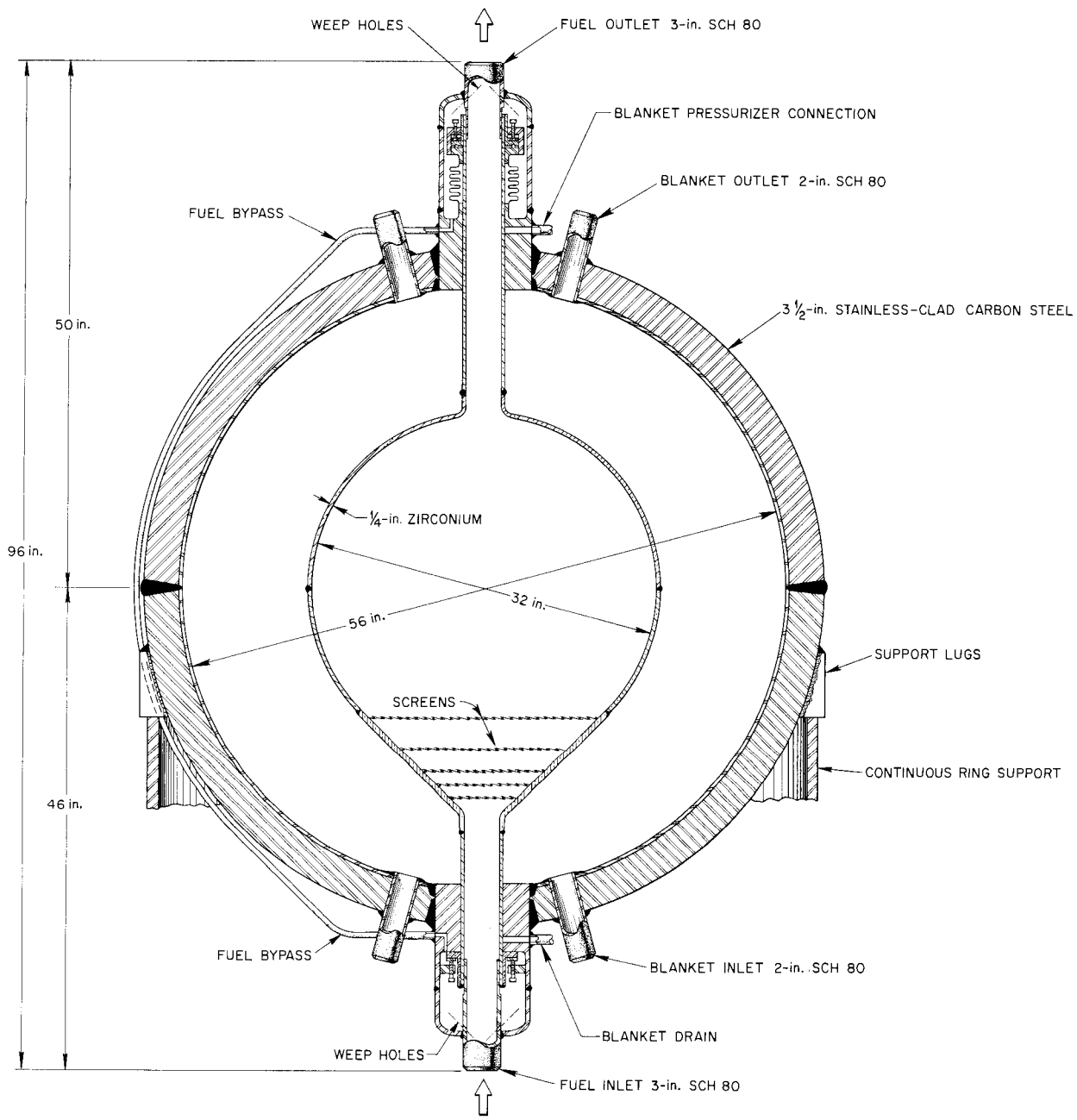

Fig. 14. Proposed HRT Reactor Core.

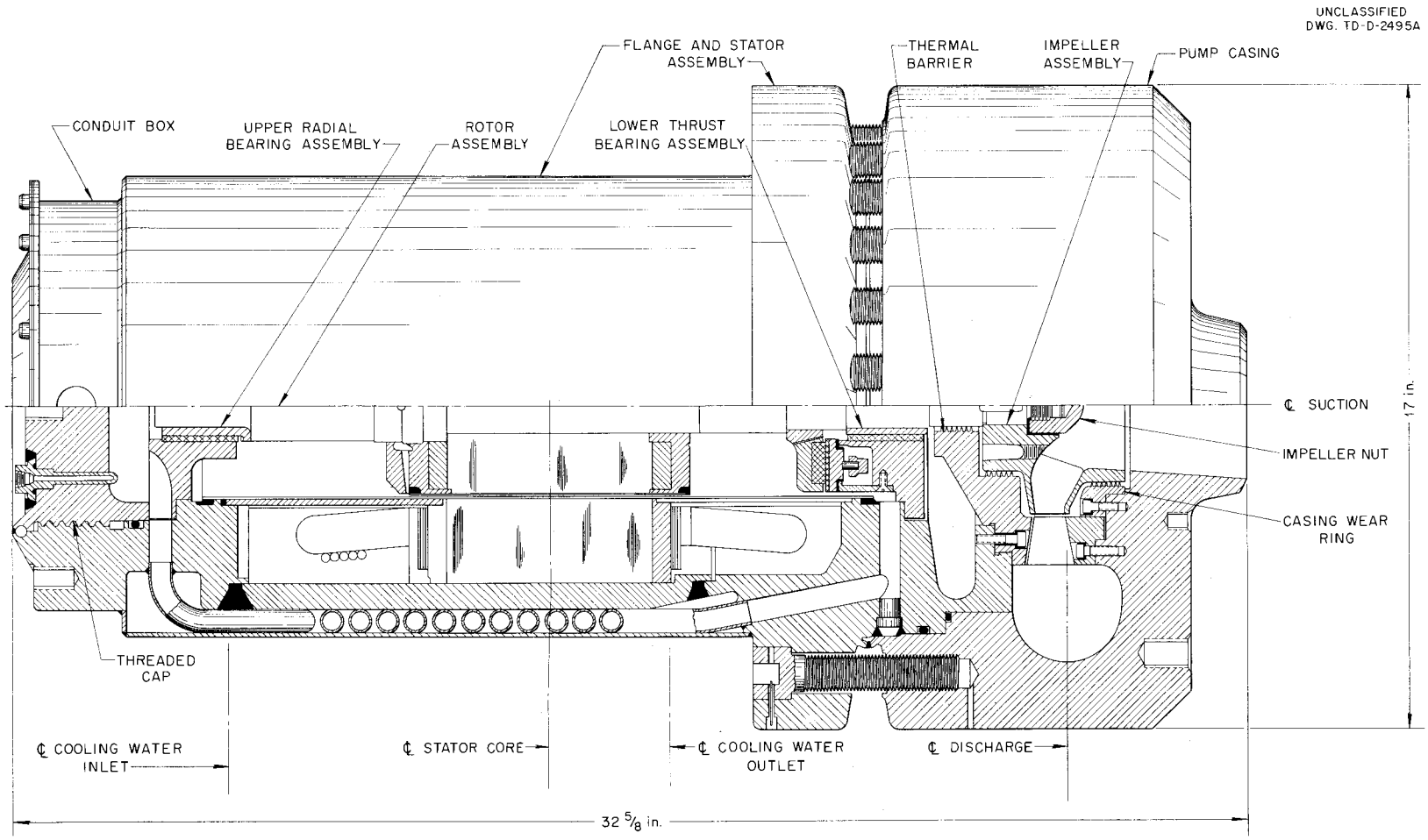

Fig. 15. Westinghouse Model 400A Centrifugal Pump.

18,000-psi yield strength of Zircalloy II is exceeded. There are not sufficient design data available to make a good calculation of the collapsing pressure for the core tank; however, the best estimates indicate that elastic buckling will occur if the pressure in the blanket exceeds that in the core by 170 psi.

"Straight-through" flow has been selected as the flow pattern for the core in preference to the "rotational" flow in the HRE core because it is considered to be more promising for large power reactors. As the core diameter increases, the pressure drop with rotational flow increases rapidly for a given inlet velocity, and the core becomes less effective as a gas separator. The pressure drop through the HRT core and diffuser screens is estimated to be two inlet velocity heads or 4.8 psi.

The pressure vessel has an inside diameter of 56 in. and a wall thickness near 3½ in. Present proposals are for a stainless-steel-clad carbon steel construction, although the final vessel may be stainless steel. The pressure vessel is to be designed to withstand an internal pressure of 2000 psi, with a maximum stress of 15,000 psi including thermal stresses.

The core and reflector will contain 290 and 1200 liters of liquid, respectively. Approximately 650 lb of zirconium will be contained in the core tank, and the pressure vessel will weigh about 6 tons.

Pumps

The fuel solution in the HRT will be circulated by a Westinghouse model 400A canned rotor pump as shown by Fig. 15. This pump is a modification of the model 150C pump. The motor is the same as that of the model 150C, but the pump has been redesigned for a flow capacity of 400 gpm at a 100-ft head. Estimated performance curves are reported in Fig. 16.

The circulating pump for the reflector has not yet been specified.

Feed pumps are required for both the fuel and reflector systems; they probably will be the pulsafeeder type of pump.

Main Heat Exchanger

Calculations have been made[2] for the heat transfer surface area, number of tubes, length of tubes, holdup volume, and pressure drop through the tubes for the main heat exchanger for the HRT. Results of the calculations and the basic design

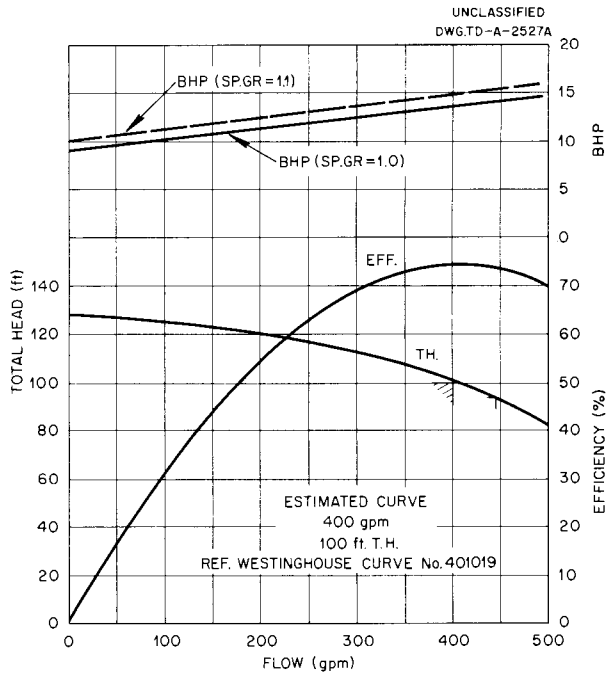

Fig. 16. Estimated Performance Curve for Westinghouse Model 400A Pump.

data are given in Table 3. The composition and properties of the fuel were changed to those reported in Table 2 after the design calculations were completed. Although the calculations will be repeated, no important changes in specifications are anticipated.

The initial design of the exchanger is shown in Fig. 17. It is similar to the exchanger used in the HRE, but enough larger that experience gained in its manufacture and operation should be applicable to the very large units required for power reactors.

Gas Separator

The gas separator for the core system is shown in Fig. 18. The design of the separator is similar to that which has been discussed in previous reports dealing with the ISHR. Fluid entering the separator is caused to rotate by the inlet vanes. The gas is centrifuged to the center and withdrawn through a nozzle at the exit end of the separator. Vanes are provided at the exit to recover some of the energy of rotation. In the present design of the HRT, gas removed in the separator will be vented to the

[2] C. L. Segaser, *Calculations for HRE No. 2 Heat Exchanger*, ORNL CF-53-12-94 (Dec. 16, 1953).

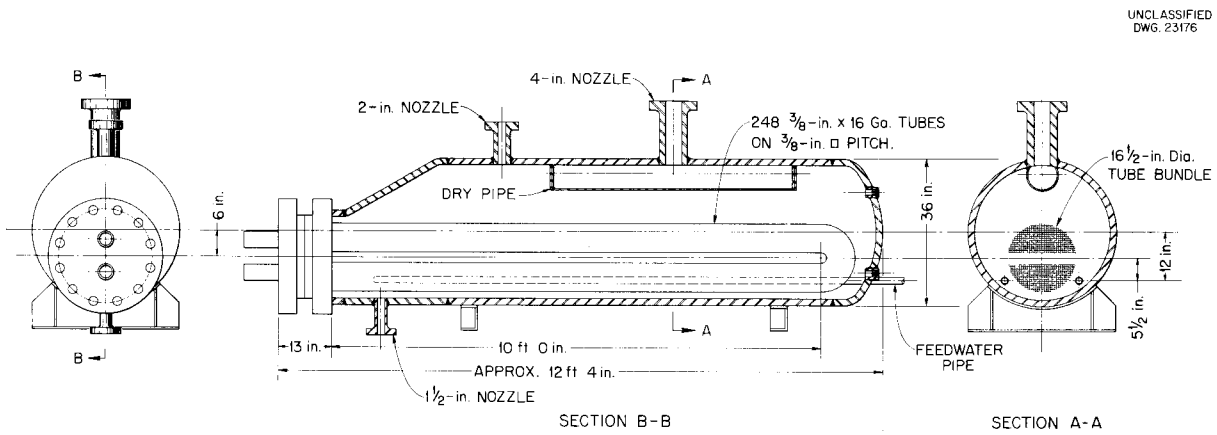

Fig. 17. Main Heat Exchanger.

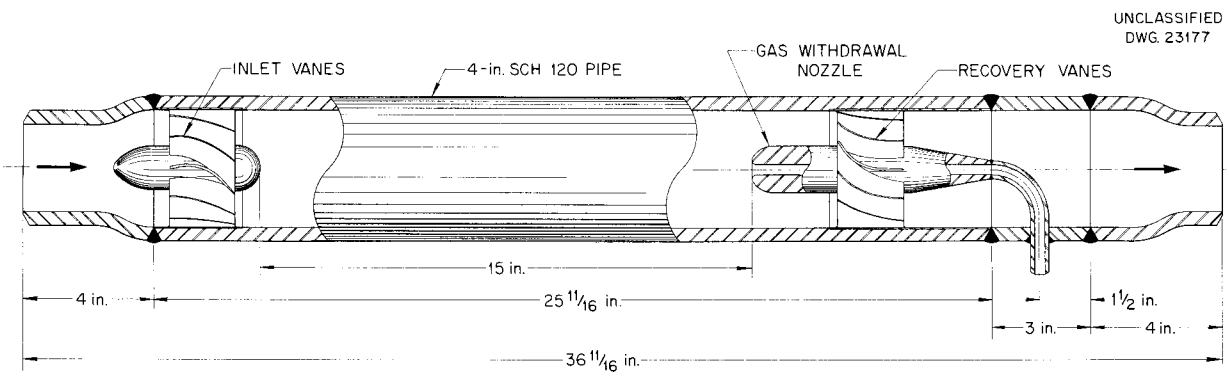

Fig. 18. HRT Gas Separator.

low-pressure system to be recombined. If, at some future time, high-pressure recombiner equipment is added to the system, a new separator will have to be provided.

Valves

One of the more important problems in ensuring continuous operation of the HRT is that of providing reliable valves. Studies are being made in cooperation with the instrument groups in order to improve upon the construction of valves used in the HRE. In general, all the valves are sealed with bellows which will be capable of withstanding a pressure of 2000 psi and are designed for easy assembly and repair. The initial effort is being directed toward the use of Stellite for both the seats and the poppets. The use of Stellite would require that the solution be cooled below 125°C before it is passed through the valve or that the valve be used infrequently. It is intended that the valves be designed with interchangeable seats and poppets so that other materials can be substituted for Stellite when their reliability has been established. Two of the recent designs are shown in Figs. 19 and 20.

Steam System

The steam system for the HRT will utilize as much of the HRE equipment as possible. By operating the present turbogenerator to exhaust near atmospheric pressure, 3000 kw of heat can be dissipated while 310 kw of electrical power is being produced. The total electrical capability is limited by the size of the generator. A condenser operated at a pressure near 150 psia will be installed in parallel with the turbogenerator to remove the remaining 2000 kw of heat.

TABLE 3. DESIGN DATA FOR MAIN HEAT EXCHANGER

Total heat transferred, kw	5000
Btu/hr	1.7×10^6
Fuel inlet pressure, psia	2000
Fuel inlet temperature, °C	300
°F	572
Fuel properties	
Uranium cancentration, g/liter	25
Solvent	H_2O
Density, lb/cu ft	49.8
Specific heat, Btu/lb/°F	1.19
Viscosity, lb/hr/ft	0.27
Thermal conductivity, Btu/hr/ft^2/°F/ft	0.35
Flow rate, gpm	400
lb/hr	163,000
Fuel exit temperature, °C	256
°F	493
Steam temperature, °F	471
Steam pressure, psia	520
Tube size: outside diameter, in.	3/8
wall thickness, in.	0.065
Number of tubes	250
Average length, ft	21
Heat transfer surface, sq ft	500
Liquid volume in tubes, liters	49
Fuel velocity, fps	11
Pressure drop, ft of fluid	33

AQUEOUS HOMOGENEOUS REACTORS FOR CENTRAL STATION POWER

Work on the study of large aqueous homogeneous reactors for producing central station power has been completed and will be published.[3] A summary of the thorium–U^{233} fueled reactors was presented in ORNL-1658.[4] A summary of that section of the report devoted to reactors fueled with uranium and plutonium is presented here.

Basis for Power Study

The basic power plant is one which will produce approximately 300 Mw of electricity. A study of uranium fuels and aqueous homogeneous reactor types resulted in the consideration of a two-region reactor with a solution of plutonium flowing through the core and a uranium oxide–plutonium oxide slurry in the blanket and of a one-region reactor with a uranium oxide–plutonium oxide slurry fuel. The two-region reactor is designed so that natural or depleted uranium is fed into the blanket, and the net production of plutonium in the blanket is sufficient to supply the plutonium requirements of the core. The important difference between the one- and two-region reactors, based upon the plutonium system, is that the two-region reactor utilizes natural or depleted uranium as a fuel, whereas the one-region reactor requires enriched fuel. Details of the reactor designs can be obtained from ORNL-1642[3] or ORNL-1658.[4]

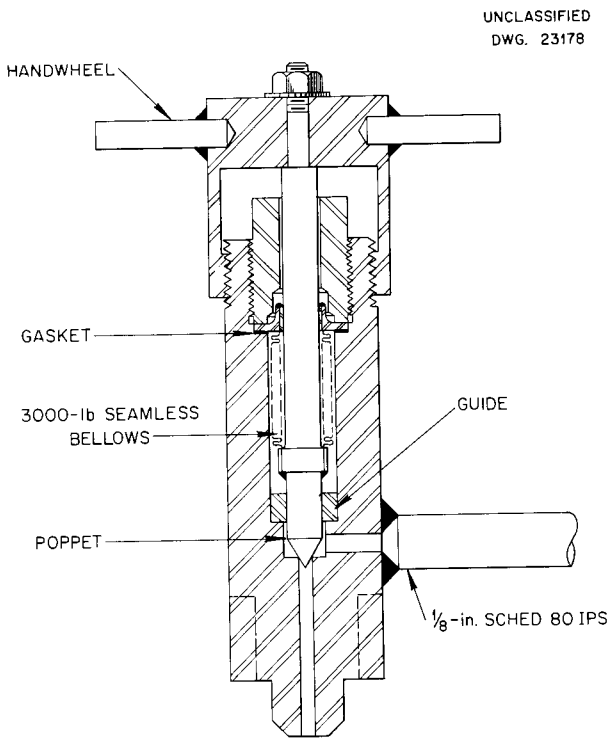

Fig. 19. Sample Valve.

Fuel Processing

Purex processing was assumed for both core and blanket of the two-region reactor and for fission product removal from the one-region reactor. A study of several Purex plant designs resulted in the following relationship between processing cost and plant capacity:

$$C = \$5000 + \$3.00\, W_U + \$3.50\, W'_U + \$1.00\, w_{Pu},$$

[3] R. B. Briggs *et al.*, *Aqueous Homogeneous Reactors for Producing Central Station Power*, ORNL-1642 (in press).

[4] R. B. Briggs *et al.*, *HRP Quar. Prog. Rep. Oct. 31, 1953*, ORNL-1658, p 21.

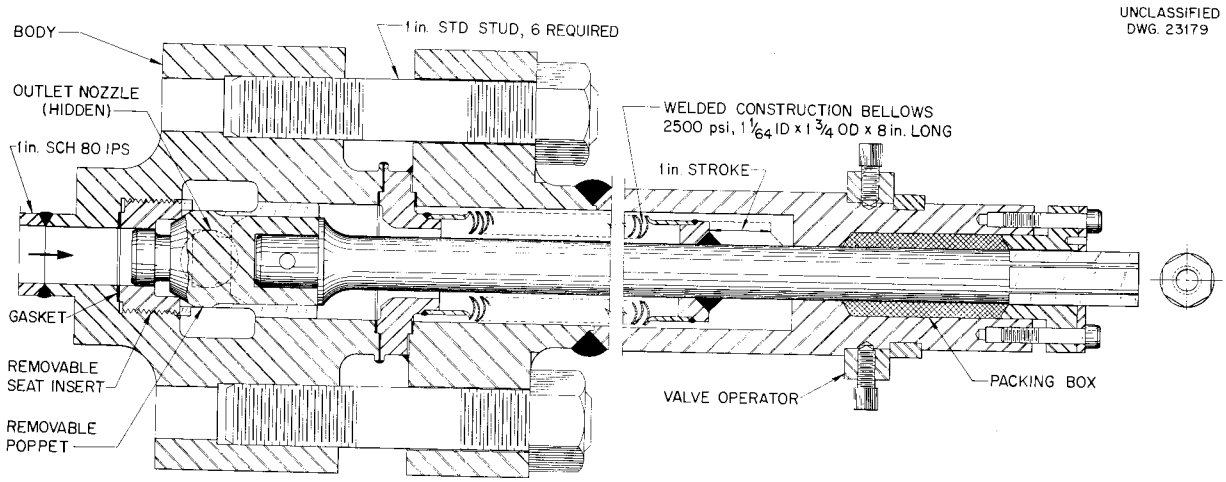

Fig. 20. Shut-Off Valve.

where C is the cost in dollars per day, W_U is the kilograms of uranium partially decontaminated per day, W'_U is the kilograms of uranium completely decontaminated per day, and w_{Pu} is the grams of plutonium decontaminated separately from the uranium per day. In the one-region reactor there was essentially no separate processing of plutonium and uranium, since the plutonium was recycled with the fuel back to the reactor. In the two-region reactor separation of a part of the plutonium from the blanket and removal of fission products from plutonium in the core were required. No continuous process similar to the calcium fluoride process has yet been suggested for removal of fission products from the core of a two-region, plutonium-fueled reactor. With both the one-region reactor and the two-region reactor, lowest fuel costs were obtained when some of the uranium was recycled through a diffusion plant for re-enriching.

Cost of Power

The components of the total cost of power are the fixed charges on the reactor plant, the operating and maintenance cost, and the cost of the fuel. The fixed charges on the reactor plant were based upon a 15% annual charge on the investment in the plant and a plant-operating factor of 0.8.

Operating costs were based upon similar costs for conventional power plants. Yearly maintenance costs were assumed to be $1\frac{1}{2}$% of the investment in the plant, which is equivalent to 10% of the fixed charges. The fuel costs include inventory and consumption charges on plutonium, uranium, D_2O, and the cost of chemical processing. Costs assumed in the analysis were \$20 per gram of fissionable material for plutonium, \$88 per kilogram for D_2O, and projected costs for uranium of the required U^{235} concentration.

Studies were made of the effect upon power costs of uranium concentration and enrichment, poison level, and reactor size. Minimum costs for one-region reactors were obtained with a 15-ft-dia reactor containing 180 to 200 g of slightly enriched uranium in D_2O and operating with a poison fraction of 0.07. Too few studies were made to determine an optimum two-region reactor. It appeared that minimum costs for a station producing about 300 Mw of electricity would be obtained by using a 15-ft-dia reactor with a core diameter of 7.2 ft, assuming that the specific power in the core is limited to 100 kw/liter. The blanket contained 300 to 500 g of partially depleted uranium per liter. A poison fraction of 0.07 was found to be near the optimum.

Fixed charges and operating and maintenance costs were the same as those obtained for thorium-fueled reactors. Fuel costs for the uranium-plutonium systems were higher by about 1 mill/kwhr than those reported for thorium fuels. This resulted largely from uncertainties in values for η for Pu^{239} and Pu^{241}. The values used in this study were $\eta_{49} = 1.75$ and $\eta_{41} = 1.9$. If the higher values $\eta_{49} = 1.9$ and $\eta_{41} = 2.4$ had been used, the cost difference would have been less than 0.5 mill/kwhr.

Typical operating and cost data are presented in Tables 4 and 5.

TABLE 4. OPERATING AND COST DATA FOR PLUTONIUM-FUELED REACTOR STATIONS

	TWO-REGION REACTORS		ONE-REGION REACTORS	
Reactar operating temperature, °C	250	300	250	300
Reactor pressure, psia	1000	2000	1000	2000
Number of reactors per station	1	1	1	1
Reactor diameter, ft	15	15	15	15
Core diameter, ft	7.2	7.2		
Total heat output, Mw	1350	1350	1350	1350
Heat produced in core, Mw	550	550		
Uranium concentration, g/liter	500	450	200	180
Ratio of U^{235} atoms to U^{238} atoms	0.0045	0.0045	0.0083	0.0109
Ratio of plutonium atoms to U^{238} atoms	0.0022	0.0018	0.016	0.019
Plutonium concentration in core, g/liter	~1.5	~1.5		
Poison fraction	0.07	0.07	0.07	0.07
Total plutonium inventory, kg	220	250	390	520
Total uranium inventory, metric tons	90	90	44	41
D_2O inventory, metric tons	130	130	153	153
Steam pressure, psia	215	560	215	560
Steam temperature, °F	388	478	388	478
Gross efficiency of turbogenerator plant	0.264	0.307	0.264	0.307
Gross electrical capability, Mw	356	415	356	415
Net station efficiency	0.234	0.274	0.234	0.274
Net electrical capability, Mw	316	370	316	370
Reactor plant cost: millions of dollars	16	19	15	18
$/kw net capability	50	51	48	49
Power plant cost: millions of dollars	44	48	44	48
$/kw gross capability	123	116	123	116
$/kw net capability	139	130	139	130
Total plant cost: millions of dollars	60	67	59	66
$/kw net capability	189	181	187	179

TABLE 5. COST OF POWER FROM PLUTONIUM-FUELED REACTORS

	TWO-REGION REACTORS		ONE-REGION REACTORS	
Reactor temperature, °C	250	300	250	300
Fixed charges, mill/kwhr	4.1	3.9	4.1	3.9
Operating and maintenance, mill/kwhr	0.8	0.7	0.8	0.7
Fuel cost, mill/kwhr				
Asymptotic chemical processing	0.4	0.3	0.1	0.1
Fissile and fertile materials: consumption	1.0*	0.9*	1.4*	1.4*
inventory	0.3	0.3	0.3	0.3
D_2O inventory and losses	1.0	0.9	1.0	0.9
Total fuel cost, mill/kwhr				
Without fixed chemical processing charge	2.7	2.4	2.8	2.7
With fixed chemical processing charge	3.4	3.0	3.5	3.3
Total cost, mill/kwhr				
Without fixed chemical processing charge	7.6	7.0	7.7	7.3
With fixed chemical processing charge	8.3	7.6	8.4	7.9

*Values are based upon $\eta_{41} = 1.9$. If $\eta_{41} = 2.4$ they are reduced by 1/3 to 1/2, with corresponding decreases in total costs.

ENGINEERING DEVELOPMENT

C. B. Graham, Section Chief

CORE AND GAS SEPARATOR DEVELOPMENT

R. Goodman L. B. Lesem
J. A. Hafford I. Spiewak

Alternate HRT Core

The straight-through core using screens in the inlet diffuser has been discussed in previous quarterly reports.[1,2] This type of design is also feasible for the HRT.

An alternate core model has been tested and found to be satisfactory[3] for copper-catalyzed systems. A sketch of this core, which has concentric inlet and outlet pipes, is shown in Fig. 21.

[1]C. B. Graham *et al.*, *HRP Quar. Prog. Rep. Jan. 1, 1953*, ORNL-1478, p 45-46.

[2]C. B. Graham *et al.*, *HRP Quar. Prog. Rep. Oct. 31, 1953*, ORNL-1658, p 32-35.

[3]L. B. Lesem and I. Spiewak, *Alternate Core Proposal for the HRT*, ORNL CF-54-1-80 (Jan. 19, 1954).

UNCLASSIFIED
DWG. 22786A

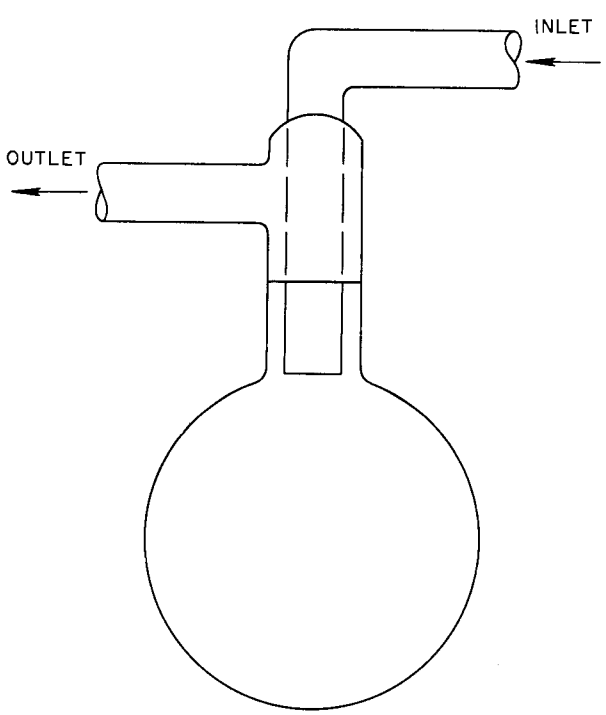

Fig. 21. Alternate Core Model.

In comparison to the straight-through core design, the alternate core has some structural advantages which make it easier to design and fabricate. The bellows expansion joint, which is necessary to allow for thermal expansion in the straight-through design, is eliminated. The inlet pipe is not joined to the core; so only one major zirconium-to-stainless-steel joint is necessary. The reactor core would require a small dump line at the south pole and another small bimetallic joint in that line. No conical section or baffles of any sort are required to realize a satisfactory flow distribution; hence, fabrication of the core vessel is simplified and parasitic neutron capture is decreased somewhat.

Flow tests indicate that the alternate core is highly turbulent and well mixed. The temperature distribution in a core of this configuration would consist of a cool region in the entering jet with the remainder of the sphere at essentially outlet temperature.

The key factor in deciding whether this type of core is feasible is gas holdup. If it is assumed that an internal copper catalyst is not used, gas production in the HRT is estimated at 2.27 cfm (5 Mw, 2000 psi, 300°C). This amounts to 4.2% of the liquid flow volume and would also be the void percentage in the core. In the straight-through core, the corresponding void percentage would be below 2% for upward flow. Nuclear instabilities resulting from gas would be much more pronounced in a well-mixed core. On the other hand, with an internal copper catalyst gas bubbles are no longer considered to be a problem. Operation with a well-mixed core essentially at 300°C may allow the copper concentration to be reduced considerably from that required for the straight-through reactor.

The comparatively high gas holdup of the alternate core is a disadvantage in the HRT unless internal recombination by means of copper is used.

Gas Separators

The proposed intermediate-scale gas separator serves to remove the reactor gases and also to provide a pressurizer for the system. A full-scale experimental model of the separator operating at

low temperature and pressure has been built and has undergone initial testing with water. A diagram of the experimental separator is shown in Fig. 22, and Fig. 23 is a preassembly photograph of the parts.

In testing, 400 cfm of air was introduced into the central void of the separator, thus simulating the diluent gas of the reactor system. In addition, a small amount of gas was introduced into the liquid stream ahead of the inlet elbow.

The initial tests revealed that a cylindrical void about 6 in. in diameter extends from the gas inlet to the gas takeoff. Gas bubbles in the entering liquid are all centrifuged into the center. When the unit is operated properly, all the gas and some entrained liquid leave via the gas takeoff.

Instabilities were noted in the experimental system, and these promote the bypassing of gas around the takeoff nozzle. It is believed that the long-radius elbow preceding the rotation vanes disturbs the flow pattern so that the void is not so smooth in appearance as the voids observed in smaller models. Also, the gas-discharge system was too restricted.

A vaned elbow will be substituted for the present elbow and greater flow area will also be provided around the island.

The model was operated at flow rates varying from 4600 to 5900 gpm. The pressure drop observed at the rated 5000 gpm is about 2.5 psi. The recovery vanes performed very well. Although not yet evaluated, their efficiency is believed to be about 75%.

HIGH-PRESSURE CATALYTIC RECOMBINER TEST

I. Spiewak R. H. Wilson

Future designs of large-scale homogeneous reactors may include a high-pressure catalytic recombiner for burning the radiolytic gas formed in the core. This unit would be used during startup or at any other time during operation at low fuel temperature.

In order to obtain operating experience on a high-pressure recombiner, a small test loop is under construction. This system will operate at pressures from 1000 to 2000 psi and with a flow rate of hydrogen and oxygen of 1.0 standard scfm and has been described in a previous quarterly report.[2]

Of particular interest are the electrolytic cells which have been designed to produce stoichiometric gas for the small test loop. One of the two cells in the system is illustrated in Fig. 24. The hydrogen, produced at the central cathode, is allowed to mix with the oxygen coming off at the anode. There are no moving parts in contact with the explosive gas at any time; so the danger of an explosion is considered to be remote. However, the cells are designed for 2000 psi rating, and rupture disks are provided to prevent damage from overpressure. The design temperature is 70°C.

Other features of the cell are fluorothene gaskets and insulators and nickel-plated electrodes to protect the metal from the concentrated caustic electrolyte.

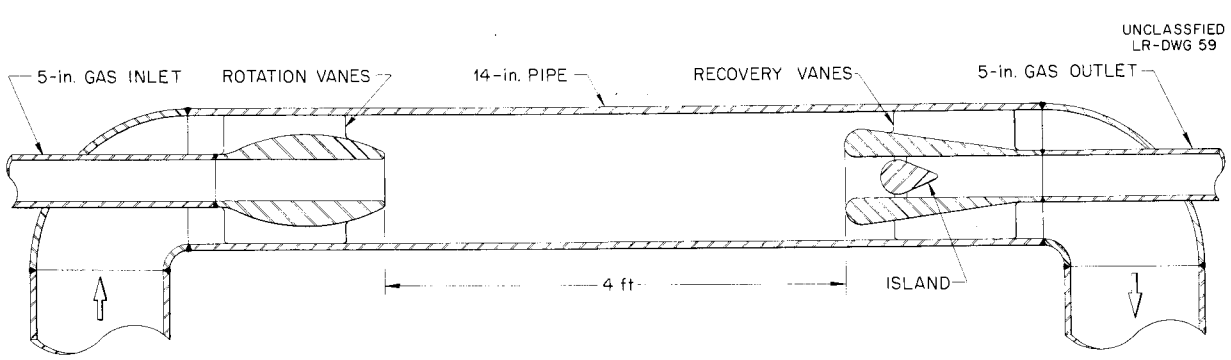

Fig. 22. Schematic Diagram of Experimental Gas Separator.

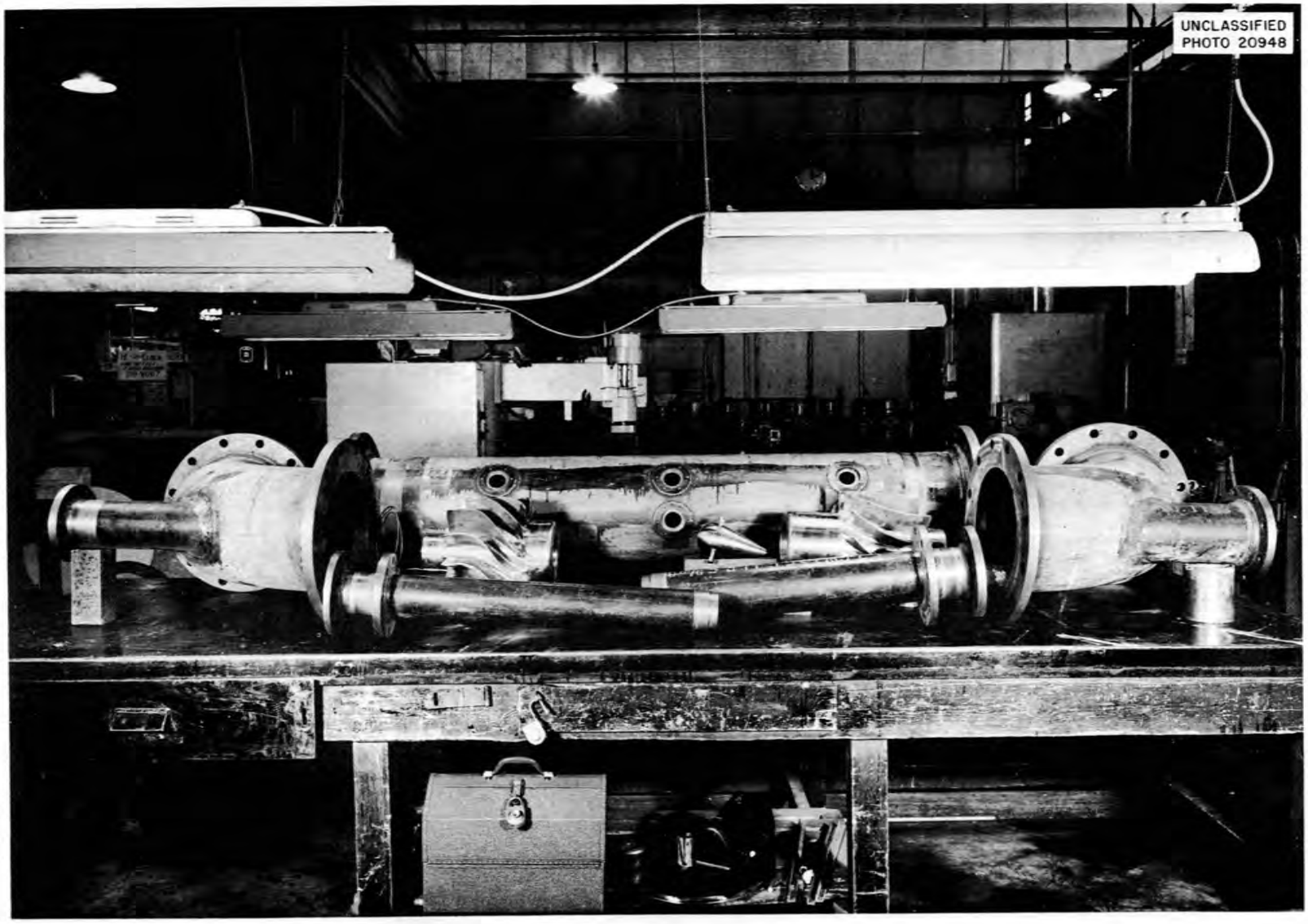

Fig. 23. Preassembly Photograph of Experimental Gas Separator.

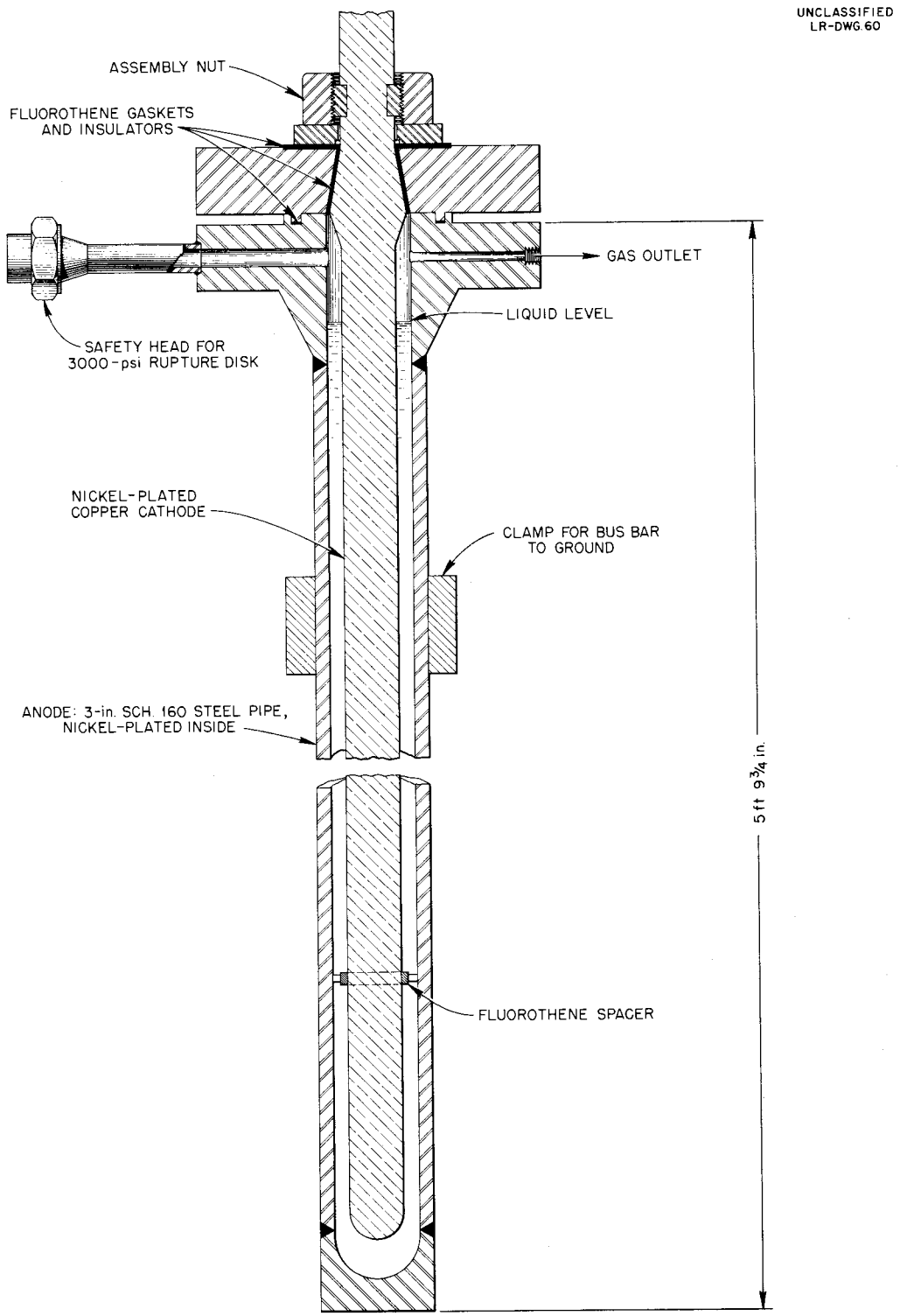

Fig. 24. Electrolytic Cell.

TEST OF THORIA PELLETS IN FLUIDIZED BED

R. Goodman J. A. Hafford
I. Spiewak

A number of types of ceramic, pressed, cylindrical, $\frac{1}{8}$-in. pellets that were obtained from the American Lava Company are being tested for abrasion against each other and against samples of brass, stainless steel, and zirconium by fluidizing with water.

The pellets showed a fairly high initial rate of wear, averaging about 15% weight loss in the first week of operation. Most of the abrasion appeared to be at the corners of the cylinders, which were worn smooth. The thoria dust which was produced was extremely fine.

Abrasion of the metal samples in the first week was: brass, 6 mpy; stainless steel, 0.2 to 1.5 mpy; and Zircalloy-II, 1 to 5 mpy. These tests are being continued in order to determine whether the initial rates will continue.

LARGE REACTOR COMPONENTS

L. F. Goode W. L. Ross

Preliminary discussions of contracts for the following components have been held and contracts are expected to materialize very shortly. The extension of time schedules has not significantly affected the proposals received from prospective manufacturers.

Main Fuel and Gas Condenser Heat Exchangers

The development and the predesign of two major heat exchangers are under way. The first, similar to one discussed previously,[4] is to be a single-drum, horizontal U-tube, 50-Mw exchanger which will generate steam at 560 psia with a tube pressure of 2000 psia. The second exchanger will be a gas cooler-condenser similar to the condenser proposed previously.[5] Tube operating pressure in this unit has also been raised to 2000 psia. The capacity will be about $3\frac{1}{2}$ Mw, and it will generate steam under the same conditions as those of the main heat exchanger. Several small test models of these exchangers will be made by the contractor as the developmental work progresses in order that materials, welds, and construction techniques may be thoroughly tested. This testing will include corrosion studies.

Heat Exchanger Development

A tube-screening test has been started for comparing the corrosion stability of type 347 seamless stainless steel tubing, type 304L welded tubing, and type 347 welded tubing. Sample tubes from various manufacturers are being used and significant results will be reported. It is planned that future corrosion tests on heat exchanger components will include welded-joint tests, tube entrance- and exit-flow characteristic tests, and tests on combination rolled and welded tube joints.

Automatic Tube-Joint Welding

An automatic, heliarc, tube-joint welding machine is being made by ORNL. Linde Air Products Company designed the machine and furnished assembly drawings. Completion is expected in March 1954, and tests on automatically welded joints will begin immediately thereafter. Primary interest will be on tubes $\frac{3}{8}$-in. OD by 16 and 18 BWG. Emphasis will be placed on the attainment of sound welds which can be readily duplicated under actual fabrication conditions for a large heat exchanger.

Worthington Corporation Pump Development

A 20,000-gpm centrifugal pump proposed by the Worthington Corporation has been described[6,7] and a development contract has been active for approximately two years. Some of the early difficulties encountered with the bearing testing equipment have been overcome, and more than 600 hr of successful operation has been attained. Bearings have been operated at loads of 50 and 100 lb per square inch of projected bearing area. Journal and bearing combinations that have been employed are: Stellite 1 vs Graphitar 14, Stellite 1 vs Stellite 6, and Stellite 3 vs Stellite 6 (the last named is the bearing material in each case).

Two failures have occurred because of seizure of the journals after short periods of operation.

[4] C. B. Graham *et al.*, *HRP Quar. Prog. Rep. July 31, 1953*, ORNL-1605, p 58 and Fig. 16.

[5] R. B. Briggs *et al.*, *HRP Quar. Prog. Rep. July 31, 1953*, ORNL-1605 p 42 and Fig. 20.

[6] C. B. Graham *et al.*, *HRP Quar. Prog. Rep. July 1, 1952*, ORNL-1318, p 112.

[7] C. B. Graham *et al.*, *HRP Quar. Prog. Rep. Oct. 1, 1952*, ORNL-1424, p 65.

In each case the clearance between the journal and the bearing was considerably smaller than that specified in the design. As the damage was slight, the bearings were rebored to the approximate design clearance and successful runs were attained.

SMALL REACTOR COMPONENTS

W. L. Ross

Contracts covering the design, finalizing of specifications, and the submission of a proposal to fabricate and test the following components have been negotiated with one manufacturer and proposals have been requested of a second manufacturer. If the proposals are satisfactory, the contractors will fabricate components and conduct short performance tests with each pump and loop prior to shipment to Oak Ridge, provided trouble-free, satisfactory operation has been attained.

Small Gas Circulators for Recombiner Systems

It is planned to develop a gas circulator of about 20-cfm capacity which will aid in the development of the large gas circulator and other necessary components of a high-pressure, catalytic recombiner system and which will provide equipment which may be used in future homogeneous reactors in the size range of about 5 Mw.

Model 150C and 400A Westinghouse Pumps

Models 150C and 400A pumps have been on order for some time; delivery is expected in early summer of this year. Westinghouse has been requested to make proposals for the design and fabrication of two test loops for 150C pumps and two test loops for 400A pumps.

500-gpm Fuel Circulating Pump

Preliminary specifications have been developed for a 500-gpm fuel circulating pump, similar to a 5000-gpm fuel circulating pump, which will aid in the development of a larger pump. The 500-gpm pump will provide an alternate circulating pump for future reactors.

Status of the 4000-gpm Loop

J. S. Culver

Construction of the loop is essentially complete, as can be seen in Fig. 25. All instrumentation and the pump electrical supply are complete and have been checked out. Several weeks will be required for pressure testing and component testing before actual operation can begin. The loop will then be given an initial shakedown run on water, gradually working up to 1000-psi, 250°C operation.

A complete record of all welds in the main loop, including x rays, has been kept. Some welds on 6-, 8-, and 10-in. pipe have been made entirely by the heliarc method, and welding-time records have been kept. All other welds consist of three heliarc root passes followed by coated-rod welding.

Although the initial root pass must give full penetration and no bleed-through, there is a small ring of metal pushed through as subsequent passes are put in. Most welds have 180 deg of this ring ($\frac{1}{32}$ to $\frac{1}{16}$ in. high) ground out so that corrosion and errosion effects under both conditions can be compared.

HRE-Type Pulsafeeder as a Slurry Pump

J. M. Baker R. Meza
J. S. Culver

The pulsafeeder pump loop previously set up to pump UO_3 slurry[8] is being used for exploratory tests with thoria slurry. After an initial shakedown run on water, sufficient thorium oxide was added to give a concentration of 500 g per liter, and the pump successfully pumped this slurry for an accumulated 63 hr. Since the system cannot be run continuously without attention, it was shut down each evening and restarted in the morning. After settling overnight it took 10 min of pumping to re-establish full flow rate. A priming tank was added which reduced startup time. This was accomplished by holding up 1 or 2 liters in a vessel 4 ft above the diaphragm head in the suction line. The pump would start immediately when the valve was opened to allow the undispersed material and water to flow into the pump.

At atmospheric pressure the pump delivered 0.846 gpm and at 1000 psi 0.548 gpm. Both tests were made at room temperature.

When additional operating time has been accumulated, the pump will be dismantled and examined for signs of wear.

[8] C. D. Zerby, *HRP Quar. Prog. Rep. Jan. 1, 1953*, ORNL-1478, p 59.

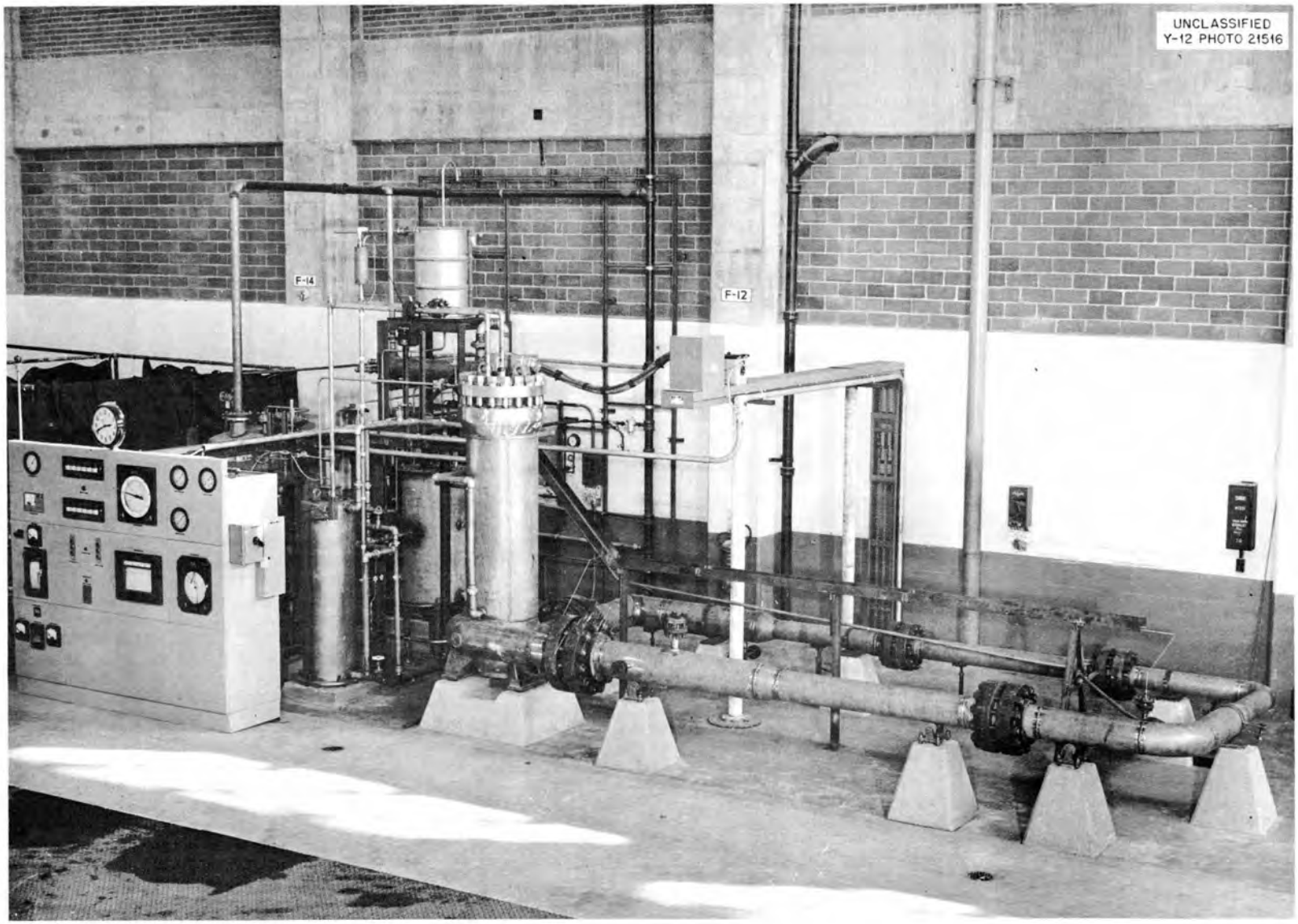

Fig. 25. 4000-gpm Loop.

REACTOR ANALYSIS

M. C. Edlund, Section Chief
H. C. Claiborne P. R. Kasten
T. B. Fowler L. C. Noderer
M. Tobias

CRITICALITY CALCULATIONS FOR HRT

Critical conditions for the proposed HRT have been calculated for several mixtures of H_2O and D_2O moderator in the core and for three blankets, heavy water, ThO_2 slurries, and low-enrichment uranyl sulfate solutions.

As was pointed out by G. M. Safonov,[1] the critical concentration of fuel for a reactor of given size may be less for a mixture of light and heavy water than for either moderator alone if the critical fuel concentration lies within a limited range. At an average moderator temperature of 300°C this range is from about 10 to 25 g of uranium per kilogram of moderator for highly enriched fuel (Fig. 26).

Mixed H_2O-D_2O Moderator

Initially, interest was expressed in a reactor with a 24-in. core diameter, a ¼-in. zirconium alloy core tank, and a 12-in. heavy-water reflector. Calculations for this configuration were made for various H_2O-D_2O mixtures by use of the usual two-group method.[2] The fast-group constants were obtained by matching fast nonleakage probabilities for the equivalent bare reactors to Safonov's bare reactor calculations.

A comparison of Safonov's calculations for the two limiting cases of pure H_2O moderator with the experimental data of Beck *et al.*[3] and of pure D_2O with calculations in which the Gaussian-Yukawa kernel of Friedman and Wattenburg[4] was used shows excellent agreement (Fig. 27). For these reasons it is felt that the results given in Safonov's report[1] can be used as a basis for obtaining the fast-group constants for mixtures of H_2O and D_2O.

The minimum critical concentration occurs for a volume fraction of H_2O in the H_2O-D_2O mixture of about 55% and is about 19% lower than the critical concentration for pure H_2O moderator (Fig. 28). In this particular case the reactor was not critical as a thermal reactor with pure D_2O moderator.

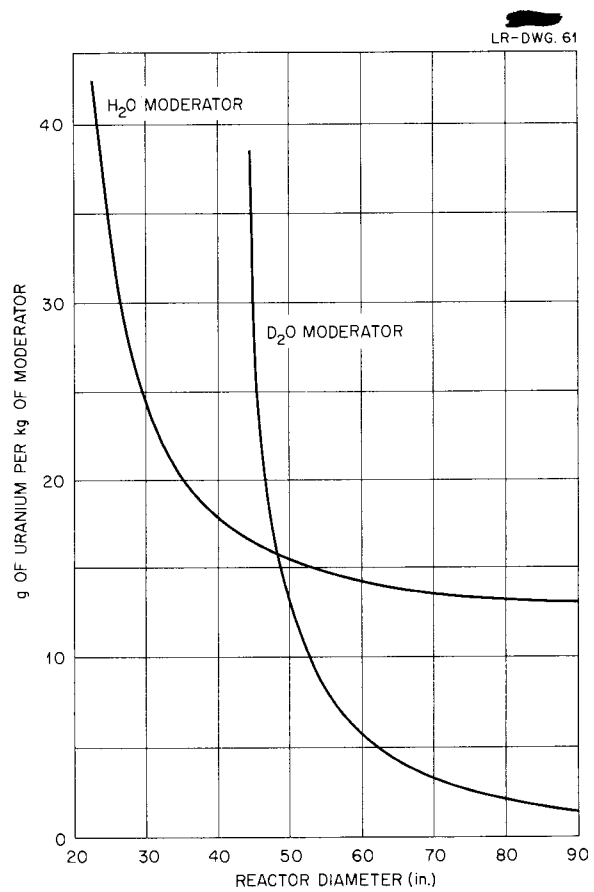

Fig. 26. Critical Concentration of Bare Spherical Reactors vs Diameter at 300°C.

[1] G. M. Safonov, *A Study of Homogeneous H_2O, D_2O, U-235 Reactors with a Note on Optimum Moderating Mixtures for a Minimum U^{235} Requirement*, RM-842 (May 1, 1952).

[2] M. Tobias, *Critical Mass Calculations for a Proposed Rebuilt HRE*, ORNL CF-54-1-45 (Jan. 4, 1954).

[3] C. K. Beck, A. D. Callihan, J. W. Morfitt, and R. L. Murray, *Critical Mass Studies, Part III*, K-343 (April 19, 1949).

[4] F. L. Friedman and A. Wattenburg, *Age of Fission Neutrons in D_2O*, CP-3453 (May 1945).

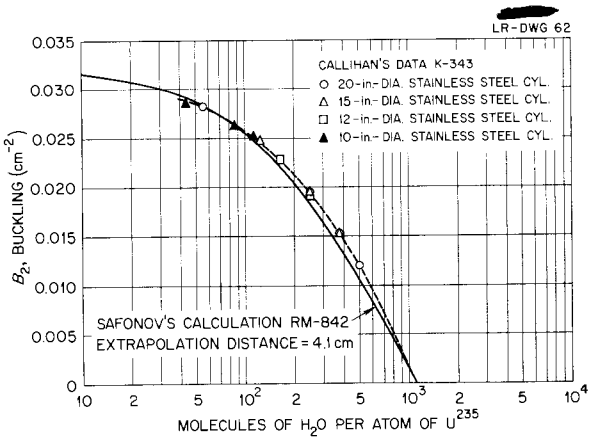

Fig. 27. Buckling for H_2O-U^{235} Reactors at 20°C.

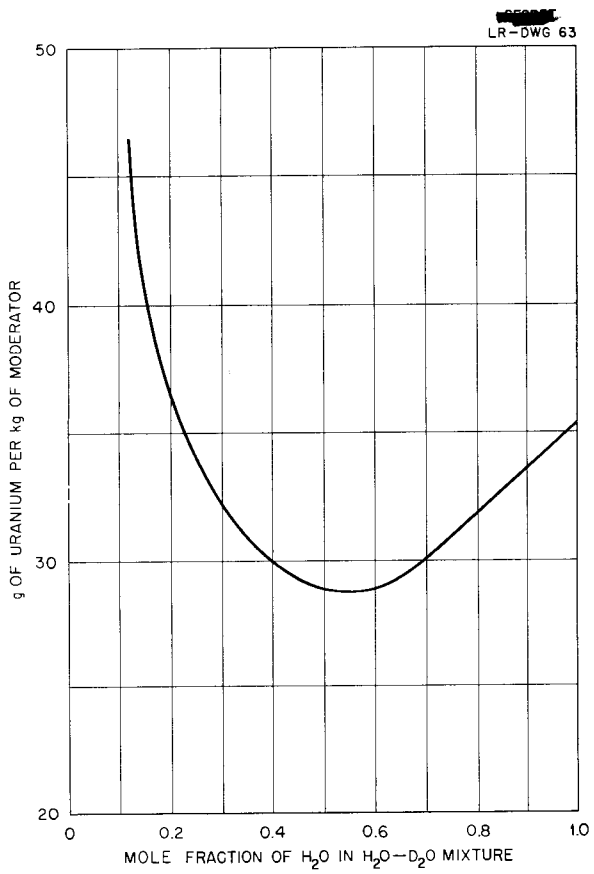

Fig. 28. Critical Concentration as a Function of Mole Fraction of H_2O in a D_2O-H_2O Moderator Mixture. Reactor temperature, 300°C; core diameter, 2 ft; D_2O reflector thickness, 1 ft; core tank, ¼-in. Zr; enrichment of fuel, 93.5% U^{235}; core voids, 3%.

Small D_2O Reactors

Due to velocity effects on corrosion, interest was shifted to lower fuel concentrations than those estimated for the 2-ft core. At lower uranium concentrations (larger reactors) no advantage accrues from the mixing of H_2O with D_2O, and hence pure D_2O moderator was selected. The core diameter was increased to 32 in., bringing the critical fuel concentration down to about 10 g of uranium per kilogram of D_2O with a 12-in. D_2O reflector.

Results of calculations made for ThO_2 slurry and low-enrichment uranyl sulfate solution blankets are given in Fig. 29. The ratio of blanket fissions to core fissions for the case of the natural uranium blanket (300 g of uranium per liter) increases almost linearly with blanket thickness. It increases from 0.2 for a 12-in. blanket to 0.9 for a 24-in. blanket. The conversion ratio (Pu produced per atom of U^{235} destroyed in the core) for the natural

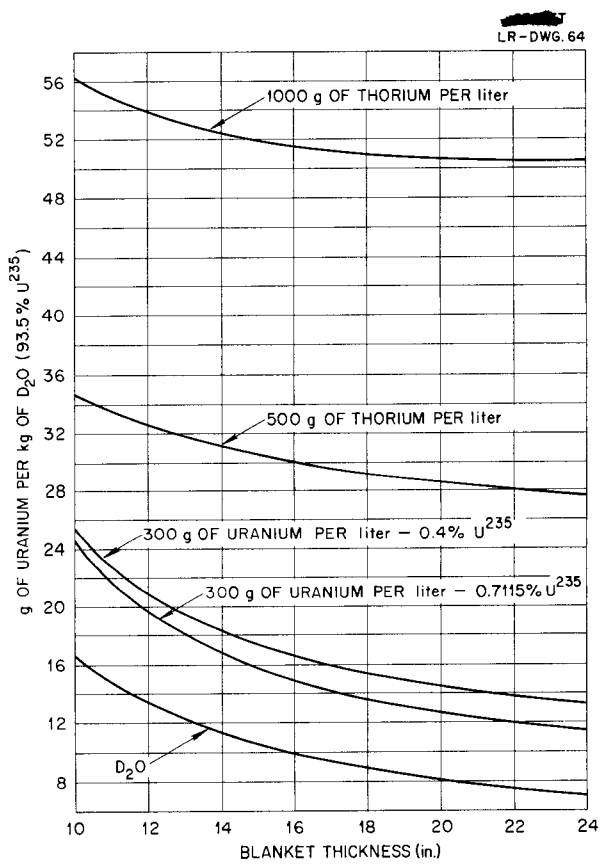

Fig. 29. Critical Concentration vs Blanket Thickness. Core diameter, 32 in.; core tank, ¼-in. Zr; moderator, D_2O; temperature, 280°C.

uranium blanket increases from 0.36 for the 12-in. blanket to 1.06 for the 24-in. blanket.

As a preliminary step to making calculations for the HRT, the general problem of calculating small D_2O moderated and reflected reactors was studied. For small reactors, the critical mass depends strongly on the shape of the assumed slowing-down kernel. The only experimental information[4] which is available indicates that the best slowing-down kernel for D_2O is a convolution of a Gaussian-Yukawa kernel.

The harmonics method[5] for solving the reactor equation which is applicable when the slowing-down properties of the core and reflector are the same was investigated and found to give rapid convergence for the core and reflector dimensions of interest. A comparison of the results for Gaussian, Gaussian-Yukawa, and Yukawa kernels is given in Fig. 30. The core radius is 39 cm in all cases; the age of the thermal neutrons is 237 cm^2, which is based on 120 cm^2 for D_2O at 20°C corrected for density change to 300°C. For the Gaussian-Yukawa kernel the "age" parameters are 95 and 142 cm^2, the larger value referring to the Gaussian part of the kernel. The parameter z is the ratio of the fuel absorption to moderator absorption.

To check the convergence, two-group calculations were made and compared with the results of the harmonics method for the Yukawa kernel. The critical z obtained from retaining the leading 4×4 subdeterminant of the infinite-order critical determinant gives excellent agreement with the closed form solution. In fact, the results obtained from the 2×2 subdeterminant yielded results which were in error by less than 4% in z over the entire range of reflector thickness considered.

The harmonics method has been extended to take into account multiplication in the blanket and resonance capture. The $i - j$ element of the critical determinant is

$$M_{ij} = \left(DB_i^2 + \Sigma_{aB}\right)\delta_{ij} + \left(\Sigma_{aC} - \Sigma_{aB}\right)\lambda_{ij} - \sum_k \bar{P}\left(B_k^2\right)\left[\left(p_C - p_B\right)\lambda_{ik} + p_B\,\delta_{ik}\right]\left[\left(\frac{k_C}{p_C}\Sigma_{aC} - \frac{k_B}{p_B}\Sigma_{aB}\right)\lambda_{kj} + \frac{k_B}{p_B}\Sigma_{aB}\,\delta_{ij}\right],$$

where

D = diffusion coefficient for thermal neutrons,

Σ_{aC} = thermal macroscopic absorption cross section in core,

Σ_{aB} = thermal macroscopic absorption cross section in blanket,

k_C = multiplication constant in core,

k_B = multiplication constant in blanket,

p_C = resonance escape probability in core,

p_B = resonance escape probability in blanket,

$\bar{P}(B_k^2)$ = Fourier transformation of slowing-down kernel,

B_k^2 = buckling for the kth mode,

$$\lambda_{ij} = \frac{\sin\left(i - j\right)\frac{\pi a}{b}}{\pi(i - j)} - \frac{\sin\left(i + j\right)\frac{\pi a}{b}}{\pi(i + j)}$$

(for spherical geometry),

a = core radius,

b = outer radius of reflector.

Convergence of the extended harmonics method is still under investigation. The reliability of the results of the calculations for the thorium and uranium blankets has not yet been established so well as have the results for the D_2O reflector.

WATER BOILER KINETICS EXPERIMENT

Some preliminary results on the rate of formation of decomposition gases have been obtained from the water boiler experiment[6] conducted last August. Immediately following an addition of reactivity there is a decrease in reactivity, primarily due to the formation of decomposition gases, since at least 10% of the decomposition products of water appear in the vapor phase within 0.1 sec. In all cases the measured rate of reactivity decrease immediately after the addition of reactivity

[5] A. M. Weinberg and L. C. Noderer, *Theory of Neutron Chain Reactions, Vol. II, Part I, Homogeneous Nuclear Chain Reactions*, ORNL CF-51-9-58, p VII-57 (Aug. 10, 1951).

[6] R. N. Lyon *et al.*, *HRP Quar. Prog. Rep. July 31, 1953*, ORNL-1605, p 19; *HRP Quar. Prog. Rep. Oct. 31, 1953*, ORNL-1658, p 14.

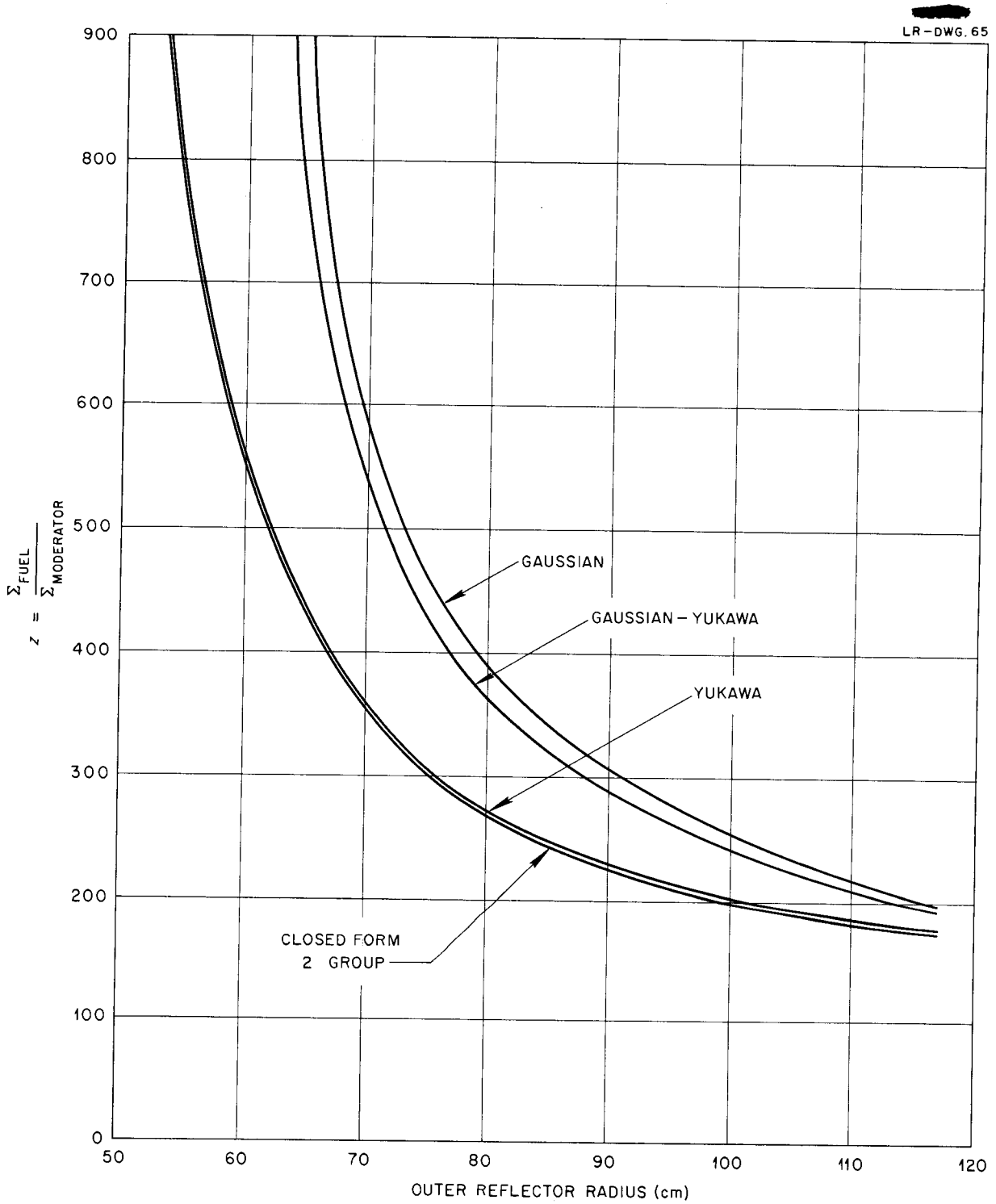

Fig. 30. Comparison of Critical Fuel-to-Moderator Absorption Ratios for Three Slowing-Down Kernels in D_2O at 300°C. Core radius, 39 cm.

by withdrawal of the absorber rod was greater than five times that which can be attributed to the core-temperature rise. As the gas bubbles leave the core, reactivity effects which result from the increase in core temperature become relatively more important.

A portion of the data obtained during a typical experimental run is given in Fig. 31 in which reactor power and poison-rod position are shown as a function of time. The initial power was 10 kw and the initial core temperature was 54°C. The calculated results are given in Fig. 32 in which the reactivity decrease and the rate of reactivity decrease are given as a function of the excess energy injected into the reactor during a run (excess energy being defined as the time integral of the difference between the power and the initial power). Reactivity is measured in terms of m, the excess grams of U^{235} added to the core which give the corresponding reactivities. (Instantaneous addition of 26 g of U^{235} is equivalent to a Δk_{eff} of 0.0085.) The change in m with excess energy input is written as $\Delta m/\Delta kw$-sec, which is the rate of reactivity decrease.

From the known steady-state rates of formation of gases within the water boiler, the maximum reactivity effect due to gas formation was calculated. In the above runs, the observed rate of reactivity decrease was below the maximum rate obtained by assuming immediate formation of gas saturated with water vapor, except for one run. The data reveal no trend in initial rate of reactivity decrease with core temperature or power level.

The remaining experimental runs, including those in which the reactor fluid was initially in a boiling state, are now being analyzed.

[redacted]
DWG. 22826A

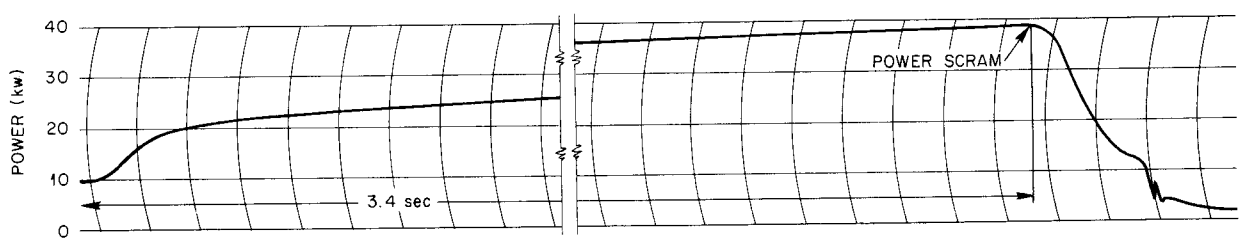

Fig. 31. Reactor Power vs Time. T_0 = 54°C; P_0 = 10 kw.

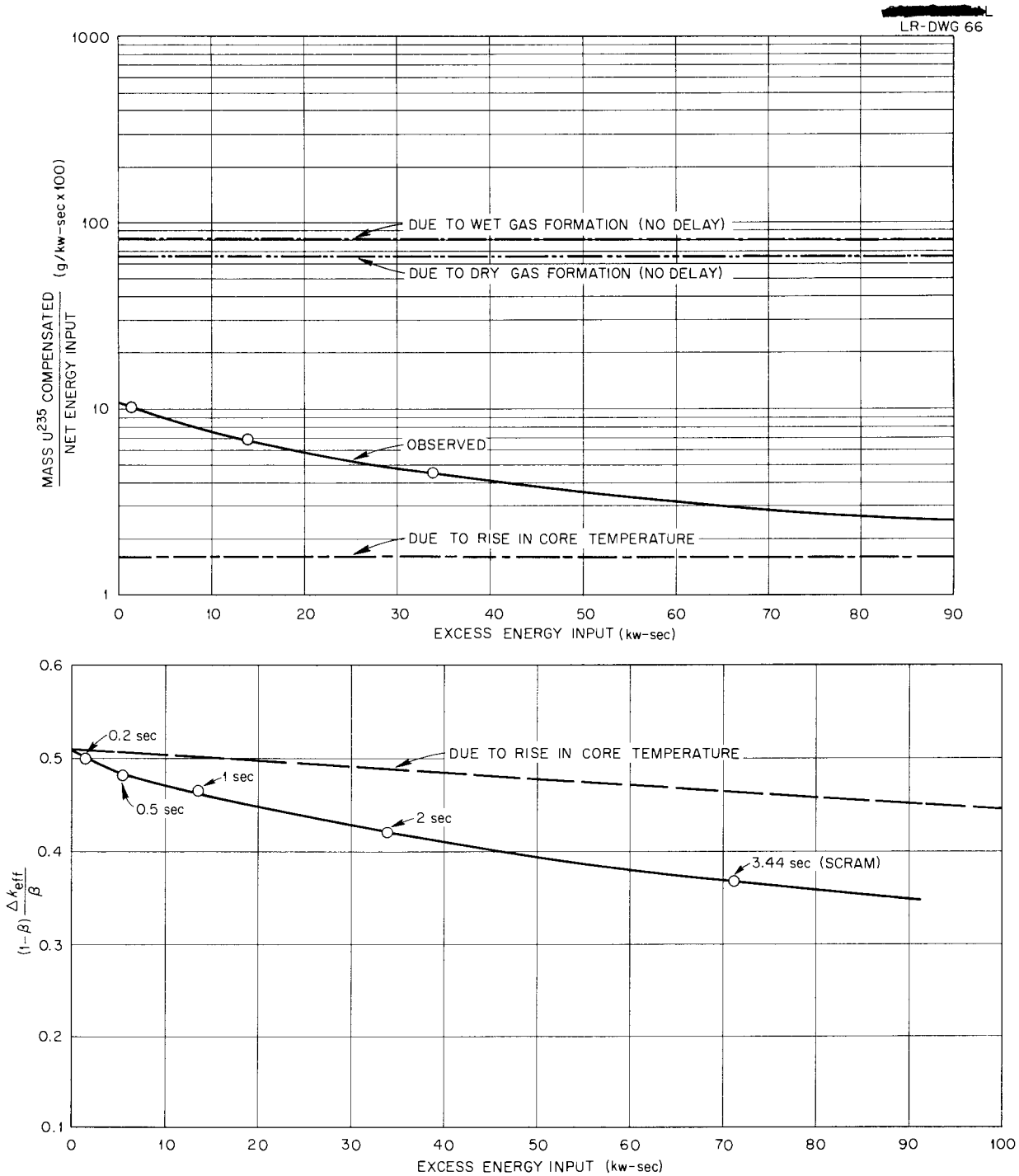

Fig. 32. Reactivity Decrease and Rate of Reactivity Decrease vs Excess Energy Generated in Core During Experimental Run.

CONTROLS AND INSTRUMENTATION

J. N. Baird, Jr.
A. M. Billings
D. G. Davis
R. L. Moore
J. L. Redford
D. S. Toomb
W. P. Walker

IN-PILE CORROSION-LOOP EXPERIMENTS

Instrumentation for the development loop has been operating quite satisfactorily for the past three months and has provided almost perfect control. A difference of several degrees has been observed between the pressurizer temperature and the temperature equivalent to the measured pressurizer steam pressure when the system is operated with water. This difference has been constant for a number of runs and appears to be a summation of the tolerances of all the temperature- and pressure-measuring components plus some intangible effects that result from location of thermocouples.

A delay in delivery of a special precision multirange potentiometer for indicating loop-pressurizer pressures will delay completion of mockup loop instrumentation by about three weeks. However, the panel will otherwise be complete and should permit shakedown tests of the loop itself one week after the target date of February 1.

A major portion of instruments for the panel to be used in the LITR is scheduled for shipment February 15. This has forced postponement of the target completion date of this panel from March 1 to March 22. Installation should be completed by April 1.

HOMOGENEOUS REACTOR TEST INSTRUMENTATION

Control-Valve Program

A number of companies that manufacture control valves have been contacted with regard to providing control valves for the intermediate scale reactor. Twelve major companies showed no interest; one major company wanted a development program; three small companies expressed interest and submitted tentative drawings for a suitable valve. Some of the drawings displayed obvious design shortcomings. It is evident from these findings that no known valve makers are expert at designing and producing all the three major valve components of bodies, sealing bellows, and actuators. Therefore, these items should be investigated separately. For this reason, the valve-development program within the Laboratory should be expanded, with more attention given to stress analysis, design, evaluation, and testing.

The sealing bellows is one of the most vulnerable spots in high-pressure valve design. An interview with a representative of Breeze Corporations, Inc., Union, New Jersey, disclosed that that company has been supplying the Navy with welded diaphragm bellows of type 347 stainless steel which have been operating at 2500 psi and about 300°F. This bellows is heliarc welded by machines and leak tested by the mass spectrograph.

Valve-Test Loop

Five prototype valves have been tested in the valve-test loop for a total of 415 hr at 1000 psi and 150°C with water. The loop is now dismantled for modifications to permit operation at 2000 psi. Strain gages will be mounted on the surge tank during a hydrostatic test at 3000 psi. The surge tank will be equipped with auxiliary fittings to provide a facility for testing level controllers suitable for use on the HRT pressurizer.

Pressurizer-Level Controller

The present HRE pressurizer-level controller is being redesigned for improved operation at 2000 psi and 300°C. A buoyant member consisting of solid titanium is being considered. This body would weigh approximately 50% more than a hollow stainless steel member of adequate wall thickness, but it should be relatively immune to pressure and temperature effects.

Waterproofing of Instrumentation

The plan for flooding portions of the reactor with water to permit mechanical repairs will require that a number of measuring and controlling components be able to withstand submergence. This will require improved insulation of thermocouple and electrical lines. Pneumatic devices will have

to have waterproof housings which are equipped with "snorkels" to permit exhausting above water level. To date only a cursory examination has been made of this problem.

ULTRASONIC LIQUID-LEVEL INDICATOR

Occasional troubles with the liquid-level controller of the HRE pressurizer have pointed out the need for a secondary system of level indication to check the accuracy of the primary measuring system. The practicality of an ultrasonic system for this purpose has been investigated. Quartz piezoelectric transducers clamped to a water-filled tank were energized with damped pulses of a frequency of 5 Mc/sec. The pulses and echoes from inserted metallic surfaces and from the surface of the water were observed on an oscilloscope connected to an amplifier. The tests were repeated with solutions containing $2\frac{1}{2}$ to 40 g of uranyl sulfate per liter.

The method bears some promise as a means of providing visual indication of level, but it would not be suitable for recording or controlling. As in radar, spurious echoes are present which can hardly be screened out electronically and must be evaluated visually by observation on an oscilloscope.

Measurements made in uranyl sulfate solutions indicated that attenuation of the sound waves varied markedly with concentration. Thus, determination of concentration might be obtained by measuring the attenuation in the solution. One method of doing this would be a measurement of the log slope of attenuation vs frequency, which should be independent of amplifier and apparatus errors.

Further testing at lower frequencies and higher temperatures seems to be justified.

RECOMBINER AND ENTRAINMENT-SEPARATOR LOOPS

Instrumentation for the recombiner and entrainment-separator loops has been selected and is either on order from outside vendors or is being fabricated in ORNL shops.

AXIAL-FLOW GAS-SEPARATOR LOOP

Instrumentation for the 14-in. axial-flow gas separator has been completed and is operating satisfactorily.

SALT LOOP

Procurement and installation of a modular frame and panels and power controls for the salt loop have been completed. Other instrument procurement is about 75% complete.

THERMAL CONDUCTIVITY ELECTRICAL ANALOGUE

A number of helipots, resistors, and other components were supplied and wired in a voltage-distribution network to a piece of conductive paper to present an electrical analogy of thermal conduction in a specimen-testing apparatus.

CORROSION

E. G. Bohlmann, Section Chief

DYNAMIC-CORROSION TESTS

Pump Loop Operation and Maintenance

H. C. Savage F. J. Walter

Thirteen dynamic-corrosion test loops are now in operation. Four of these loops (A, I, K, and M) are the multiple-bypass type described in a previous quarterly report.[1] In general, each loop contains standard pin and coupon corrosion specimens.

During most of this quarter, loop A[2] has operated at 225°C with 0.17 M UO_2SO_4 solution (40 g of uranium per liter) and dissolved O_2 (1000 to 5000 ppm). A special line heater has been installed and the loop is now operating at 320°C with 0.02 M UO_2SO_4 (5 g of uranium per liter), 0.005 M excess H_2SO_4, and dissolved O_2. Special impact specimens[3] and standard corrosion specimens were installed for this run which has been in continuous operation for over 500 hr.

A series of short-term runs (~200 hr) at 250°C with 0.17 M UO_2SO_4, dissolved O_2, and SiO_2 additives has been performed to investigate the inhibitive effect of silica.[4] A special heated bypass packed with stainless steel turnings has been installed on loop B, which is now operating at 250°C with 0.17 M UO_2SO_4 and dissolved O_2.

Due to a shortage of model 100A pumps, loop C has not been in operation for the last two months. During a long-term run at 100°C with 0.02 M UO_2SO_4 (5 g of uranium per liter), 0.005 M excess H_2SO_4, and dissolved O_2, the pump rotor shaft broke off at the point where it contacts the impeller. The broken rotor shaft has been turned over to the Metallurgy Group for investigation. A repaired pump has been received for this loop.

Loop D is being used to investigate the inhibitive effect of various additives. One 200-hr test at 250°C with 0.17 M UO_2SO_4 and O_2 in which D_2O was used as a solvent has also been completed.

During the early part of this quarter, loop E was used to test a spare pump for the HRE. The HRE spare pump has been seal-welded and is now being used for a long-term run at 100°C with 0.02 M UO_2SO_4, 0.005 M excess H_2SO_4, and dissolved O_2.

Loop F is still being used for correlation tests on the in-pile type of specimen.[5] At the present time the pump is being fitted with a titanium impeller and a thermal spacer with a titanium face.[6] Since the titanium face is removable, it is hoped that the thermal spacer can be used to investigate the possibility of crevice corrosion between stainless steel and titanium.

Special line heaters have been installed on loop G, and during this quarter the loop has been operated at 300°C with 0.02 M UO_2SO_4, 0.005 M excess H_2SO_4, and dissolved O_2 for about 700 continuous hours. At the present time the loop is being prepared for another long-term run at 300°C.

Loop H is being used to make a series of short-term runs at less than 250°C with 1.26 M UO_2SO_4 and dissolved O_2.

Loop I is being used to make a series of long-term runs at 250°C with 0.04 M UO_2SO_4 (10 g of uranium per liter), 0.006 M excess H_2SO_4, and dissolved O_2. The present run is to continue to 2000 hr.

Loop J is being used to make a series of long-term runs at 200°C with 0.02 M UO_2SO_4, 0.005 M excess H_2SO_4, and dissolved O_2. It is planned to continue the present run to 2500 hr.

Loop K has not been operated this quarter because of a shortage of model 100A pumps. A repaired pump has been received and assembled in the loop. The new loop contains the special fabricated weld sections from the old loop B[7] and

[1] E. G. Bohlmann *et al.*, *HRP Quar. Prog. Rep. March 31, 1953*, ORNL-1554, p 43.

[2] H. C. Savage, F. J. Walter, and R. A. Lorenz, *HRP Quar. Prog. Rep. Oct. 31, 1953*, ORNL-1658, p 42.

[3] E. G. Bohlmann *et al.*, *HRP Quar. Prog. Rep. Oct. 31, 1953*, ORNL-1658, p 42.

[4] Results are given in the section "Loop Test Results."

[5] H. C. Savage, R. A. Lorenz, and F. J. Walter, *HRP Quar. Prog. Rep. July 31, 1953*, ORNL-1605, p 69.

[6] H. C. Savage, R. A. Lorenz, and D. Schwartz, *HRP Quar. Prog. Rep. March 31, 1953*, ORNL-1554, p 47.

[7] H. C. Savage, F. J. Walter, and R. A. Lorenz, *HRP Quar. Prog. Rep. Oct. 31, 1953*, ORNL-1658, p 42.

from the special heat exchanger test assembly.[8]

During this quarter two 1000-hr runs at 250°C with 0.004 M UO_2SO_4 (1 g of uranium per liter), varying amounts of excess H_2SO_4, and dissolved O_2 have been completed in loop L.

A series of short-term runs (50 to 200 hr) at 250°C with 0.06 to 0.17 M UO_2SO_4, excess H_2SO_4, and dissolved O_2 are being performed in loop M to study entrance effects at velocities from 10 to 50 fps. Special tubing samples, consisting of 1-in.-long sections of heavy-wall, ¼-in., type 347 stainless steel tubing of the type used in the HRE heat exchanger, are ground flat on the ends and honed out to 0.155-in. ID. The tubing specimens are clamped in a special holder (Fig. 33) and placed in the loop in the usual manner.

Two additional 200-hr tests at 250°C with 0.17 M UO_2SO_4 and dissolved O_2 have also been completed. These tests were made to expose special welded specimens for the Metallurgy Group.

The special venturi type of coupon holder (Fig. 34) has been completed and was tested in loop M. This holder was designed to provide maximum liquid velocities in the range of 100 fps.

HRE Mockup. The HRE mockup was not operated this quarter because of higher priority projects.

Westinghouse Model 100A Pumps. Three Westinghouse model 100A pumps failed during this quarter. One failure was electrical and the other two failures were due to leaks in the Inconel cans. Three pumps have been repaired and returned to service, bringing the total number of pumps with new windings and stainless steel diaphragms to 14. All the reworked pumps continue to give excellent service as evidenced by no pumps with stainless steel diaphragms having failed during corrosion-testing service.

Three new titanium impellers have been received from the Y-12 machine shop. A total of five titanium impellers has been fabricated. During this

[8]H. C. Savage, R. A. Lorenz, and D. Schwartz, *HRP Quar. Prog. Rep. March 31, 1953*, ORNL-1554, p 49.

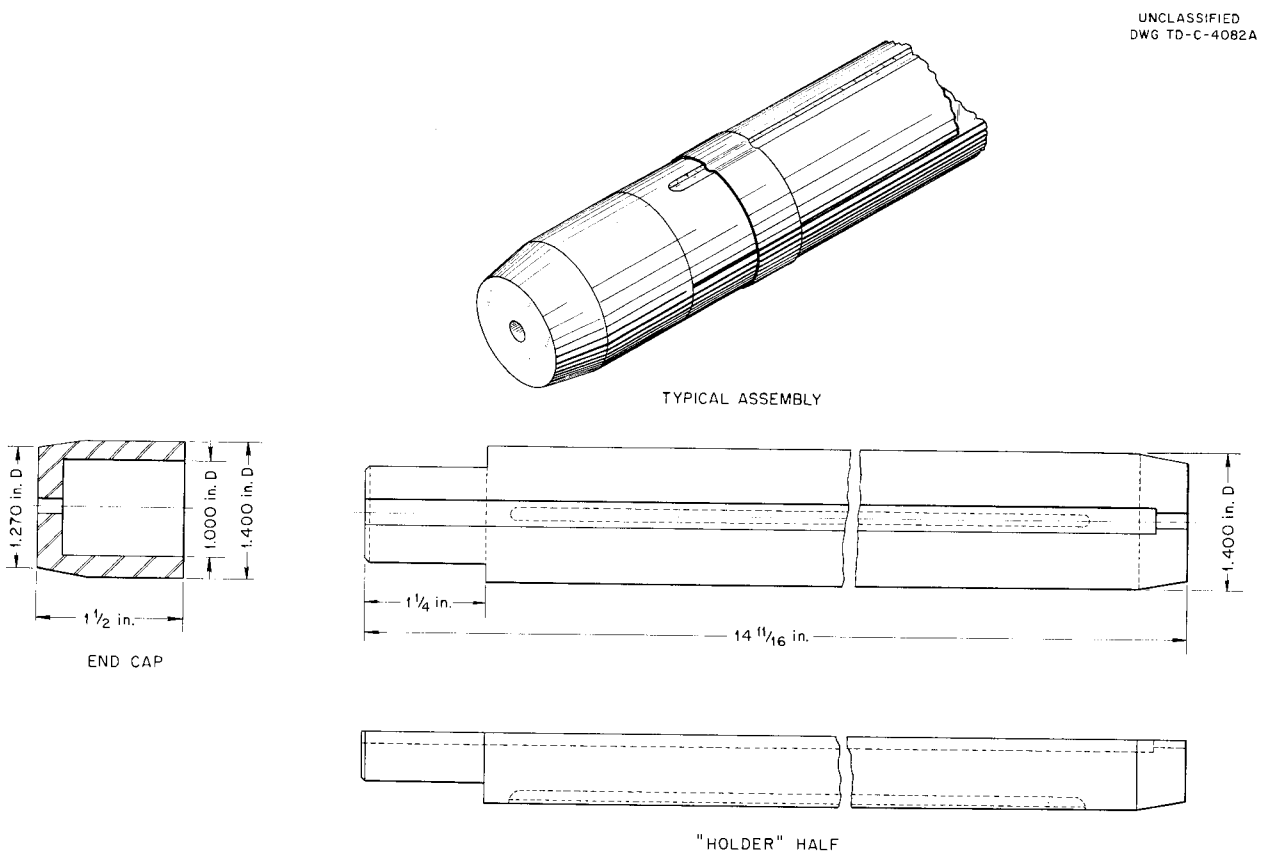

Fig. 33. Tubing-Sample Holder.

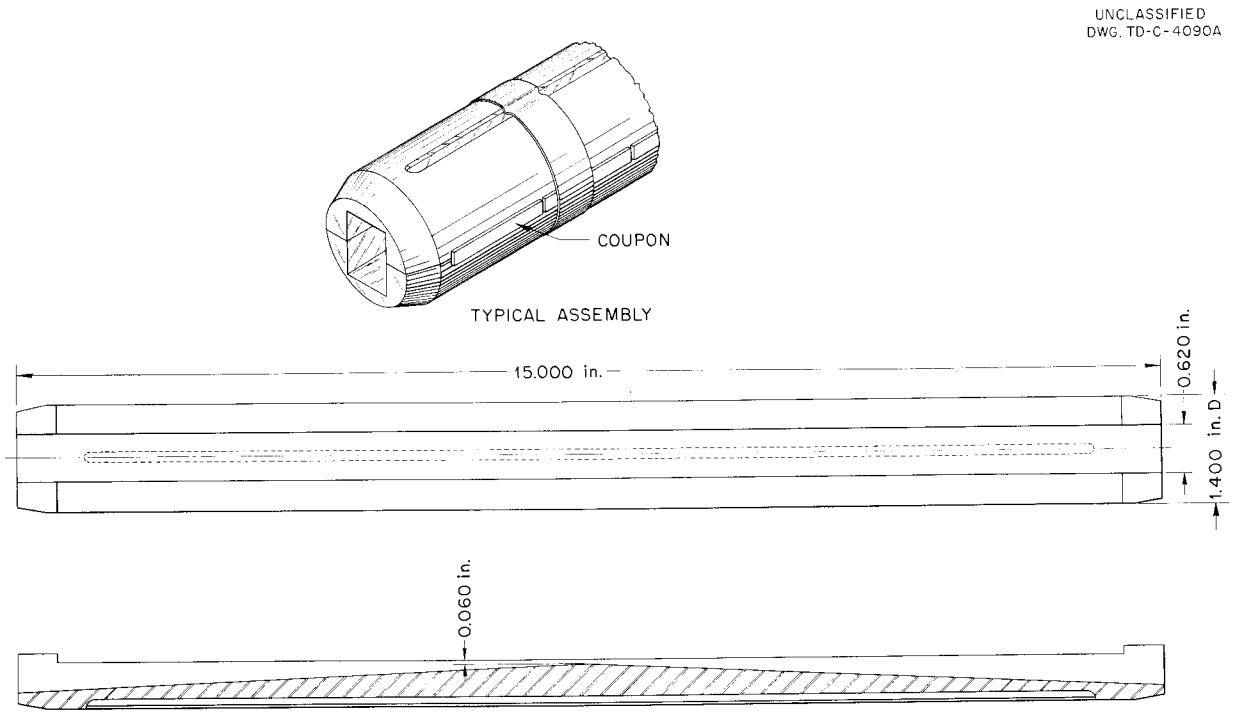

Fig. 34. Venturi Taper Coupon Holder.

quarter, five model 100A pump rotors have been reclaimed by replacing either the stainless steel can, the front stub shaft, or both.

Loop Test Results

J. C. Griess R. E. Wacker

The dynamic-corrosion test program has continued with a number of short-term tests having been run during the last quarter, but at present increased emphasis has been placed on longer-term testing. In addition, a substantial number of metallurgically treated specimens have been tested for the Metallurgy Group; the results are reported by them.

Molybdate, phosphate, pertechnetate, and silicate ions have been added to 0.17 *M* uranyl sulfate at 250°C to determine their effectiveness as corrosion inhibitors for stainless steel in this environment. Of the four additives, only silica showed a slight tendency to reduce corrosion at high flow rates but the effect was not significant.

Preliminary data have indicated that 0.02 *M* uranyl sulfate solutions behave similarly to higher concentrations in the temperature range of 200 to 225°C, that is, the corrosion rate is measurable even at low flow rates; however, the rate of corrosion is very low.

General Corrosion Rates. The average corrosion rates of pin-type corrosion specimens exposed to various uranyl sulfate solutions during the past quarter are presented in Table 6. The corrosion rates are expressed in mils of penetration per year (mpy) and are determined by weight loss during the exposure. Before each final weighing the adherent oxide film on the specimen was cathodically removed from the metal so that the weight loss represented the actual amount of the alloy oxidized. It should be pointed out that the corrosion rates given in Table 6 are average rates for the entire exposure time. At low flow rates corrosion is seldom a constant-rate process; hence care must be exercised in utilizing the data.

Effect of Condition of the Loop on Corrosion of Stainless Steel. In the last quarterly report[9] data were presented on the corrosion of stainless steel by 0.17 *M* uranyl sulfate at 225°C. These data were obtained from a loop which had been used extensively at 250°C, with the result that the

[9] J. C. Griess and R. E. Wacker, *HRP Quar. Prog. Rep. Oct. 31, 1953*, ORNL-1658, p 45.

TABLE 6. CORROSION RESULTS OF PIN-TYPE SPECIMENS

RUN NO.	TEST CONDITIONS						PIN MATERIAL	NO. OF PINS	CORROSION RATE (mpy)		
	Solution	Uranium Concentration (g/liter)	Temperature (°C)	Time (hr)	Additions	Flow Rate (fps ±10%)			Minimum	Average	Maximum
A-58	UO_2SO_4	40	225	500	1000 to 2000 ppm O_2	16	Type 347 stainless steel	4	2.1	2.2	2.3
							Type 304 ELC stainless steel	4	1.7	1.9	1.9
							Type 304 stainless steel	1		2.3	
							Type 321 stainless steel	1		2.0	
							Type 309 SCb stainless steel	1		2.1	
							Type 316 ELC stainless steel	1		1.6	
							Type 310 stainless steel	1		2.4	
							Type 430 stainless steel	1		1.2	
						62	Type 347 stainless steel	6	4.7	12	30
							Type 304 ELC stainless steel	7	0.7	29	51
							Type 304 stainless steel	2	1.1	3.6	6.1
							Type 321 stainless steel	3	18	22	27
							Type 309 SCb stainless steel	3	1.6	4.3	9.7
							Type 316 ELC stainless steel	3	10	40	53
							Type 310 stainless steel	2	13	15	17
							Type 430 stainless steel	2	0.5	1.7	2.8
A-59	UO_2SO_4	40	225	283	1000 to 2000 ppm O_2	16	Type 347 stainless steel	3	15	16	16
							Type 304 ELC stainless steel	3	16	23	35
							Type 321 stainless steel	3	22	31	38
							Type 17-4 PH stainless steel[a]	1		15	
							Type 322W stainless steel[a]	1		9.3	
							Type 416 stainless steel	1		16	
							Type 430 stainless steel	1		12	
							Carpenter-20 stainless steel	1		29	
						62	Type 347 stainless steel	6	51	65	77
							Type 304 ELC stainless steel	6	68	75	88
							Type 321 stainless steel	6	57	62	68
							Type 17-4 PH stainless steel[a]	2	9.4	55	100
							Type 322W stainless steel[a]	2	16	24	32
							Type 416 stainless steel	2	17	40	62
							Type 430 stainless steel	2	61	63	64
							Carpenter-20 stainless steel	2	80	82	84
A-60	UO_2SO_4	40	250	283	1000 to 2000 ppm O_2	16	Type 347 stainless steel	3	12	12	12
							Type 304 ELC stainless steel	3	13	17	22
							Type 321 stainless steel	3	3.4	16	27
							Type 17-4 PH stainless steel[a]	1		13	
							Type 322W stainless steel[a]	1		9.6	
							Type 416 stainless steel	1		20	
							Type 430 stainless steel	1		7.4	
							Carpenter-20 stainless steel	1		27	

TABLE 6. (continued)

RUN NO.	TEST CONDITIONS						PIN MATERIAL	NO. OF PINS	CORROSION RATE (mpy)		
	Solution	Uranium Concentration (g/liter)	Temperature (°C)	Time (hr)	Additions	Flow Rate (fps ±10%)			Minimum	Average	Maximum
A-60	UO_2SO_4	40	250	283	1000 to 2000 ppm O_2	68	Type 347 stainless steel	6	150	170	220
							Type 304 ELC stainless steel	6	170	200	220
							Type 321 stainless steel	6	160	180	230
							Type 17-4 PH stainless steel[a]	2	150	160	160
							Type 322W stainless steel[a]	2	22	30	38
							Type 416 stainless steel	2	15	19	22
							Type 430 stainless steel	2	140	150	150
							Carpenter-20 stainless steel	2	200	210	210
A-61	UO_2SO_4	40	225	200	1000 to 2000 ppm O_2	16	Type 347 stainless steel	5	21	25	32
							Type 304 ELC stainless steel	5	26	39	46
							Type 416 stainless steel	1		27	
							Type 430 stainless steel	2	17	18	18
						68	Type 347 stainless steel	10	68	77	81
							Type 304 ELC stainless steel	10	75	84	99
							Type 416 stainless steel	1		34	
							Type 430 stainless steel	2	72	76	80
							Misco A[b]	1		240	
							Misco B[b]	1		67	
							Misca C[b]	1		94	
							Miscro 4[b]	1		120	
B-32	UO_2SO_4	40	250	200	1000 to 2000 ppm O_2, 140 ppm SiO_2[c]	17	Type 347 stainless steel	6	15	27	42
							Type 304 ELC stainless steel	6	17	89	120
							Titanium, Ti-75A	1		(d)	
							Zircalloy II	1		(d)	
						75	Type 347 stainless steel	6	200	210	220
							Type 304 ELC stainless steel	6	180	200	210
							Titanium, Ti-75A	1		(d)	
							Zircalloy II	1		(d)	
B-33	UO_2SO_4	40	250	200	1000 to 2000 ppm O_2, 300 ppm Si as Na_2SiO_3[e]	19	Type 347 stainless steel	4	14	20	23
							Type 304 ELC stainless steel	4	11	37	91
							Type 316 stainless steel	1		64	
							Type 416 stainless steel	1		28	
							Platinum	1		0.7	
							Type 430 stainless steel	1		10	
							Titanium, Ti-75A	1		(d)	
							Zircalloy II	1		(d)	
						75	Type 347 stainless steel	4	170	180	180
							Type 304 ELC stainless steel	4	160	170	180
							Type 316 stainless steel	1		110	
							Type 416 stainless steel	1		130	
							Type 430 stainless steel	1		160	
							Platinum	1		1.0	
							Titanium, Ti-75A	1		(d)	
							Zircalloy II	1		(d)	

TABLE 6. (continued)

RUN NO.	TEST CONDITIONS						PIN MATERIAL	NO. OF PINS	CORROSION RATE (mpy)		
	Solution	Uranium Concentration (g/liter)	Temperature (°C)	Time (hr)	Additions	Flow Rate (fps ± 10%)			Minimum	Average	Maximum
B-34	UO_2SO_4	40	250	200	1000 to 2000 ppm O_2, 320 ppm Si as Na_2SiO_3[e]	17	Type 347 stainless steel	4	14	20	27
							Type 304 ELC stainless steel	4	1.2	18	58
							Type 316 stainless steel	1		53	
							Type 416 stainless steel	1		12	
							Type 430 stainless steel	1		1.4	
							Titanium, Ti-75A	1		(d)	
							Zircalloy II	1		(d)	
						75	Type 347 stainless steel	4	150	160	170
							Type 304 ELC stainless steel	4	14	120	160
							Type 316 stainless steel	1		91	
							Type 416 stainless steel	1		160	
							Type 430 stainless steel	1		150	
							Titanium, Ti-75A	1		(d)	
							Zircalloy II	1		(d)	
D-15	UO_2SO_4	40	250	200	1000 to 2000 ppm O_2	17	Type 347 stainless steel	5	15	17	18
							Type 304 ELC stainless steel	6	4.3	16	32
							Titanium, Ti-75A	1		(d)	
							Zircalloy II	1		(d)	
						71	Type 347 stainless steel	5	270	270	280
							Type 304 ELC stainless steel	6	250	260	270
							Titanium, Ti-75A	1		(d)	
							Zircalloy II	1		(d)	
D-16	UO_2SO_4	40	250	200	1000 to 2000 ppm O_2, 100 ppm Mo as H_2MoO_4	16	Type 347 stainless steel	5	21	24	27
							Type 304 ELC stainless steel	6	29	33	44
							Titanium, Ti-75A	1		(d)	
							Zircalloy II	1		(d)	
						71	Type 347 stainless steel	5	250	270	280
							Type 304 ELC stainless steel	6	250	270	310
							Platinum	1		3.2	
							Titanium, Ti-75A	1		(d)	
							Zircalloy II	1		(d)	
D-18	UO_2SO_4	40	250	200	1000 to 2000 ppm O_2, 500 ppm Mo as H_2MoO_4	13	Type 347 stainless steel	4	33	34	35
							Type 304 ELC stainless steel	5	38	45	53
							Titanium, Ti-75A	1		(d)	
							Zircalloy II	1		(d)	
						71	Type 347 stainless steel	5	240	260	270
							Type 304 ELC stainless steel	6	230	240	260
							Titanium, Ti-75A	1		(d)	
							Zircalloy II	1		(d)	
D-19	UO_2SO_4	40	250	200	1000 to 2000 ppm O_2, 200 ppm PO_4 as $(UO_2)_3(PO_4)_2 \cdot 4H_2O$	17	Type 347 stainless steel	5	31	40	44
							Type 304 ELC stainless steel[f]	6	93	150	180
							Titanium, Ti-75A	1		(d)	
							Zircalloy II	1		(d)	

TABLE 6. (continued)

RUN NO.	TEST CONDITIONS						PIN MATERIAL	NO. OF PINS	CORROSION RATE (mpy)		
	Solution	Uranium Concentration (g/liter)	Temperature (°C)	Time (hr)	Additions	Flow Rate (fps ±10%)			Minimum	Average	Maximum
D-19	UO_2SO_4	40	250	200	1000 to 2000 ppm O_2, 200 ppm PO_4 as $(UO_2)_3(PO_4)_2 \cdot 4H_2O$	71	Type 347 stainless steel	4	300	320	360
							Type 304 ELC stainless steel	6	280	340	360
							Titanium, Ti-75A	1		(d)	
							Zircalloy II	1		(d)	
D-20	UO_2SO_4	40	250	200	1000 to 2000 ppm O_2, D_2O instead of H_2O	16	Type 347 stainless steel	3	30	33	36
							Type 304 ELC stainless steel	3	35	59	86
							Type 304 stainless steel	1		40	
							Type 416 stainless steel	1		31	
							Type 430 stainless steel	1		15	
							Miscro 4[b]	1		47	
							Titanium, Ti-75A	1		(d)	
							Zirconium, crystal bar	1		(d)	
						54	Type 347 stainless steel	7	130	190	210
							Type 304 ELC stainless steel	7	140	160	190
							Type 304 stainless steel	1		190	
							Type 310 stainless steel	2	130	140	140
							Type 316 ELC stainless steel	2	120	140	160
							Type 416 stainless steel	1		170	
							Type 430 stainless steel	2	150	180	200
							Miscro 4[b]	1		220	
							Zirconium–2.5% tin	1		(d)	
							Zircalloy II	1		(d)	
D-21	UO_2SO_4	40	250	200	1000 to 2000 ppm O_2, 50 ppm Tc as NH_4TcO_4	17	Type 347 stainless steel	4	15	17	18
							Type 304 ELC stainless steel	4	12	16	19
							Type 316 ELC stainless steel	1		17	
							Type 416 stainless steel	1		21	
							Type 430 stainless steel	1		5.9	
							Titanium, Ti-75A	1		(d)	
							Zirconium–2.5% tin	1		(d)	
						71	Type 347 stainless steel	4	200	230	280
							Type 304 ELC stainless steel	4	210	230	280
							Type 316 ELC stainless steel	1		150	
							Type 416 stainless steel	1		140	
							Type 430 stainless steel	1		220	
							Titanium, Ti-75A	1		(d)	
							Zircalloy II	1		(d)	
F-29	UO_2SO_4	40	250	200	1000 to 2000 ppm O_2, 0.01 M $CuSO_4$	12	Type 347 stainless steel	7	18	22	27
							Type 304 ELC stainless steel	6	2.7	29	39

TABLE 6. (continued)

RUN NO.	TEST CONDITIONS						PIN MATERIAL	NO. OF PINS	CORROSION RATE (mpy)		
	Solution	Uranium Concentration (g/liter)	Temperature (°C)	Time (hr)	Additions	Flow Rate (fps ±10%)			Minimum	Average	Maximum
F-30	UO_2SO_4	40	250	200	1000 to 2000 ppm O_2, 0.01 M $CuSO_4$[g]	12	Type 347 stainless steel[h]	5	0.51	0.71	1.0
							Type 304 ELC stainless steel[h]	5	0.42	0.56	0.85
							Type 347 stainless steel[i]	2	21	22	23
							Type 304 ELC stainless steel[i]	2	27	30	33
H-25	UO_2SO_4	5	225	400	1000 to 2000 ppm O_2, 0.005 M H_2SO_4	16	Type 347 stainless steel	3	2.4	2.6	2.8
							Type 304 ELC stainless steel	3	2.0	2.2	2.6
							Type 321 stainless steel	2	2.3	2.3	2.3
							Type 316 ELC stainless steel	2	2.3	2.4	2.5
							Type 309 SCb stainless steel	2	2.0	2.3	2.5
						77	Type 347 stainless steel	3	11	16	20
							Type 304 ELC stainless steel	3	18	19	20
							Type 321 stainless steel	2	19	19	19
							Type 316 ELC stainless steel	2	21	22	22
							Type 309 SCb stainless steel	2	18	18	18
H-26	UO_2SO_4	5	225	563	1000 to 2000 ppm O_2, 0.005 M H_2SO_4	16	Type 347 stainless steel	4	1.6	1.9	2.1
							Type 304 ELC stainless steel	3	1.5	1.6	1.7
							Type 304 stainless steel	1		1.8	
							Type 321 stainless steel	1		1.6	
							Type 316 ELC stainless steel	2	1.6	1.8	1.9
						77	Type 347 stainless steel	4	19	20	21
							Type 304 ELC stainless steel	2	10	15	20
							Type 321 stainless steel	2	21	22	22
							Type 316 ELC stainless steel	2	23	24	24
J-32	UO_2SO_4	5	200	406	1000 to 2000 ppm O_2, 0.005 M H_2SO_4	15	Type 347 stainless steel	3	4.1	4.5	4.9
							Type 304 ELC stainless steel	3	2.6	3.7	4.3
							Type 321 stainless steel	2	4.0	4.2	4.3
							Type 309 SCb stainless steel	2	2.9	3.1	3.2
							Type 322W stainless steel[a]	1		7.1	
							Type 17-4 PH stainless steel[a]	1		5.7	
							Type 430 stainless steel	1		2.4	
						75	Type 347 stainless steel	3	7.3	8.7	9.2
							Type 304 ELC stainless steel	3	8.6	9.3	10
							Type 321 stainless steel	2	7.5	7.7	7.9
							Type 309 SCb stainless steel	2	5.8	7.0	8.1
							Type 17-4 PH stainless steel[a]	1		14	
							Type 430 stainless steel	1		5.8	
J-33	UO_2SO_4	5	200	1000	1000 to 2000 ppm O_2, 0.005 M H_2SO_4	16	Type 347 stainless steel	3	1.8	1.9	1.9
							Type 304 ELC stainless steel	3	1.8	1.9	2.0
							Type 321 stainless steel	2	1.9	2.0	2.0
							Type 309 SCb stainless steel	2	2.1	2.1	2.1

TABLE 6. (continued)

RUN NO.	TEST CONDITIONS						PIN MATERIAL	NO. OF PINS	CORROSION RATE (mpy)		
	Solution	Uranium Concentration (g/liter)	Temperature (°C)	Time (hr)	Additions	Flow Rate (fps ±10%)			Minimum	Average	Maximum
J-33	UO_2SO_4	5	200	1000	1000 to 2000 ppm O_2, 0.005 M H_2SO_4	16	Type 322W stainless steel[a]	1		2.5	
							Type 17-4 PH stainless steel[a]	1		2.2	
							Type 430 stainless steel	1		1.4	
						75	Type 347 stainless steel	3	1.7	6.2	9.2
							Type 304 ELC stainless steel	3	9.2	9.5	10
							Type 321 stainless steel	2	5.8	7.4	9.0
							Type 309 SCb stainless steel	2	7.8	8.0	8.2
							Type 322W stainless steel[a]	1		3.7	
							Type 17-4 PH stainless steel[a]	1		5.5	
							Type 430 stainless steel	1		7.8	
L-22	UO_2SO_4	1	250	909	1000 to 2000 ppm O_2, 0.0025 M H_2SO_4	14 to 25	Type 347 stainless steel	7	0.39	0.50	0.56
							Type 304 ELC stainless steel	10	0.30	0.39	0.45
							Type 304 stainless steel	4	0.39	0.49	0.62
							Type 321 stainless steel	3	0.47	0.52	0.58
							Type 309 SCb stainless steel	3	0.41	0.45	0.50
							Type 310 stainless steel	3	0.39	0.45	0.49
							Type 316 ELC stainless steel	3	0.43	0.46	0.50
							Carpenter-20 stainless steel	3	0.69	0.83	0.90
							Type 17-4 PH stainless steel[a]	1		0.64	
							Type 322W stainless steel[a]	1		0.49	
							Titanium, RC-70	1		(d)	
							Titanium, Ti-75A	2		(d)	
							Zircalloy II	1		(d)	
						75	Type 347 stainless steel	4	0.50	0.58	0.64
							Type 304 ELC stainless steel	4	0.34	0.42	0.52
							Type 304 stainless steel	1		0.79	
							Type 321 stainless steel	1		0.50	
							Type 309 SCb stainless steel	1		0.73	
							Type 316 ELC stainless steel	1		0.47	
							Carpenter-20 stainless steel	1		1.1	
L-23	UO_2SO_4	1	250	1000	1000 to 2000 ppm O_2, 0.005 M H_2SO_4	17 to 25	Type 347 stainless steel	7	1.0	1.2	1.3
							Type 304 ELC stainless steel	8	0.77	0.89	1.1
							Type 304 stainless steel	2	1.2	1.2	1.2
							Type 304 stainless steel[i]	2	1.4	1.5	1.6
							Type 321 stainless steel	3	0.31	0.58	1.1
							Type 310 stainless steel	3	0.77	0.90	1.1
							Type 316 ELC stainless steel	3	0.85	0.97	1.1
							Type 322W stainless steel[a]	1		0.63	
							Type 17-4 PH stainless steel	1		1.3	
							Carpenter-20 stainless steel	3	1.1	1.4	1.8
							Miscro 4[b]	1		10	
							Titanium, RC-70	1		(d)	
							Titanium, Ti-75A	2		(d)	
							Zircalloy II	1		(d)	

TABLE 6. (continued)

RUN NO.	TEST CONDITIONS						PIN MATERIAL	NO. OF PINS	CORROSION RATE (mpy)		
	Solution	Uranium Concentration (g/liter)	Temperature (°C)	Time (hr)	Additions	Flow Rate (fps ±10%)			Minimum	Average	Maximum
L-23	UO_2SO_4	1	250	1000	1000 to 2000 ppm O_2, 0.005 M H_2SO_4	75	Type 347 stainless steel	5	1.4	1.7	2.2
							Type 304 ELC stainless steel	4	1.2	1.4	1.6
							Type 304 stainless steel[i]	1		2.3	
							Type 316 ELC stainless steel	1		1.7	
							Carpenter-20 stainless steel			4.1	
							Miscro 4[b]			85	
M-6	UO_2SO_4	15	250	200	1000 to 2000 ppm O_2, 0.016 M H_2SO_4	15	Type 347 stainless steel	3	10	11	13
							Type 304 ELC stainless steel	2	9.4	10	11
							Type 304 stainless steel	3	9.5	10	11
							Type 321 stainless steel	2	11	12	12
							Type 309 SCb stainless steel	2	2.3	6	10
							Type 410 stainless steel	1		39	
							Titanium, RC-70	1		0.3	
						61	Type 347 stainless steel	2	96	98	100
							Type 304 ELC stainless steel	3	71	76	89
							Type 304 stainless steel			38	
							Type 321 stainless steel	2	58	71	84
							Type 309 SCb stainless steel	2	66	70	74
M-10	UO_2SO_4	40	250	200	1000 to 2000 ppm O_2	26	Type 347 stainless steel	12	14	35	66
							Type 304 ELC stainless steel		10	52	76
M-11	UO_2SO_4	40	250	201	1000 to 2000 ppm O_2	23	Type 347 stainless steel	10	15	33	55
							Type 304 ELC stainless steel	10	8.0	72	150

[a]Hardened by suitable heat treatment.

[b]These alloys were obtained from the Michigan Steel Casting Company and had the following composition (the balance being iron):

	COMPOSITION (%)			
	Ni	Cr	C	Si
Misco A	37.9	19.2	0.26	1.57
Misco B	13.3	25.4	0.36	1.45
Misco C	10.0	28.7	0.22	1.73
Miscro 4	0.15	13.1	0.07	1.41

[c]In this run the original solution had only 10 ppm of silicon at the beginning; however, a bundle of quartz tubing was included in a bypass line of the loop and during the run silica was dissolved from the quartz. The 140 ppm of silicon represented the amount in solution at the completion of the run.

[d]These specimens were not defilmed; all showed weight gains due to the deposition of iron and chromium oxide on their surfaces.

[e]During the run the silicon concentration of the solution decreased to 200 to 250 ppm. The pH also decreased to about 2.0. At the conclusion of the run, a small amount of a yellow precipitate was observed in the loop.

[f]The surface of the type 304 ELC stainless steel pins was only partially covered with a black film.

[g]Prior to this run the entire system was treated with a very dilute chromic acid solution.

[h]These specimens were in the system during the pretreatment.

[i]These specimens were placed in the system after the pretreatment.

[j]The type 304 stainless steel specimen was sensitized by suitable heat treatment before exposure.

interior surface of the loop was completely covered with an adherent, protective oxide film; consequently, the loop itself was only very slightly attacked during the runs at 225°C and the concentration of corrosion products in solution was comparatively low.

The construction of a new loop, loop A, presented an opportunity to observe the corrosion of specimens as well as of the loop itself at 225°C when the whole system was new. Previously reported data[10] showed that at 250°C the specimens in a new loop were less severely corroded than in an old loop but that the loop itself was rather heavily attacked during the first run. It appeared that corrosion products, ferric and chromic oxides, originating from the loop itself were laid down on the specimens, thereby minimizing corrosion of the specimens.

The first run, A-58, in the new loop was made at 225°C with 0.17 *M* uranyl sulfate, and the duration was 500 hr. Immediately following this, run A-59 was made at 225°C. The duration was 283 hr. A third run, A-60, was made at 250°C and a final run, A-61, was made at 225°C. All runs were made with newly machined specimens and a new solution of the same uranium concentration.

The pin data for the above series are summarized in Table 6, and it is interesting to note that in all these runs in the new loop A the corrosion rates observed at 225°C were lower by approximately a factor of 2 than those previously reported[9] under the same conditions. It should also be noted that during the first run, A-58, the corrosion rates were very much lower than in subsequent runs.

The coupon data for the runs at 225°C are shown in Fig. 35. The data from run L-21, which were obtained from an old loop operated at 225°C for 200 hr, are shown for comparison. It can be seen that the coupon data generally agreed with the pin data at a given flow rate and that the critical-velocity region shifted to lower velocities with increased use of the loop. Whether or not the critical velocity would ultimately reach that of run L-21 is a matter of conjecture, but at least the trend is in the correct direction. That the shift is related to the concentration of corrosion

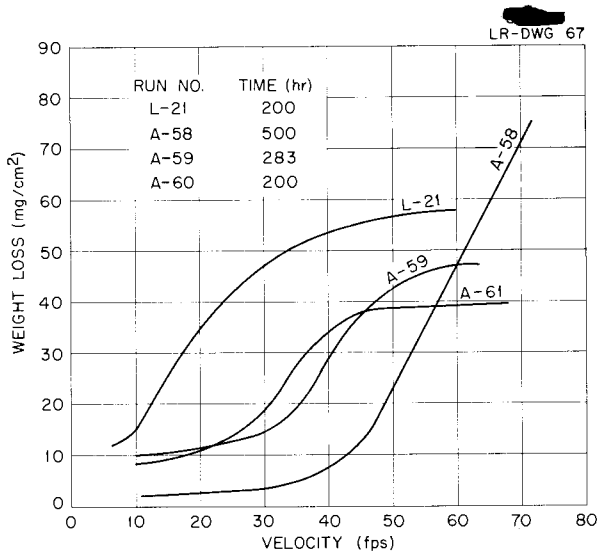

Fig. 35. Effect of Loop Condition on Corrosion of Type 347 Stainless Steel in 0.17 M UO_2SO_4 at 225°C.

TABLE 7. GENERALIZED CORROSION RATE OF THE SYSTEM DURING SEVERAL RUNS IN 0.17 *M* URANYL SULFATE AT 225°C

RUN NO.	CORROSION RATE (mpy)
L-21	1.9
A-58	4.4
A-59	3.7
A-61	3.0

products in solution is shown in Table 7. Thus, at 225°C the corrosion of steel specimens seems to be as related to the total corrosion of the system as it is at 250°C.

Both x-ray and electron diffraction examination of the oxide coating formed at 225°C showed the scale to consist largely of $Fe_2O_3 \cdot H_2O$ (and probably $Cr_2O_3 \cdot H_2O$), whereas at 250°C the film consisted chiefly of alpha Fe_2O_3 and Cr_2O_3. Obviously the hydrated film was not so protective as the alpha form. Thus, the corrosion specimens in run A-60, which was of 283-hr duration at 250°C, showed weight losses slightly lower than normal for such a run; however, the corrosion rate of the system was higher than usual because of the poor protection afforded by the oxide coating formed in the previous 225°C operations, and this

[10] J. C. Griess and R. E. Wacker, *HRP Quar. Prog. Rep. March 31, 1953*, ORNL-1554, p 49.

probably accounted for the lower weight losses on the specimens, consistent with the previous discussion.[9]

Effect of Additives on Corrosion of Stainless Steel. It has been demonstrated that the corrosion rate of austenitic stainless steels in uranyl sulfate solutions at 250°C and higher is very low after a short, initial period if the rate at which the solution flows past the steel is sufficiently low. Generally the more dilute the solution, the higher the flow rate that can be tolerated. For example, with 0.02 *M* uranyl sulfate, flow rates in excess of 80 fps cause no acceleration of the corrosion rate, but with a 1.26 *M* solution it is necessary to maintain flow rates less than 15 fps if the corrosion rate is to be low. Whether or not corrosion is stifled at 250°C (and higher) depends on whether or not a film forms on the surface. In the last quarterly report[9] data were presented for the effect of temperature and uranium concentration on the critical velocity – the velocity in excess of which a stable film does not form.

Since corrosion is not serious if a stable film forms, it would be desirable to raise the critical velocity of a system to such a value that a circulating system could be operated completely below the critical velocity. In such a system corrosion rates less than 1 mpy could be expected with solutions as concentrated as 0.17 *M* and perhaps even higher. In fact, loops have been operated at 250°C with 0.02 *M* uranyl sulfate, where the critical velocity is very high, with corrosion rates as low as several hundredths of 1 mpy.

As an empirical approach to improving the nature of the oxide film and thereby increasing the critical velocity, several additives have been examined in 0.17 *M* uranyl sulfate at 250°C, a system which had been investigated thoroughly in the absence of additives or "inhibitors."

The inhibitors investigated to date have been silica added as sodium silicate, runs B-32, 33, and 34; molybdate ions added as molybdic acid, runs D-16 and 18; phosphate ions added as uranyl phosphate, run D-19; and pertechnetate ions added as ammonium pertechnetate, run D-21. Table 6 shows the results that were obtained from pin-type specimens and it is evident that none of the additives had a significant effect on corrosion. Silica appeared to have a small beneficial effect at high flow rates on both pins and coupons, but it is possible that the effect may have been due to some other variable such as temperature.

The other additives had no noticeable effect except possibly in the case of uranyl phosphate where the corrosion rate was somewhat higher. In this case, however, all the uranyl phosphate did not dissolve and it is possible that the increased attack was due to erosion caused by the circulation of the suspended particles during at least part of the run.

It was suggested that uranyl sulfate solutions in heavy water may have a different degree of corrosiveness than solutions of uranyl sulfate in normal water. One run, D-20, was made in which uranyl sulfate dissolved in heavy water was circulated at 250°C. The pin data, given in Table 6, show that at low flow rates the corrosion rates were somewhat higher than usual, particularly the type 304 ELC stainless steel pins. At the higher flow rate, corrosion rates appeared to be somewhat lower than for light water.

The type 347 stainless steel coupon data gave the usual pattern and indicated no change in the critical velocity. Hence, the use of heavy water instead of light water in a uranyl sulfate solution produced no measurable change in the corrosion behavior of type 347 stainless steel and probably very little, if any, in the other steels.

Corrosion of Stainless Steel by 0.02 *M* Uranyl Sulfate at 200 and 225°C. In the last quarterly report it was shown that corrosion of stainless steel in 0.02 *M* uranyl sulfate containing 0.005 *M* sulfuric acid was very low at all flow rates (10 to 80 fps) in the temperature range 250 to 300°C. Since that time, preliminary data have been obtained at 200 and 225°C under otherwise identical conditions. The pin data can be seen in Table 6, runs H-25, H-26, J-32, and J-33. From these data and an observation of the coatings on the steel specimens after exposure, it is evident that corrosion is worse at 200 and 225°C than at 250°C. It is interesting to note that at low flow rates the corrosion rate of stainless steel is higher at 200°C than at 225°C. The reverse was true with 0.17 *M* uranyl sulfate.[9] Further runs are in progress which will better define the corrosion rates at the above-mentioned temperatures.

The oxide scales formed on the specimens at both 200 and 225°C with 0.02 *M* uranyl sulfate containing 0.005 *M* sulfuric acid looked like those formed in 0.17 *M* uranyl sulfate at the same temperatures. Both temperatures produced black to

brownish-black films which did not adhere well to the steel. Electron-diffraction and x-ray studies showed that at 225°C the oxide was the same as that formed in 0.17 *M* uranyl sulfate at the same temperature, namely, $Fe_2O_3 \cdot H_2O$. The films formed at 200°C have not been carefully examined to date.

Titanium Loop Operation. The titanium loop, loop G, has been operated for a 1000-hr period with 0.02 *M* uranyl sulfate containing 0.005 *M* sulfuric acid at 250°C. During this period of operation there was no evidence of corrosion of either the pump or the specimens. Analyses of the solution showed no change in the solution during the run. All titanium surfaces developed a bluish-purple film which resisted corrosion completely. However, three of the specimens were slightly loose in their holder and probably vibrated as the solution flowed past them. Where the specimen struck the holder, very severe corrosion of both the specimen and the holder was observed. It appeared that the continuous vibration prevented the formation of a protective film and the corrosion damage was heavy. A similar phenomenon has been observed in the case of stainless steel.

Following the successful run at 250°C an attempt was made to operate the same system at 300°C. After approximately 700 hr of operation, during which time solution analyses showed no consistent change, the loop was cooled and examined. The interior of the loop was covered with a thin, yellow film but the titanium surfaces showed no evidence of attack. The yellow precipitate was examined by electron and x-ray diffraction and was analyzed chemically. Both x-ray and electron examination indicated a compound which matched no known compounds of uranium or titanium. Chemical analysis showed that the precipitate contained 70% uranium and 19% titanium. This compound was identical to the one found following run G-2 in which 0.02 *M* uranyl sulfate without added acid was circulated at 250°C.[10] Since at 250°C the formation of the compound was prevented by the addition of acid (see run G-4 above), it seems likely that its formation can be prevented at 300°C by the addition of a larger amount of acid than the 25 mole % used in run G-5. This will be attempted in the future.

At 300°C the corrosion of the titanium loop and of the titanium and zirconium specimens was evident only by the thin, colored films developed on all surfaces; the specimens showed no weight change.

In-Pile Loop Experiments. In the last quarterly report[9] it was stated that the agreement between corrosion rates observed in 0.17 *M* uranyl sulfate containing 0.01 *M* copper sulfate at 250°C on corrosion specimens normally used in the out-of-pile loops and those designed for the in-pile loop was very good. In fact, the weight loss per unit area and the effect of flow rate were the same in both cases. The corrosion rates were about the same as those normally observed in 0.17 *M* uranyl sulfate at the low flow rates, but at high flow rates the presence of cupric ions seemed to increase the rate of attack of the steel.

Shortly after the last report was written, a complete in-pile loop was placed in operation (out-of-pile) by C. D. Zerby *et al.* (see section "Loop Package" in this report for details). After the system was operated on water and oxygen at 250°C for about four days, the loop was drained and filled with a solution containing 0.17 *M* uranyl sulfate and 0.01 *M* copper sulfate. After the system was operated at 250°C for 200 hr, the corrosion specimens were removed and examined. The specimens had a shiny, black film, and after the film was cathodically removed the specimens showed no evidence of corrosion either by weight change or by visual observation.

The difference in the extent of corrosion between the above-mentioned run and the runs made in the standard out-of-pile loops was not easily explainable except on the basis of pretreatment. It was observed that at the conclusion of the water run in the in-pile loop, the water had a yellow color which was probably due to chromate ions. This same observation was made in run M-1 where the same conditions prevailed.[10] It seemed possible that the slow buildup of chromate ions in the solution may have produced a passive film which retarded corrosion in the subsequent uranyl sulfate solution exposure.

In order to determine whether or not the chromate hypothesis could be responsible for the nearly complete passivity of the steel, the following experiment was carried out. Two in-pile coupon assemblies were flanged into loop F and a standard pin and coupon holder were placed in a bypass line of the same loop. The system was filled with water, pressurized with 200-psi oxygen, and operated at 250°C for 19 hr. Then over a period of

88 hr a solution of chromic acid was continuously added to the loop by means of a pulsafeeder pump. The rate of addition of the chromic acid was constant and the final loop solution showed a chromium concentration of 104 ppm. The loop was then operated for an additional 55 hr, at the end of which time the chromic acid solution was removed from the loop. At this point both the pins and the standard coupons were examined. Regardless of the flow, all had thin, copper-colored films and showed no weight change. Four of the pins were replaced with newly machined ones and the specimens were returned to the loop which was then filled with 0.17 M uranyl sulfate containing 0.01 M copper sulfate, pressurized with 200-psi oxygen, and operated for 200 hr at 250°C. Solution samples were withdrawn during the run to determine the increase of corrosion products in solution.

At the conclusion of the run, the specimens showed essentially the same result observed in the in-pile loop, that is, practically no corrosion of the specimens. In Table 6, run F-30, it can be seen that the pretreated pins showed very little attack and that the untreated pins showed the usual corrosion rate. The difference in corrosion of the standard coupon specimens between runs F-29 and F-30 is shown in Table 8, and the weight losses of the in-pile specimens are shown for both runs in Table 9. It is obvious that corrosion was nil on both types of specimens in run F-30 at velocities of 50 fps and lower.

TABLE 8. CORROSION OF STANDARD TYPE 347 STAINLESS STEEL COUPONS IN RUNS F-29 AND F-30

VELOCITY RANGE (fps)	WEIGHT LOSS (mg/sq cm)	
	Run F-29	Run F-30
6.8– 7.6	8	0.1
7.6– 9.5	8	0.1
9.5–11.7	10	0.1
11.7–15.4	14	0.1
15.4–23.9	19	0.1
23.9–27.1	31	0.1
27.1–31.2	66	0.1
31.2–36.3	104	0.1
36.3–44.4	125	0.2
44.4–56.0	159	12.0

TABLE 9. CORROSION OF IN-PILE LOOP TYPE 347 STAINLESS STEEL SPECIMENS IN RUNS F-29 AND F-30

VELOCITY RANGE (fps)	WEIGHT LOSS (mg/sq cm)	
	Run F-29	Run F-30
9.2–10.5	19	0.2
10.5–12.7	18	0.03
12.7–15.9	21	0.03
15.9–21.5	25	0
21.5–33.4	41	0
33.4–38.5	99	0
38.5–47.3	140	0.03
47.3–26.7	102	0
26.7–18.7	34	0.03
18.7–14.0	22	0.06
14.0–11.4	18	0.03
11.4– 9.5	1	0
10.0–11.5	21	0.2
11.5–13.9	19	0.06
13.9–17.4	22	0.03
17.4–23.5	27	0.03
23.5–36.4	27	0.03
36.4–42.0	150	0.1
42.0–51.6	159	0.03
51.6–29.1	143	0
29.1–20.4	59	0.03
20.4–15.3	37	0.03
15.3–12.5	22	0.03
12.5–10.6	1	0.03

The solution analyses in run F-30 showed that the nickel concentration of the uranyl sulfate solution increased slowly and uniformly to a high value of 54 ppm which corresponded to an average corrosion rate of 0.8 mpy. In the preceding run F-29, which was operated under exactly the same conditions except for the pretreatment, the average corrosion rate was 2.6 mpy.

The data presented in Table 6 generally show a pattern consistent with that presented in previous reports. There are, however, at least two particulars in which the data appear to deviate from previously reported trends. In several cases given in Table 6, particularly runs M-10, M-11, B-32, and D-19, the corrosion resistance of type 304 ELC stainless steel at low flow rates was definitely inferior to that of type 347 stainless

steel, although in most previous runs there was very little, if any, difference between the two. The reason for the lack of resistance of the type 304 ELC stainless steel was immediately apparent if the specimens were examined as they were removed from the loop. All the type 304 ELC stainless steel specimens which showed unusually high corrosion rates were at least partially free of film, while the type 347 specimens were always completely covered with film. The reason for the difference in film adherence between types 304 ELC and 347 is not evident at present. It should be pointed out, however, that in runs D-19 and B-32 it was possible that a small amount of suspended matter may have circulated with the solution, at least in the early parts of the run, and that it may have been abrasion which was responsible for removing the film from the type 304 ELC. In runs M-10 and M-11 the flow rates were near the critical velocity, and in these cases the data indicated that the critical velocity may be lower for type 304 ELC than for type 347 under the conditions of the test.

The general reproducibility of the corrosion data presented in this and previous reports can be seen by comparing the spread of the data for a given alloy under a given set of conditions. Most of the time the disagreement is largest at the low flow rates (15 to 25 fps). At high flow rates the agreement is usually satisfactory in a given run although the data may differ substantially from run to run.

At low flow rates the film formed on the surface greatly reduces the rate of corrosion after a short exposure and therefore any factors which change the rate or completeness of film formation also change the extent of attack. In addition to the usual variables such as concentration, temperature, and acidity, two other variables which have a large effect are flow conditions and the corrosion rate of the system as a whole. The effect of the corrosion of the system as a whole has been discussed in an earlier section. The flow conditions existing in a system are important since they determine to a large extent whether or not a film will form on the steel surface. For example, even at low flow rates the first specimen in a holder is usually more severely attacked than the other pin in the holder. In an effort to understand better the influence of flow conditions on the corrosion of the system, several special loop runs are being made at present to obtain data for H. Hoffman who is attempting to relate film stability (and consequently corrosion rate) to flow conditions in a given system.

At high flow rates where a film does not form, perhaps the two most important variables are temperature and uranium concentration. From the relationship between temperature and corrosion presented in the last quarterly report, it can be seen that in 0.17 M uranyl sulfate solutions at 250°C the corrosion rate can be varied from about 200 to 300 mpy by changing the temperature ±5°C. In the dynamic loops with the present instrumentation, the control is no better than ±5°C and in some cases is even poorer. Hence, most of the discrepancies in the corrosion data at high flow rates can be explained on the basis of temperature variation although it has been shown that other variables are important. At high flow rates the only concern is generally with factors which influence the rate of dissolution of the metal. On the other hand, at low flow rates not only must the factors which influence the rate of dissolution of the metal be considered but also those which affect film formation.

Run F-30 and the run made in the in-pile loop by C. Zerby represent a new approach to the art of pretreatment. Previously, chromic acid in much larger amounts (2%) has been used as a pretreating agent, but a heavy black film was formed and in the process of pretreating, an appreciable amount of metal was oxidized. In the new pretreatment the oxidizing agent (and the corresponding acid) was added slowly to the system, and then only in relatively small amounts; this produced a very thin film, showing interference tints, on the surface of the steel. When this thin film was cathodically stripped from the steel, the surface was as bright as before the exposure and all the fine machining marks were clearly visible. Even after exposure in the uranyl sulfate solution containing copper sulfate, the films did not change appreciably in appearance, and, similarly, the base metal itself showed only a very slight etch in a few places. At flow rates of 50 to 60 fps the film did not withstand the flow and some corrosion actually occurred. But even at this point the extent of attack was not great and visually it appeared that corrosion had ceased.

It should be made clear that all the data discussed above are based on only two experiments.

Before detailed consideration can be given to the applications of such a process, it will be necessary to establish how good the film actually is and how long it will actually remain at moderately high flow rates.

At present it seems that such a process would involve a risk in that once the chromic acid is removed from the system, the film-repair mechanism may not be so effective as during the pretreatment. On the other hand, if as little as 100 ppm of chromium in solution is sufficient to maintain the film, it is possible that this amount could be added to the uranyl sulfate solutions. Further experimentation will be necessary to determine the merit of such a pretreatment or the use of other pretreating agents such as nitric acid or dilute uranyl sulfate solutions.

Small-Scale Dynamic-Corrosion Program

G. E. Moore

The preliminary tests on the operation of the 20-toroid, De Rieux-McWherter rotator No. I have been completed; the mechanism has shown satisfactory performance. The furnace design for the rotator has been completed and will soon be sent to the machine shop for fabrication.

The toroid rotator No. II has been operated with four toroids containing 40 g of uranium per liter as UO_2SO_4 at an average velocity of about 20 fps with approximately 430 psi excess O_2 pressure at about 250°C. Uninterrupted periods of operation have included two 100-hr intervals and intervals of 136 and 170 hr. Minor difficulties have prevented longer continuous operation. These tests will be continued in an attempt to improve the basic design.

IN-PILE LOOP

Complete Installation

G. H. Jenks R. A. Lorenz
D. T. Jones A. R. Olsen
H. C. Savage

Status of Design and Construction of Operating Equipment. The design of disassembly equipment for installation in a cell in Building 4501 has been completed, and part of the equipment is installed. The balance of the equipment will be installed as it is completed, and will be ready for use by March 1.

The design of the loop installation is complete except for the carrier to transport the loop and plug assembly from Y-12 to the LITR. This design will be completed by February 5. Construction of equipment is near completion except for the valve boxes; however, construction of the boxes is on schedule.

Work has started at the LITR on the hot drain installation, service alterations, etc. It is expected that the completion date of March 1 will be met.

A decision has recently been made to provide, for the final disassembly of loop components, a facility that will be independent of the Solid State installation. The additional facility will be installed in the hot storage room of Building 4501. It will be capable of handling pieces up to 8 in. in diameter and 30 in. in length and of making cuts on either axis of the object. These dimensions were selected so that the available space will be used and so that equipment from the HRE can be handled. This area will also contain defilming equipment and a remotely operated balance of 200-g capacity. Tentative designs for this installation are complete, and a cost estimate is in preparation. Design completion is scheduled for early April, fabrication completion for June 1, and installation completion by July 1.

Special Problems Investigated in Connection with the Loop Installation. Approximately 50 valves are used in the operational equipment of the in-pile loop. Very tight shutoff is demanded of a few of these valves, but the others may leak slightly without injury to the experiment or the equipment. In all cases it is desirable that the valves have a small holdup volume and be free of crevices which would hinder decontamination by washing. All valves operate at room temperature.

The valves which have been selected for this service are of the autoclave, 30,000-psi series. The valve bodies are of type 304 or 303 stainless steel, and the stems are of hardened type 420 stainless. A Teflon gasket comprises the packing. For the present service, it is specified that the packing nut and retaining washer be made of bronze.

After the valves are received from the factory, they are prepared for loop service as follows. They are disassembled and degreased in a vapor degreaser in which trichloroethylene is used; then

they are washed in distilled water and dried in an oven at 110°C. While still hot, the seats of the valves and the threads on the stems are coated with a thin layer of Aquadag. When cool, the valves are reassembled and tested for tightness of shutoff and for tightness across the packing.

A helium leak detector is used in the leak testing because of the ease and rapidity with which such tests may be made. The following rough relationship has been experimentally established between the leak rate indicated by the helium detector and the rate at which water at room temperature will pass through the same leak:

1 cc of He/day/15 psi pressure difference

= 1 cc of H_2O/day/1000 psi pressure difference.

The helium detector will sense leak rates as small as 5×10^{-4} cc of helium per day per atmosphere. A pressure difference of 1 atm was used in all helium leak testing.

In all valves tested to date the Teflon packing has been tight to the helium detector. The shutoff has also been highly satisfactory. Slight leaks have been found after a given valve has been opened and closed repeatedly, but the rate of leakage has not exceeded 10^{-3} cc/day. In addition, water was flushed through the valve for 2 hr at a rate of 0.3 gpm from a head of 70 psi. The leak rate during and at the conclusion of the test did not exceed the above value.

An explanation is necessary regarding the use of Aquadag on the valve seats. The valves will be used in oxygen service, and it is considered necessary to degrease them. However, it was found that completely degreased valves may develop leaks as large as 1 cc/day/atm of helium after several openings and closings. Suitably lubricated valves shut off as described above. Lubrication of the seats clearly improves the performance of the valves, and Aquadag appears to be a suitable lubricant. It is fairly unreactive, and the thin film which is applied adheres strongly to the metal. Flushing water through a valve as described above did not visibly affect the coating.

It is tentatively concluded that the valves will be suitable for loop service. Final evaluation will be made in the mockup.

In the previous report, plans were described for the incorporation of a neutron shutter in the in-pile loop installation.[11] The shutter was to be comprised of a cadmium foil 3 in. wide and 8 in. long. The foil moved in a beryllium "L piece" directly in front of the hole. To provide a basis for estimating the effect of the shutter, measurements have been made of the flux along the axis of hole HB-4 with and without a cadmium foil positioned at the inner end of the hole.

The foil used in these measurements was 3 in. wide and 4 in. high. Its thickness was sufficient for stopping more than 99% of incident thermal neutrons.

The center of the foil was on the approximate center line of the hole. It was held in position against the end of the hole by means of an aluminum holder designed for this purpose. Small cobalt specimens which were used in measuring the flux were also contained and positioned by the aluminum holder.

The magnesium "L piece" which was in front of the hole at the time of the previous measurements was replaced with beryllium before the present measurements were begun.

Two sets of specimens were irradiated, one with cadmium and one without. The duration of each irradiation was one week, and the nominal power of the pile was 3 Mw for this period.

The results with and without cadmium are shown in Fig. 36. The flux determined by a given cobalt specimen is plotted as a function of the distance which separated the specimen from the front of the hole. The flux depression caused by the cadmium amounted to roughly 40% for the points lying between 8 and 23 cm from the cadmium. For points closer than 8 cm the depression was greater; no measurements were taken beyond 23 cm.

The shutter which is planned will be about 6 cm from the front of the loop core, which is about 18 cm long. The above data indicate that, with these spacings, a 3 × 4 in. cadmium shutter will reduce the flux at the core by 40%. The larger 3 × 8 in. shutter which is planned will probably effect a greater reduction.

Previous flux data,[12] shown in Fig. 36, were obtained by using cobalt specimens held within a stainless steel, loop core assembly. The magnesium "L piece" was in front of the hole at the time of the measurements. The lower flux in this case was probably due both to the presence of

[11] G. H. Jenks *et al.*, *HRP Quar. Prog. Rep. Oct. 31, 1953*, ORNL-1658, p 67.

[12] *Ibid*, p 70.

the magnesium and to neutron absorption in the stainless steel. As stated above, the magnesium has now been replaced with beryllium; however, the final loop assembly will contain as much or more stainless steel as the holder in the previous measurement. It is expected then that the value of the flux for the loop experiments will be between the values found in the previous measurements and the present measurements without cadmium.

No further flux determinations are planned prior to installation of the first loop. The actual power developed in the core from fission will be determined during loop operation.

A series of static bomb tests has been initiated to determine the effect of gamma radiation on the Graphitar 14 bearings which are under consideration for the in-pile loop pump. The approximate conditions which will prevail in the pump are the following:

Solution: 0.17 *M* UO_2SO_4 with 0.01 *M* $CuSO_4$

Temperature: 70 to 100°C

Pressure of dissolved gas: About 300 psi of oxygen and 200 psi of hydrogen

Radiation level: Gamma-ray intensity in the rotor region estimated to be such that about 10^{-3} w/g will be generated by absorption of the radiations; contribution of beta rays, fission recoils, and neutrons to the radiation absorbed by the Graphitar will probably not exceed 10^{-3} w/g.

In tests made to date, a titanium bomb of 17.9-ml capacity and equipped with a type 347 stainless steel cap was used. Ten milliliters of solution was placed in the bomb, and four Graphitar specimens from bearing material were submerged in the solution. The specimens were cylindrical in shape, 0.8 in. in length and 0.18 in. in diameter, with a 0.10-in. hole drilled lengthwise along the axis. The stainless steel cap was connected to a Baldwin pressure cell and a valve through 28 ft of 30-mil stainless tubing. The total volume of the system was 29.3 ml. Each run was pressurized initially with 290 psi of oxygen at room temperature.

At the completion of a run, the gas remaining in the bomb system was collected and analyzed for oxygen and carbon dioxide. A 1-liter glass flask was used to collect the gas, and the analyses were made by weighing the gases within the flask. Oxygen was separated by evacuation at liquid-nitrogen temperature. The residual carbon dioxide and water vapor were separated by evacuation at dry-ice temperature.

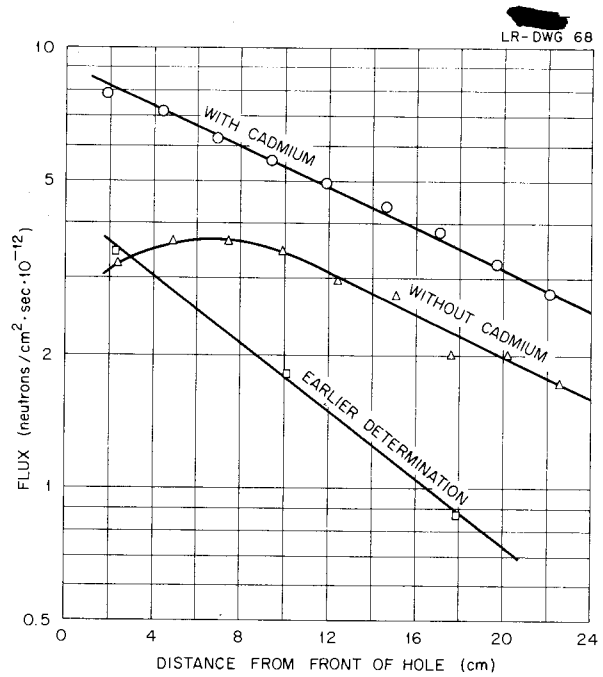

Fig. 36. Neutron Flux in Hole HB-4.

Three runs have been completed. The radiation exposure and the copper content were varied as shown in Table 10. The radiation test was made in the cobalt gamma-ray source in Building 3001.

Studies of the Graphitar samples after exposure indicate that in addition to direct oxidation to CO_2 there are other chemical changes. Samples from run No. 1 were placed in boiling distilled water for 15 min and then dried overnight at 110°C. They were then leached in water at 70°C for 2 hr; a suspension of a yellow material formed in the water during the leach, but a subsequent 70°C water leach for 4 hr gave no coloration. The samples were then leached for 1 hr in 0.1 *M* NaOH solution at 70°C, and again a yellow suspension formed which was similar to that mentioned above but in greater quantity. A small amount of flaked graphite was also observed. Two additional NaOH leaches produced similar yellow suspensions. Samples from run No. 2 were tested similarly, and the water leach remained clear. The NaOH

TABLE 10. SUMMARY OF BOMB TESTS OF GRAPHITAR

	RUN		
	No. 1	No. 2	No. 3
Solution	0.17 M UO_2SO_4 0.01 M $CuSO_4$	0.17 M UO_2SO_4 0.01 M $CuSO_4$	0.17 M UO_2SO_4 No $CuSO_4$
Gamma radiation	1.3×10^{-3} w per gram of solution	None	None
Exposure time, hr	505 under irradiation, 22 without irradiation	185	179
Temperature, °C	106	100	99
Initial system pressure (at temperature), psi	325	320	320
Graphitar surface area, sq cm	19.4	19.4	19.4
Initial O_2 charge, mg	470	462	468
Rate of pressure drop, psi/day	2	2	Varied, averaged 2.2
Final O_2 collected (weighed as O_2 and CO_2), mg	413	433	435
Final CO_2 collected, mg	86	25	19
Graphitar oxidation rate (from CO_2 and surface area), mpy	4.9	4.0	3.2

leaches, however, gave the yellow suspended material.

Dried samples from run No. 1 were weighed before and after the different leaches mentioned above. After the initial hot water rinse the samples showed an average weight gain of 0.62 mg from the original weight. After the third NaOH leach, the sample weights averaged 4 mg less than the original weights.

As mentioned previously, the titanium bomb was equipped with a stainless steel cap. When the cap was removed at the end of the radiation test, it was found to be badly corroded. No corrosion of the steel was observed in the runs made in the absence of radiation. Solution from run No. 1 was found to contain a total of 130 μg of chloride ion. No chloride ion was found in the solution from the other runs or in the original solution. The corrosion of the stainless cap in run No. 1 was probably due to the presence of chloride.

A sample of the Graphitar has been submitted to the Analytical Chemistry Division for determination of chlorine. A reliable value has not yet been obtained, but a preliminary analysis indicates considerable chlorine content.

The yellow material has not been positively identified but it is probably graphitic oxide (analyses for uranium gave negative results). This material is discussed at length by Emeléus and Anderson.[13] Briefly, it is an interstitial compound with oxygen formed when graphite is treated with strong oxidizing agents. Oxygen penetrates the solid, entering between the sheets and bonding to the carbon atoms within the sheets. The character of the graphite is changed by this reaction. In particular, graphitic oxide is hydrophilic, and

[13] H. J. Emeléus and J. S. Anderson, *Modern Aspects of Inorganic Chemistry*, Van Nostrand, New York, 1945.

water may penetrate between the sheets. Swelling takes place which corresponds to an increase in the interplanar spacing. In alkaline media, increased swelling and separation of sheets from the solid are observed.

Another material of the same nature, called graphite bisulfate, is formed when graphite is treated with sulfuric acid and an oxidizing agent. In this case, the bisulfate ion is considered to penetrate between the sheets. Some graphitic oxide is usually formed along with the bisulfate. The bisulfate reverts to graphite when washed with water, but some oxygen remains in the graphite bound as a surface oxide. The resulting material is hydrophilic and may form colloidal graphite.

The studies made to date have not established any effect of radiation on the formation of the interstitial compounds. The simple tests made on the samples after the different exposures indicated that more graphitic oxide had been formed in the irradiated samples than in the others. However, the longer period of exposure to uranyl sulfate of the irradiated specimens may account for this difference.

No appreciable effect of radiation was found on the oxidation of graphite to CO_2. The rate of formation of CO_2 was roughly the same for the irradiated and unirradiated specimens.

Evidence exists from these studies that the Graphitar specimens tested contained chlorine and that radiation brought about solution of the chlorine. It should be emphasized that the specimens tested were from one bearing and were machined in the machine shops. A possible explanation for chlorine being present is that it was introduced through some unknown treatment to the specimens. Further tests for chlorine are planned on other samples of Graphitar 14 and on other graphite bearing materials.

Mockup. A mockup of the in-pile loop system including loop, beam-hole liner, loop can, shield plug, valves, valve boxes, accessory equipment, and instrumentation is now under construction in the Y-12 Area. The orientation of the beam-hole liner, valve boxes, and instrument panel is almost identical with the planned installation at hole HB-4 of the LITR.

The loop package for the mockup is virtually complete. Final welding of the loop assembly is being done in a recently designed and fabricated welding jig that will ensure proper fit of the loop in the loop can. A beam-hole liner is in place along with the two chambers for valves and accessory equipment. All valves have been installed in these chambers and interconnections between valves are now being made. The instrument panels are in place and about 75% of the instruments have been installed. Preliminary tests of the in-pile system mockup should begin by February 1. All accessory equipment is being fabricated and performance-tested at X-10 prior to installation in the mockup.

Personnel to operate the in-pile loop in the LITR are now engaged in construction of the loop package, operation of the development loop, and construction of the in-pile system mockup. With operating experience on the mockup, a well-trained group, familiar with all details of the in-pile system, will be available for operation of the loops installed in the LITR.

Loop Package

C. D. Zerby T. H. Mauney
R. J. Kedl H. C. Savage
R. E. Wascher

Development and Design. Two short-term tests have been completed with the initial model of the in-pile loop circulating UO_2SO_4 containing 40 g of uranium per liter plus 0.01 *M* $CuSO_4$ at a temperature of 250°C in the main circulating loop and 280°C in the pressurizer. The main purpose of the tests was to observe the behavior of the pump and of corrosion-coupon holders in conjunction with the other components of the loop under design operating conditions.

The first test ran for 215.1 hr, during which time there was no operating difficulty. Observation of the coupons from the core and in-line coupon holder after the test showed negligible corrosion. The coupons were not etched and showed no differential corrosion rate due to velocity differences. The lack of corrosion was attributed to the pretreatment of the loop which resulted from a run in which oxygenated water was used for approximately 100 hr at temperature. This pretreatment is being used in other work described in the section "Dynamic Corrosion Tests."

The second test ran for 211.6 hr. During the run two different leaks occurred at threaded fittings; the loop had to be cooled to lower the pressure before the fittings were tightened and the leaks stopped. The threaded fittings are used in the

loop model for ease in assembly and disassembly; there will be only welded fittings in the final loop package. There were no other operating difficulties.

Observation of the corrosion coupons from the second test showed a maximum average corrosion rate of 33 mpy on the coupon in the core where the velocity gradient across the coupon was 41 to 50 fps. The coupons from the in-line coupon holder, however, showed a maximum corrosion rate of 2.8 mpy. The low corrosion rates can be attributed to formation of protective films during the cooling-down periods; however, the difference in the behavior of the coupons from the two holders is not easily explained.

The nickel concentration in the main circulating stream is shown for both runs in Fig. 37. The differences in nickel concentration buildup between runs 1 and 2 can be attributed to a low over-all corrosion rate in run 2 that resulted from the formation of a protective film in run 1. The loop had not been run on fuel before run 1.

The same pump was used in the loop for both runs and operated with no difficulty throughout the tests. Additional information on the pump is given in the next section, "ORNL In-Pile Pump." In general, during the two tests all the components of the loop were proved to operate as predicted.

The designs for all the components and the loop layout are now complete except for minor changes resulting from construction expediency or additional testing. The initial development of the loop is now considered to be complete.

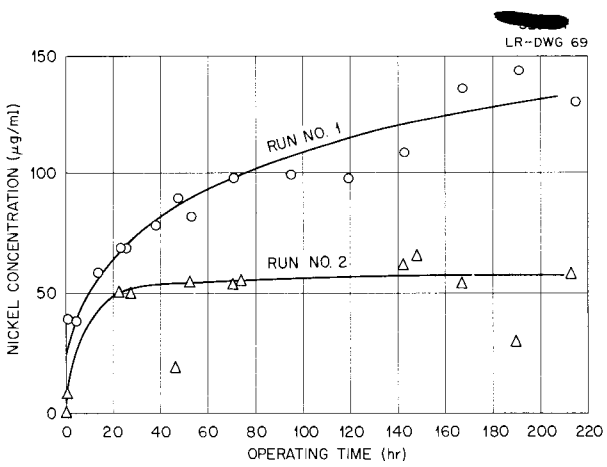

Fig. 37. Nickel Concentration in Initial Model of In-Pile Loop with 40 g of Uranium per Liter as UO_2SO_4 Plus 0.01 M $CuSO_4$ at 250°C.

ORNL In-Pile Pump. As was described above, the in-pile pump operated successfully for a total of 426.7 hr in circulating 0.17 M UO_2SO_4 solution, 0.01 M in $CuSO_4$ at a temperature of 250°C. The total operating time of the particular pump used in the test was 124.5 hr in circulating water and 426.7 hr in circulating the solution. There was no indication of unusual wear on any of the parts, including the bearings, after this operating time. The pump used the redesigned Graphitar bearing described in the last quarterly report.[14]

Cooling the back of the pump has proved to be satisfactory for retarding corrosion attack on the rotor or bearings. Examination of the pump parts after the fuel runs showed no indication of film formation or corrosion attack. The surfaces of the parts in the cool region remained as brilliant as when they were assembled into the pump.

The pump design has been changed to include a Stellite 98M2 sleeve on the rotor journal similar to the sleeves which have worked so successfully in the Westinghouse model 100A pump. Some minor modifications have also been made in the bearing design as a result of testing. All drawings have now been completed and approved for construction for the pump, and major development is considered to be complete. A long-term operating test is now under way to observe the wear characteristics of the bearings after 1000 hr of operation.

In-Pile Development Loop. One in-pile loop was completed during the past quarter and general performance studies have been made. The design of the loop is as previously reported except for a heating jacket that has been added around the pressurizer. It was believed that the addition of the jacket would prevent possible gas stratification in the pressurizer by maintaining a uniform temperature throughout.

Static pressure taps were installed on either side of the core sample holder, in-line sample holder, and pressurizer circuit to measure flow rates in the loop and pressurizer. Measurement of flow rate vs pressure drop is made on each of these units prior to final assembly of the loop.

Measured flow rates in the development loop are as follows: core sample unit, 5 gpm; in-line sample unit, 5 gpm; pressurizer, 5 cc/sec. Temperature and pressure controls of the loop were found to be

[14] C. D. Zerby, T. H. Mauney, and C. B. Graham, *HRP Quar. Prog. Rep. Oct. 31, 1953*, ORNL-1658, p 74.

excellent. It was quite feasible to shut down and then to return to a given set of operating temperatures within ± 1°C. Under normal operating conditions there is no detectable change or drift of any of the control conditions. All the loop components equal or exceed the design requirements. The pressurizer line heater (1500 w) will maintain the pressurizer temperature at the required 30°C above the main stream temperature with about 800 w. The cooling capacity of the loop cooler was evaluated at about 1000 w with a cooling-water flow rate of 0.15 gpm. At a cooling-water flow rate of 2 gpm, the cooling capacity is increased to approximately 2000 w.

Tests on the in-pile development loop included a study of the steady-state equilibrium and distribution of gas between the main stream and pressurizer. Water and helium were used in these tests. After a large number of liquid samples taken from the main stream were analyzed for contained gas it was noted that actual contained gas was higher than that calculated for equilibrium at operating conditions. As a result of this discrepancy, the control instruments were calibrated by evacuating the gas space of the loop and operating with no gas in order to compare measured temperatures and pressures with absolute steam-pressure data. It is apparent that this type of calibration does not detect the individual errors of the various thermocouples, pressure cells, and indicating instruments but is the summation of all errors. For ease of calculation and definition, the total error found by the above calibration can be applied as a correction to either temperature or pressure measurements. Application of the "total error" correction found in the development loop resulted in agreement between calculated and actual values of contained gas in the main stream well within the limits of the sampling techniques and analytical methods (± 10%). The total error existing in the development loop was within the combined accuracy limits of the instruments and thermocouples. Thus it is planned to make this calibration on each in-pile loop during the test period prior to operation under radiation, along with flow measurements and general operating performance.

There has been no evidence of gas stratification in the pressurizer in the development loop.

The development loop is now operating with 0.17 *M* UO_2SO_4 solution containing 0.01 *M* $CuSO_4$. Prior to the start of the run (run 3) an instrument calibration of the loop was made as described above. The total error in the indicated temperature and pressure measurements was the same, within experimental limits, with the 0.17 *M* UO_2SO_4 + 0.01 *M* $CuSO_4$ as with water. The loop contains sample units previously described[15] and the flow rate of 5 gpm in the loop gives a maximum velocity of about 40 fps in the venturi type of sample holders as installed. The test coupons were exposed to all operations of the loop prior to the start of the uranyl sulfate run. This treatment consisted of 45 hr at 200 to 250°C with water and helium gas, 2.6 hr at 100°C with 3% trisodium phosphate and helium gas, 48 hr at 100°C with 5% nitric acid solution with helium gas.

Present operating conditions are 250°C in the main stream, 282°C in the pressurizer, with an initial partial pressure of oxygen of 116 psi. Initially 30 psig of oxygen was added to the loop (this is equivalent to ~ 1500 ppm). Results of this run, along with others, will be reported at a later date.

STATIC CORROSION STUDIES

J. L. English

Corrosion by Decontamination Solutions

A study was completed of metal-loss rates for seven different metals and alloys exposed in chemical solutions which were recommended for the decontamination of stainless steel surfaces. The materials examined in the investigation were restricted to those metals and alloys generally used in the construction and fabrication of dynamic corrosion test loops and which would be in contact with the chemical solution during the decontamination procedure. These metals were Stellite 6, Stellite 98M2, Inconel, Inconel X, tantalum, Zircalloy II, and type 347 stainless steel. The decontamination solutions were recommended by C. D. Watson and R. J. McNamee of the Chemical Technology Division and were of the following compositions:

1. 20 wt % HNO_3–3 wt % HF–balance, water;
2. inhibited 1.2 *M* HCl–1.8 *M* H_2SO_4;
3. inhibited 1.2 *M* HCl–1.8 *M* H_2SO_4–0.05 *M* H_2O_2.

[15] C. D. Zerby, R. J. Kedl, T. H. Mauney, R. E. Wascher, and W. L. Ross, *HRP Quar. Prog. Rep. Oct. 31, 1953*, ORNL-1658, p 73.

The inhibitor used in the $HCl-H_2SO_4$ solutions was an alkyl pyridine type and was added in concentrations of 2 ml/liter.

The corrosion tests were run in quiescent solutions at room temperature (~28 ± 2°C) and at 85 ± 2°C. The room-temperature tests were contained in covered, Polythene beakers and the tests at 85°C were operated under total reflux in flanged, stainless steel vessels. The total time for each test was 100 hr, and the specimens were removed for weighing and microscopic examination at cumulative periods of 1, 4, 24, 72, and 100 hr. The original solution was used for each 100-hr test.

The experimental results obtained with duplicate specimens are reported in Tables 11, 12, and 13. The apparent metal-thickness losses were calculated from the as-removed weight losses on the specimens.

The 20% HNO_3–3% HF solution at room temperature was the most corrosive of the three solutions tested. Stellite 6, with a metal-removal rate of less than 0.1 mil after 100 hr, was the best corrosion-resistant material of the six metals tested in this solution. The other metals – tantalum, type 347 stainless steel, Stellite 98M2, Inconel X, and Inconel – showed average thickness losses of 0.6, 0.9, 2.4, 2.8, and 17.7 mils, respectively, for 100-hr exposure periods. A localized type of corrosion attack was observed on all metals except Stellite 6 and type 347 stainless steel. The surfaces of the Stellite 6 were virtually unattacked; the type 347 stainless steel surfaces were severely roughened in appearance but there were no positive indications of localized corrosion attack observed at a magnification of 30X.

Corrosion attack on the metals exposed in inhibited 1.2 M HCl–1.8 M H_2SO_4 solution at room temperature was fairly mild in intensity and the metal-removal rates for the 100-hr tests did not exceed 0.1 mil. The attack was of a uniform nature in all cases. With the exception of the Stellite 6 specimens and specimens of type SAE 1015 carbon steel which were included in this particular series of tests, none of the other metals showed a definite susceptibility toward increased corrosion attack as the solution temperature was increased from 28 to 85°C. At the higher temperature, the metal loss rates remained at nominal values of 0.1 mil and less. The corrosion behavior

TABLE 11. APPROXIMATE METAL-THICKNESS LOSSES ON MATERIALS EXPOSED IN 20 wt % HNO_3–3 wt % HF SOLUTION AT 28 ± 2°C

MATERIAL	METAL REMOVED (mils)					TYPE OF ATTACK
	1 hr	4 hr	24 hr	72 hr	100 hr	
Stellite 6	<0.1	<0.1	<0.1	<0.1	<0.1	Uniform
	<0.1	<0.1	<0.1	<0.1	<0.1	
Stellite 98M2	<0.1	<0.1	0.2		2.0	Localized
	<0.1		0.1	0.8	2.8	
Inconel	0.2	0.6	1.6	9.1	17.5	Localized
	0.2	0.6	1.5	8.9	17.9	
Inconel X	0.1	0.5	2.3	2.5	2.8	Localized
	0.1	0.4	2.2	2.4	2.7	
Tantalum	<0.1	<0.1	0.1	0.3	0.6	Localized
	<0.1	<0.1	0.1	0.3	0.6	
Type 347 stainless steel	0.1	0.2	0.4	0.7	0.9	Heavy surface roughening
	0.1	0.2	0.4	0.7	0.9	

of Stellite 6 was temperature-dependent, however, and the metal-removal rate increased from 0.1 mil at 28°C to 1.7 mils at 85°C. Corrosion attack was localized at this temperature. Type SAE 1015 carbon steel was severely attacked after 27 hr at 85°C, and the nominal depth of metal removed was nearly 32 mils.

The addition of 0.05 *M* hydrogen peroxide to the 1.2 *M* HCl–1.8 *M* H_2SO_4 solution at 28 and 85°C resulted in little over-all change in corrosion behavior of the metals from their behavior in the peroxide-free solution. The only significant difference noted was with the Stellite 98M2 specimens at 85°C. In the peroxide-free solution, the

TABLE 12. APPROXIMATE METAL-THICKNESS LOSSES ON MATERIALS EXPOSED IN INHIBITED 1.2 *M* HCl–1.8 *M* H_2SO_4 SOLUTION AT 28 AND 85 ± 2°C

MATERIAL	TEMPERATURE (°C)	METAL REMOVED (mils)					TYPE OF ATTACK
		1 hr	4 hr	24 hr	72 hr	100 hr	
Stellite 6	28	*	*	<0.1		0.1	Uniform
		<0.1	<0.1	<0.1	0.1	0.1	
	85	<0.1	0.2	1.3	1.6	1.6	Localized
		0.1	0.3	1.6	1.7	1.7	
Stellite 98M2	28	<0.1	<0.1	<0.1		<0.1	Uniform
		<0.1		<0.1	0.1	0.1	
	85	<0.1	<0.1	0.1	0.2	0.2	Uniform
		<0.1	<0.1	0.1	0.1	0.1	
Inconel	28	<0.1	<0.1	<0.1	<0.1	<0.1	Uniform
		<0.1	<0.1	<0.1	<0.1	<0.1	
	85	<0.1	<0.1	<0.1	0.1	0.1	Uniform
		<0.1	<0.1	<0.1	0.1	0.1	
Inconel X	28	*	*	<0.1	<0.1	<0.1	Uniform
		<0.1	<0.1	<0.1	<0.1	<0.1	
	85	*	*	<0.1	<0.1	<0.1	Uniform
		<0.1	<0.1	<0.1	<0.1	<0.1	
Tantalum	28	*	*	*	*	*	None observed
		*	*	*	*	*	
	85	*	*	*	*	*	None observed
		*	*	*	*	*	
Zircalloy II	28	*	*	*	*	*	None observed
		*	*	*	*	*	
	85	*	*	*	*	*	None observed
		*	*	*	*	*	
Type 347 stainless steel	28	<0.1	<0.1	<0.1	<0.1	0.1	Uniform
		<0.1	<0.1	<0.1	<0.1	0.1	
	85	<0.1	<0.1	<0.1	0.1	0.1	Uniform
		<0.1	<0.1	<0.1	0.1	0.1	
Type SAE 1015 corbon steel	85	0.1	0.5	31.8			Localized
		0.1	0.5	31.7			

*Negligible.

average metal loss on Stellite 98M2 was 0.2 mil in 100 hr; with hydrogen peroxide present in the solution, the average metal-removal rate was nearly 1 mil for the same period of time.

The 100-hr laboratory tests used to evaluate the corrosion behavior of metals in quiescent decontamination solutions served only to simulate, at best, the conditions generally encountered in standard decontamination procedures for stainless steel chemical-process equipment used for handling radioactive solutions. For example, in actual practice by the Chemical Technology Division, the

TABLE 13. APPROXIMATE METAL-THICKNESS LOSSES ON MATERIALS EXPOSED IN INHIBITED 1.2 M HCl–1.8 M H_2SO_4–0.05 M H_2O_2 SOLUTION AT 28 AND 85 ± 2°C

MATERIAL	TEMPERATURE (°C)	METAL REMOVED (mils)					TYPE OF ATTACK
		1 hr	4 hr	24 hr	72 hr	100 hr	
Stellite 6	28	<0.1	<0.1	<0.1	0.2	0.2	Uniform
		<0.1	<0.1	<0.1	<0.1	0.1	
	85	0.6	0.7	0.8	0.9	1.0	Uniform
		0.3	0.3	0.4	0.4	0.5	
Stellite 98M2	28	<0.1	<0.1		0.1	0.1	Uniform
		*	*	<0.1	0.1	0.1	
	85	0.1	0.1	0.1	0.4	0.7	Uniform
		0.1	0.2	0.4	0.9	1.2	
Inconel	28	<0.1	<0.1	<0.1	<0.1	<0.1	Uniform
		<0.1	<0.1	<0.1	<0.1	<0.1	
	85	<0.1	<0.1	<0.1	<0.1	<0.1	Uniform
		<0.1	<0.1	<0.1	<0.1	<0.1	
Inconel X	28	<0.1	<0.1	<0.1	<0.1	0.1	Uniform
		<0.1	<0.1	<0.1	<0.1	0.1	
	85	<0.1	<0.1	<0.1	<0.1	<0.1	Uniform
		<0.1	<0.1	<0.1	<0.1	<0.1	
Tantalum	28	*	*	*	*	*	None observed
		*	*	*	*	*	
	85	*	*	*	*	*	None observed
		*	*	*	*	*	
Zircalloy II	28	<0.1	<0.1	<0.1	<0.1	<0.1	Uniform
		<0.1	<0.1	<0.1	<0.1	<0.1	
	85	*	*	*	*	*	None observed
		*	*	*	*	*	
Type 347 stainless steel	28	<0.1	0.1	0.1	0.1	0.2	Uniform
		<0.1	0.1	0.1	0.1	0.2	
	85	<0.1	<0.1	<0.1	0.1	0.1	Uniform
		<0.1	<0.1	<0.1	0.1	0.1	

*Negligible.

20% HNO_3–3% HF solution is allowed to remain in contact with activated stainless steel surfaces for a period not exceeding 0.5 to 1 hr at room temperature. The 100-hr metal-removal rates reported in the present investigation would, on this basis, be roughly equivalent to between 100 and 200 decontamination cycles if the rate is linear with time. In view of the low frequency of decontamination cycles on large-scale process equipment, the time required to accumulate this number of treatments would undoubtedly be a matter of years.

In this preliminary study no attempt has been made to include the effects of variables such as solution movement and the buildup of dissolved metal ions in solution on metal-removal rates.

Other Studies

Other projects now in operation or planned for operation during the next quarter are as follows:

1. A study will be made of the corrosion of Zircalloy II at 250°C in oxygenated 0.02 *M* uranyl sulfate solutions containing 25 mole % excess sulfuric acid and 50, 200, 400, and 600 ppm of fluoride ion, respectively, added as uranyl fluoride.

2. The corrosion of Stellites 6 and 98M2 in oxygenated 0.17 *M* uranyl sulfate solution at 100°C, with and without 0.01 *M* cupric sulfate, will be studied. Various techniques for depositing Stellite 6 on type 347 stainless steel will be examined corrosion-wise, as will the galvanic corrosion behavior of both Stellite alloys with type 347 stainless steel.

3. The stress-corrosion behavior of type 347 stainless steel will be investigated in oxygenated 0.02 *M* uranyl sulfate solution containing 25 mole % excess sulfuric acid and 0.01 *M* cupric sulfate and in oxygenated 0.17 *M* uranyl sulfate solution containing 0.04 *M* cupric sulfate. Corrosion tests will be run at temperatures of 250 and 300°C and the specimens will be stressed to approximately 65,000 psi.

METALLURGY

E. C. Miller, Section Chief

CORROSION OF WELDED AUSTENITIC STAINLESS STEEL SPECIMENS

W. O. Harms W. J. Leonard

Microscopic examination of welded pin specimens, the dynamic-corrosion weight-loss data for which were reported previously,[1] indicated that, with but few exceptions, the welds were sound. In general, the corrosion appeared to proceed by a nonpreferential type of attack on both weld and base metal, except at the higher solution concentrations of 300 g of uranium per liter as UO_2SO_4, where the following results were observed:

1. Type 304 stainless steel base plate welded with type 347 stainless steel rod by use of the heliarc process exhibited intergranular type of corrosion attack with an accelerated corrosion attack, in the heat affected zone, under loop conditions of 150°C for 997 hr and 250°C for 117 hr.
2. Type 304L stainless steel base plate welded with type 347 stainless steel rod by use of the heliarc process exhibited no intergranular corrosion under similar loop conditions, the corrosion rate in the type 304L stainless steel base plate being about one-tenth that in the type 304.
3. Type 321 stainless steel base plate welded with type 347 stainless steel rod and tested at 175°C for 308 hr showed preferential attack on a microconstituent which was present as a banded, stringer structure. This constituent was identified as ferrite and has been reported elsewhere.[2] Microscopic study of types 304L and 347 stainless steel base plates, welded with type 347 stainless steel rod, show nearly identical corrosion resistance under varying corrosion conditions, both being superior to types 304 and 321.

A group of 178 welded pin specimens taken from austenitic stainless steel welds, as outlined previously,[1] was corrosion tested in 0.17 *M* UO_2SO_4 (40 g of uranium per liter) with 200-psi oxygen, at 250°C and 23 to 26 fps, for 400 hr. These welds included all possible combinations of types 347 and 304L stainless steel base plates, welded with three types of stainless steel rod: (1) commercial 347, (2) commercial 308L, and (3) an experimental fully austenitic 347 rod, referred to as composition "H" (nominal composition: 18% Cr–13% Ni, 5% Mn, and Cb). The various heat treatments employed are listed in Table 14. After cathodic defilming and weight determinations, the pins were examined macroscopically. Gross inconsistencies in weight-loss data which were observed were attributed to the fact that the flow rates used were in the transition zone for the test conditions employed. Initial evaluation of the data was made, however,

[1] W. O. Harms and W. J. Leonard, *HRP Quar. Prog. Rep. July 31, 1953*, ORNL-1605, p 112.

[2] R. J. Gray, T. M. Kegley, Jr., R. S. Crouse, and T. K. Roche, *Met. Semiann. Prog. Rep. Oct. 10, 1953*, ORNL-1625, p 72.

TABLE 14. HEAT TREATMENTS GIVEN TO WELDED PIN SPECIMENS PRIOR TO DYNAMIC-CORROSION TESTS

DESIGNATION	TREATMENT	REMARKS
A	As welded	
B	1000°F for 6 hr, air cool	Corresponds to a commercial stress relief
C	1625°F for 2 hr, furnace cool	Corresponds to a commercial stabilizing treatment
D	1625°F for 2 hr, water quench	Corresponds to a commercial stabilizing anneal
E	1625°F for 2 hr, water quench; 1000°F for 6 hr, air cool	Corresponds to a commercial stabilizing anneal plus stress relief
F	1950°F for ½ hr, water quench	Corresponds to a commercial solution anneal
G	1950°F for ½ hr, furnace cool	Corresponds to a commercial full anneal

by correlating weight-loss data with surface examinations. The results of this evaluation are given in Table 15, where it is seen that the most consistently satisfactory results were obtained for welds which were given a stress relief at 1000°F. The reason for the less satisfactory behavior of specimens solution-treated at 1950°F is not clear. The relative corrosion resistance of each of the three types of all-weld-metal specimens and the nine types of welds resulting from the several treatments will be evaluated in more detail by correlating the metallurgical data now being gathered by microscopic examination with the macroscopic observations and weight-loss data.

Special flat-plate-type corrosion specimens containing the welds discussed above were machined from each of the nine welded plates and have been prepared along with nine standards for loop testing. The standards are annealed wrought specimens of types 304, 304L, 310, 309 SCb, and 347 stainless steel. These specimens are now in a loop running under the conditions to which the pins were exposed, except that the flow rate is a subcritical 20 fps and the length of the run is to be 200 hr. The flat-plate type of specimen being used in this study possesses a raised face which makes larger flat areas available for surface study by metallographic examination. The design of the plates is planned so that several tests can be performed on a single specimen.

PROPERTIES OF TITANIUM AND ZIRCONIUM ALLOYS

W. J. Fretague

Commercial Titanium

A titanium pin-specimen holder made from Rem-Cru commercial purity RC-70 titanium (Heat No. 3102, REED Item No. 11), exposed to various loop environments for approximately 2000 hr, cracked when an attempt was made to cold-straighten it after reclaiming by welding. Specimens for impact testing will be prepared from both the specimen holder and the as-received plate from which it was machined in order to determine the effect of long-time exposure to aqueous homogeneous reactor

TABLE 15. EVALUATION OF DYNAMIC CORROSION TESTS ON HEAT-TREATED WELDED AUSTENITIC STAINLESS STEEL SPECIMENS[a]

DESIGNATION	TREATMENT	EVALUATION[b]					
		Specimens[c] in Which Only Weld Metal Was Exposed to Solution			Specimens in Which Both Base and Weld Metals Were Exposed to Solution		
		Composition "H"	Type 347	Type 308L	Composition "H"	Type 347	Type 308L
A	As welded	S	S	U	S	S	M
B	1000°F for 6 hr, air cool	S	S	S	S	S	S
C	1625°F for 2 hr, furnace cool	M	M	U	M	M	M
D	1625°F for 2 hr, water quench	M	M	M	M	M	M
E	1625°F for 2 hr, water quench; 1000°F for 6 hr, air cool	M	S	S	M	S	S
F	1950°F for ½ hr, water quench	U	U	U	M	U	U
G	1950°F for ½ hr, furnace cool	M	S	S	S	S	M

[a]Specimens tested in 0.17 M UO_2SO_4 (40 g of uranium per liter) with 200-psi O_2 at 250°C and 23 to 26 fps for 400 hr.

[b]S: satisfactory; film integrity maintained.
M: marginal; film and underlying metal removed in some places.
U: unsatisfactory; film and underlying metal completely removed.

[c]Composition "H", 347, 308L denote types of stainless steel welding rod used.

fuel solutions on the impact properties (transition temperature) of commercial titanium.

Zirconium-Tin-Iron-Chromium-Nickel-Carbon (Zircalloy II)

Specimens of Zircalloy II were swaged to 0.217-in. dia, from ⅜-in.-dia rod, which had been sand blasted, pickled, vacuum annealed at 750°C for 2 hr, and furnace cooled prior to machining. Impact tests were performed on 8 of the 16 specimens described in the previous quarterly report.[3] One set of four multiple-break specimens was exposed to UO_2SO_4 containing 5 g of uranium per liter plus 0.005 *M* H_2SO_4 at 250°C for 1010 hr with 200-psi oxygen (run G-4). The impact data obtained are listed in Table 16 and appear also in Fig. 38. The other set of four multiple-break specimens was exposed to the same solution at 300°C for 693 hr (run G-5). The data obtained from these specimens appear in Table 17 and are plotted in Fig. 39. The data presented here and in the previous quarterly progress report[3] indicate that exposure to the corrosive environments studied to date does not affect the impact properties of Zircalloy II.

Considerable assistance has been furnished by Metallurgy Group personnel in securing Zircalloy II specimens for the in-pile loop experiments. The in-pile loop program will require approximately 25 corrosion impact specimens every two months for the next twelve months.

[3] W. J. Fretague, *HRP Quar. Prog. Rep. Oct. 31, 1953*, ORNL-1658, p 77.

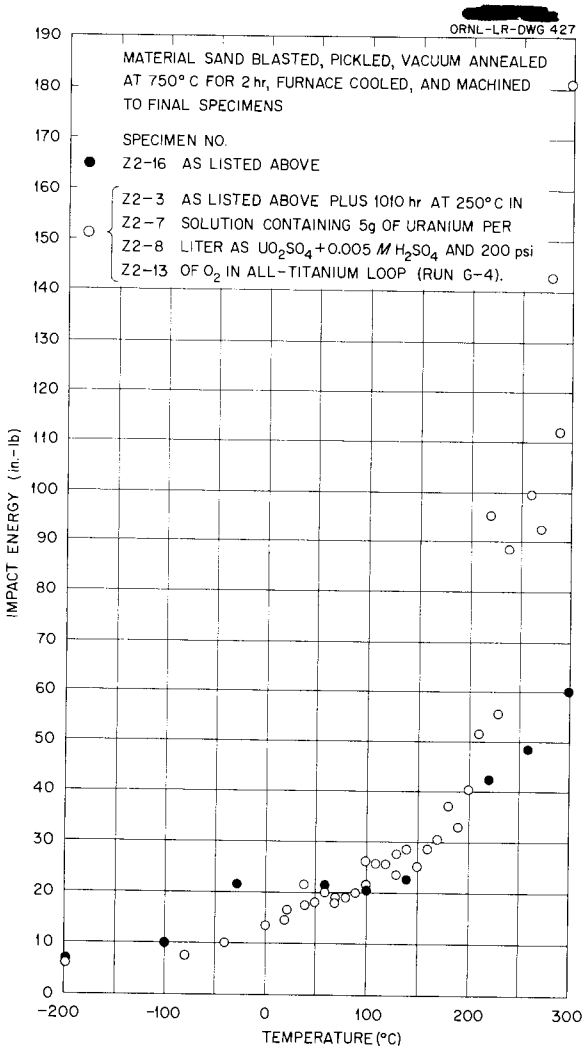

Fig. 38. Effect of Temperature on Impact Strength of Zircalloy II.

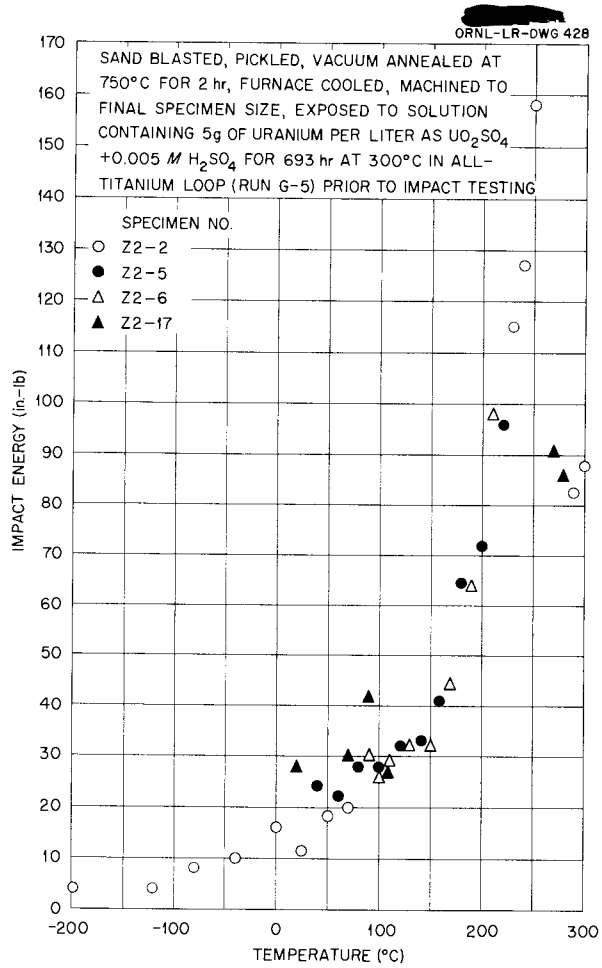

Fig. 39. Effect of Temperature on Impact Strength of Zircalloy II.

TABLE 16. IMPACT ENERGY vs TESTING TEMPERATURE DATA FOR SWAGED AND VACUUM-ANNEALED ZIRCALLOY II SPECIMENS EXPOSED IN UO_2SO_4 CONTAINING 5 g OF URANIUM PER LITER PLUS 0.005 M H_2SO_4 AT 250°C FOR 1010 hr AT 200-psi O_2

SPECIMEN NO.	NOTCH NO.	SCALE USED (in.-lb)	TEMPERATURE (°C)	IMPACT ENERGY (in.-lb)	REMARKS
Z 2-3	1	0–100	23.5	16.5	
	2	0–100	0	13.5	
	3	0–100	−40	10.0	
	4	0–100	−80	7.5	
	5	0–100	−120	50.0[a]	
	6	0–100	−195.6	6.0	
	7	0–100	50	18.0	
	8	0–100	70	19.0	
	9	0–200	290	112[b]	
	10	0–200	300	181	Did not break completely
Z 2-7	1	0–100	40	17.5	
	2	0–100	60	20.0	
	3	0–100	80	19.0	
	4	0–100	100	21.5	
	5	0–100	120	25.5	
	6	0–100	140	28.5	
	7	0–100	160	28.5	
	8	0–100	180	37.0	
	9	0–100	200	40.5	
	10	0–100	220	95.5	Did not break completely
Z 2-8	1	0–100	100	26	
	2	0–100	130	23.5	
	3	0–100	150	25	
	4	0–100	170	30.5	
	5	0–100	190	33	
	6	0–100	210	51.5	
	7	0–100	240	88.5	Did not break completely
	8	0–200	260	99.5	
	9	0–200	90	40[c]	
	10	0–200	110	43[c]	
Z 2-13	1	0–100	20	14.5	
	2	0–100	40	21.5	
	3	0–100	70	18.0	
	4	0–100	90	20.0	
	5	0–100	110	25.5	
	6	0–100	130	27.5	
	7	0–100	230	55.5	
	8	0–100	250	>100[b]	
	9	0–200	270	92.5	Did not break completely
	10	0–200	280	142.5	

[a]Pendulum struck specimen-catching tray.

[b]Specimen did not break completely, low in the vise, bent above notch.

[c]These values *do not* appear in Fig. 38.

TABLE 17. IMPACT ENERGY vs TESTING TEMPERATURE DATA FOR SWAGED AND VACUUM-ANNEALED ZIRCALLOY II SPECIMENS EXPOSED IN UO_2SO_4 CONTAINING 5 g OF URANIUM PER LITER PLUS 0.005 *M* H_2SO_4 FOR 693 hr AT 300°C (RUN G-5) PRIOR TO IMPACT TESTING

Scale Used: 0 to 200 in.-lb

SPECIMEN NO.	NOTCH NO.	TEMPERATURE (°C)	IMPACT ENERGY (in.-lb)
Z 2-2	1	25	11.5
	2	0	16
	3	−40	10
	4	−80	8
	5	−120	4
	6	−195.6	4
	7	50	18
	8	70	20
	9	290	83
	10	300	88
Z 2-5	1	40	24
	2	60	22
	3	80	28
	4	100	28
	5	120	32
	6	140	33
	7	160	41
	8	180	65
	9	200	72
	10	220	96
Z 2-6	1	90	30
	2	100	26
	3	110	29
	4	130	32
	5	150	32
	6	170	44
	7	190	64
	8	210	98
	9	250	158
Z 2-17	1	20	28
	3	70	30
	4	90	42
	6	110	27
	7	230	115
	8	240	127*
	9	270	91*
	10	280	86*

*Specimen broke loose in loop and wore flat on one side. Flat side placed away from pendulum.

SELECTIVE OXIDATION OF AUSTENITIC STAINLESS STEELS

T. W. Fulton W. O. Harms

A limited number of dynamic-corrosion tests and film studies on moist-hydrogen-pretreated austenitic stainless steel pins was carried out during this quarter. Specimens of type 304L stainless steel were pretreated for 1 hr at temperatures of 700, 1300, and 1900°F and at moisture contents of about 0.2, 2.5, and 5 to 9 vol % at each temperature. Also, pins of types 304L, 347, 321, and 309 SCb stainless steel were pretreated at 1850°F for ½ hr in hydrogen containing 0.5, 0.7, and 2.8 vol % moisture.

The pins were tested in oxygen-pressurized 0.06 M UO_2SO_4 (15 g of uranium per liter) plus 0.015 M H_2SO_4 (25 mole % excess) for 200 hr at 250°C and 61 fps. Previous tests had shown that these conditions were convenient for sorting purposes. The results are summarized in Table 18 where it is seen that, for the short times considered here, optimum pretreatment conditions include low moisture contents at high temperatures. It is of interest that these conditions, except for moisture control, are similar to those used in the full-annealing of 300-series stainless steels. It appears also that type 309 SCb (a stabilized 25-12 Cr-Ni steel) is more consistently satisfactory under these conditions than are types 304L and 347. On the other hand, at slightly higher moisture contents, type 309 SCb may fail, whereas types 304L and 347 perform satisfactorily.

Film studies on all specimens except those

TABLE 18. RESULTS OF DYNAMIC CORROSION TESTS[a] ON MOIST-HYDROGEN-PRETREATED AUSTENITIC STAINLESS STEEL PINS

PRETREATMENT CONDITIONS[b]			DEFILMED WEIGHT LOSSES[c]		
Temperature (°F)	Time (hr)	H_2O (vol %)	0 to 3 mg	12 to 15 mg	40 to 140 mg
700	1	0.2			304L (2)
		2.5			304L (2)
		5.6			304L (2)
1300	1	0.2			304L (2)
		2.4			304L (2)
		9.1			304L (2)
1900	1	0.2	304L (2)		
		2.4			304L (2)
		4.6			304L (2)
1850	½	0.5	309 SCb (2)		347 (1), 304L (2)
		0.7	309 SCb (2)	304L (1)	347 (2), 304L (1)
		2.8	304L (2), 347 (1)	309 SCb (1)	347 (1), 309 SCb (1)
As-machined pins					309 SCb (3), 347 (1)
					304L (4), 321 (2)
					304 (1)

[a]Loop run M-6: 0.06 M UO_2SO_4 (15 g of uranium per liter) plus 0.016 M H_2SO_4 (25 mole % excess), 250°C, 200 hr, 61 fps. This run also included eight specimens which were pretreated in air at 750°F for ½ hr and which lost from 107 to 127 mg in the test.

[b]Prior to the pretreatments listed, all pins were fully annealed and electropolished.

[c]Specimens are listed as to AISI designation; the number of specimens tested is given in parentheses.

treated at 1850°F, using (1) electron diffraction and microscopy and (2) x-ray diffraction and fluorescence analysis, showed that specimens which exhibited satisfactory corrosion resistance were protected by pretreatment films containing both spinels having high lattice parameters [probably $Fe(Fe_{0.5}Cr_{1.5})O_4$] and Cr_2O_3 (±10% alpha Fe_2O_3). Indications were that the rhombohedral X_2O_3 phase was contained only in the inner layer of these films. Less satisfactory films were made up of spinels of lower lattice parameter and considerably less chromium content. Films formed at higher moisture contents contained varying amounts of alpha Fe_2O_3.

The results of tests on pretreatment films thus far indicate that the corrosion resistance of austenitic stainless steels under adverse conditions of uranyl sulfate solution composition and flow rate depends to a large extent on the nature of the oxide film formed initially on the alloy. Thus it appears that the existence of a high-chromium spinel structure and perhaps the Cr_2O_3 enhance film integrity and that initial exposure to a limited oxidizing environment designed to promote the formation of this type of film should render much less probable the failure of reactor components subjected to such adverse conditions.

AQUEOUS SOLUTION AND RADIATION CHEMISTRY

HOMOGENEOUS REACTOR SOLUTIONS UNDER IRRADIATION

C. H. Secoy
H. O. Day
Q. V. Larson
M. D. Silverman
F. H. Sweeton
L. F. Woo
W. C. Yee

Microscopic Examination of Bombs

Several bombs have been cut open in order to study the corrosion of the interior walls. The irradiated bombs were examined by M. J. Feldman and co-workers in the Solid State Division, and the unirradiated bombs were examined by T. E. Willmarth and co-workers of the Analytical Chemistry Division.

Bomb H-2, which had been tested under conditions of relatively high partial pressure of oxygen and at a power density of 6 kw/liter, had resulted in an average rate of corrosion of about 2 mpy as calculated from the pressure.[1] The bomb was cut to give sections at right angles to the axis of the bomb from both the solution and vapor regions. The examination showed[2] that there had been no intergranular or void type of corrosion. There were indications that the films in the solution phase were thicker than those in the vapor phase.

In test H-11 the fission power density was 2 kw/liter, a relatively low value. The corrosion rate[3] as calculated from pressure measurements decreased during the test and averaged only about 0.2 mpy for the whole period. Examination[2] of this bomb showed, as in the previous case, that there was no intergranular or void type of corrosion and gave indications that the film in the solution phase was thicker than that in the vapor.

Bomb H-15 was made of titanium and was tested out-of-pile. The corrosion curve as calculated from pressure data[3] started off at a high rate, but after about two weeks and an apparent corrosion of about 0.15 mil it stabilized with essentially no further corrosion for the remaining three weeks of the test. When this bomb was cut open, the vapor phase was found to have a dull white coating, while the solution phase was relatively uniform in color and fairly shiny, indicating that the vapor phase had undergone more corrosion than had the liquid phase. It was found[4] that the film in both areas and also at the solution-vapor interface contained both the rutile phase of TiO_2 and a titanium-uranium compound that has been observed in an all-titanium loop test. Examination of the bomb also showed that it had been constructed of titanium containing peculiar inclusions. A stringy fibrous structure was found between the normal titanium metal and the inclusion. Where these inclusions were exposed to the solution, they served as sites for pit type of corrosion. Electron-diffraction measurements of the corrosion products found at the site of these pits indicated that the material is probably the same compound that, as mentioned above, was found in the all-titanium loop and appears to be a titanium-uranium compound.

Bomb H-16 was made of type 347 stainless steel and was tested without radiation.[3] Electron-diffraction studies[5] indicated that Fe_2O_3 was present in the film found in the vapor phase, in the solution phase, and on the outside of the bomb, which was exposed to air during the test. The ultimate crystallites in the vapor phase appeared to be the largest and those on the outside of the bomb to be the smallest. There was a heavier deposit of corrosion material in the vapor phase than in the solution phase. A spectrographic analysis of material removed from the film at the solution-vapor interface showed 21% Cr, 57% Fe, 7% Ni, and 15% Mn (at present there is no explanation for the high concentration of manganese). Electron-diffraction patterns of bulk oxide taken from the top of the vapor phase indicated the presence of manganese oxide hydrate. Chemical analysis indicated the presence of only 1 ppm of chloride ion in the solution during the test.

New Irradiations

Three bombs, H-18, H-19, and H-20, have been irradiated this quarter. All these tests were terminated before all the excess oxygen was consumed

[1] C. H. Secoy *et al.*, *HRP Quar. Prog. Rep. Oct. 1, 1952*, ORNL-1424, p 94.

[2] A. E. Richt, R. U. Acton, M. J. Feldman, and E. S. Schwartz, *Metallographic Analysis of HRE Corrosion Capsules H-2 and H-11*, ORNL CF-53-12-114 (Dec. 17, 1953).

[3] C. H. Secoy *et al.*, *HRP Quar. Prog. Rep. Oct. 31, 1953*, ORNL-1658, p 108.

[4] T. E. Willmarth, *Microscopic and Electron Diffraction Study of Titanium Bomb H-15*, ORNL CF-54-1-126 (Jan. 21, 1954).

[5] T. E. Willmarth, *Microscopic Examination of Bomb From Test H-16*, ORNL CF-54-1-39 (Jan. 12, 1954).

in order to avoid precipitation of reduced uranium. Due to instrumental difficulties, pressure data were not available for calculating the corrosion of bomb H-18, which was tested at a temperature of 290°C. However, the total-corrosion calculation based on the amount of excess oxygen added as H_2O_2 at the start of the test and on the amount and composition of the gas left in the bomb at the end of the test showed that the corrosion, if averaged over the surface of the solution phase, was 0.11 mil (if averaged over the whole internal surface, 0.07 mil) for the test period of 0.7 week. The experimental conditions of this test can be found in Table 19.

The corrosion of bomb H-19 as calculated from the partial pressure of excess O_2 read at several times during the test is shown in Fig. 40. The mathematical factor used to convert from pressure to corrosion was determined, as has been done previously in such calculations, on the assumption that the corrosion is averaged over the solution phase of the bomb surface and that there is no selective leaching of any one material out of the bomb surface. A similar calculation to give corrosion averaged over the whole of the surface would give figures about 70% as large.

The pressure data for bomb H-20 have been handled in the same manner and the calculated corrosion is shown in Fig. 41. This test differed from the others in that it contained technetium. Since there is uncertainty in how the corrosion represented by the oxygen absorption is divided between the vapor and solution phases, the evaluation of the effect of technetium will need to wait until the corrosion pins and the bomb are examined.

Solution Analyses

In the past few months the Analytical Chemistry Group working at the HRE has taken over the responsibility for analyzing the irradiated solutions. Because of increased emphasis this work has proceeded faster than heretofore, and it has been possible to make the calculations given in Table 19 (for data on previous tests see earlier report[6]). This table shows the status of the experimental work at the present time.

The uranium analyses indicate that in the majority of cases uranium has been completely recovered, within the experimental error of the determination. Tests H-10 and H-19 both showed high corrosion rates (0.1 mil in 1 to 3 weeks) and therefore in their cases the discrepancies in uranium recovery are of somewhat limited practical interest. However, in the case of test H-11 the observed corrosion amounted to only 0.05 mil in a total of 12 weeks, and the rate was continually decreasing. As far as is known, the apparent loss of uranium is a valid effect, although no confirmation of the loss of uranium was found from the analysis of the loose precipitate suspended in the solution that was removed from the bomb after the test. Future work will be necessary to clarify this situation. Test H-14 is the only one of this series to be made with titanium in pile

[6] B. O. Heston *et al.*, *HRP Quar. Prog. Rep. July 31, 1953*, ORNL-1605, p 130.

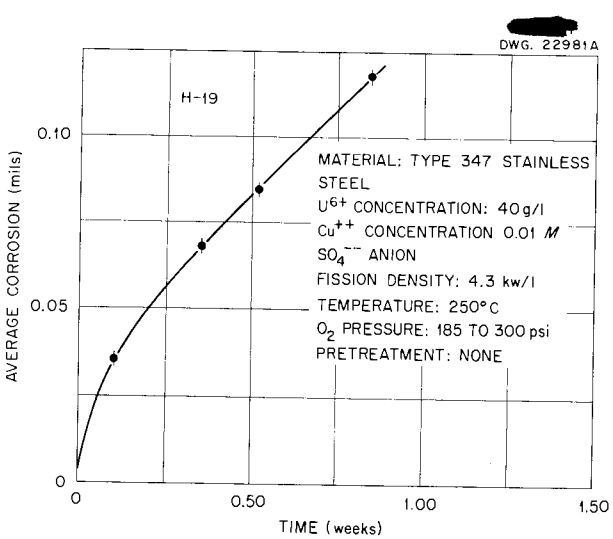

Fig. 40. Static In-Pile Corrosion Test H-19.

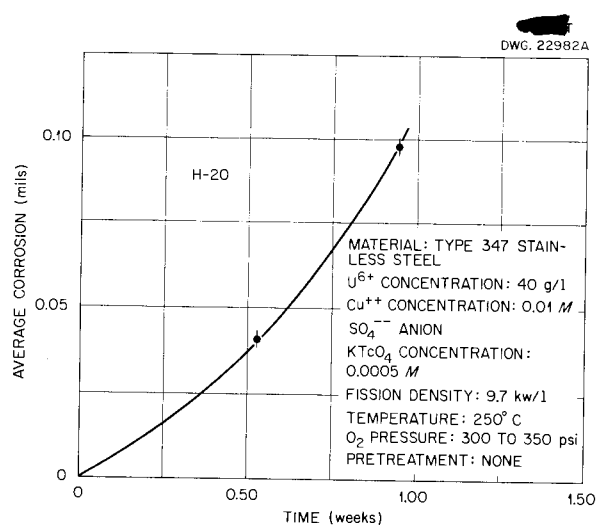

Fig. 41. Static In-Pile Corrosion Test H-20.

TABLE 19. RESULTS OF ANALYSES OF SOLUTIONS FROM TESTS

	TEST NUMBER								
	H-10	H-11	H-12	H-13	H-14	H-15	H-16	H-18	H-19
Bomb material	Type 347 stainless steel	Type 347 stainless steel	Type 347 stainless steel	Type 347 stainless steel	Titanium	Titanium	Type 347 stainless steel	Type 347 stainless steel	Type 347 stainless steel
U^{6+} concentration, g/liter	40	40	39	35	39	41	37	39	40
Cu^{++} concentration, M	0.010	0.010	0.010	0.009	0.014	0.005	0.005	0.009	0.012
Pretreatment	Etch	Etch	a	a	None	None	None	None	None
Temperature, °C	250	250	290	250	250 to 270	250	250	290	250
O_2 partial pressure: at start, psi	325	233	125	350	270	150	120	b	300
at end, psi	235	140	90	280	195	50	80	b	185
Power density,[c] kw/liter	6	2.1	6.3	3.8	5 to 10	0	0	6.4	4.3
Duration of test, weeks	3	12	1.5	0.9	8.3	5	5	0.7	0.8
Radiation dosage, kw-weeks/liter	18	25	9.4	3.4	70	0	0	4.7	3.7
Calculated[d,e] cumulative corrosion, mils	0.11 to 0.16	0.05	0.10	0.13	0.21	0.15	0.03	0.11	0.13
U^{6+} charged, mg	159	173	170	154	193	195	178	183	199
Ratio of U^{6+} recovered[f] to U^{6+} charged, %	91	84	98	98	80	98	100	98	92
Cu^{++} charged, mg	2.7	2.7	2.7	2.5	4.5	1.5	1.3	2.8	3.7
Ratio of Cu^{++} recovered[f] to Cu^{++} charged, %	60	90	100	42	109	g	g	95	84
Ni^{++} calculated[d] to be in solution, mg	5.5	2.5	5.2	6.5		0	1.7	5.0[h]	6.9
Ratio of Ni^{++} found[f] to Ni^{++} calculated, %	150	95	55	35		g	58	47	53
SO_4^{--} charged, mg	69	74	72	66	86			80	86
Ratio of SO_4^{--} recovered[f] to SO_4^{--} charged, %	103	101	107	96	103	g	g	104	122
Ratio of S^{--} found[f] to sulfur in SO_4^{--} charged, %	0.5	0.1	g	0.1	0.3	g	g	0.2	0.2
pH of solution charged	2.7[i]	2.7[i]	2.7[i]	2.7[i]	2.7[i]	2.2	2.2	2.7[i]	2.7[i]
pH of solution recovered	3.5	3.2_5	3.0_0	3.6_5	2.4	2.4	2.5	2.9_2	2.8_9

[a]Inside surface of bomb was electropolished.
[b]Pressure data were not obtained.
[c]Based on volume at room temperature.
[d]From oxygen pressure data, assuming no selective oxidation of any component of the stainless steel.
[e]Averaged over wetted surface.
[f]In solution.
[g]Not analyzed for.
[h]Calculated from amount of O_2 added (as H_2O_2) and O_2 recovered.
[i]Based on solution composition, not actually measured.

radiation and therefore will also require further work before definite conclusions can be drawn.

Both the copper and nickel analyses indicate erratic recoveries. It is difficult to determine whether the copper and nickel analyses represent anomalies in the behavior of copper and nickel in this chemical system or whether the unusual difficulties and chemical effects caused by the radioactivity in solution cause erroneous results.

In general the sulfate analyses indicate within experimental accuracy that the sulfate ion is stable. One or two tests indicate obvious errors in manipulation, since the calculation shows significantly more sulfate ion recovered than was supposedly loaded into the bombs at the beginning of the tests.

Analyses for reduced forms of sulfur do not indicate, it is believed, any experimentally significant amount of such sulfur.

Conclusions

Examination of one stainless steel out-of-pile bomb (H-16) has shown the presence of Fe_2O_3 on the walls of the bomb in both the solution and vapor phases, the Fe_2O_3 crystallites in the vapor phase being larger than those in the solution. No evidence of pit or void type of corrosion has been found in the two in-pile stainless steel bombs (H-2 and H-11) that have been examined. The uranium-titanium compound previously found in the all-titanium loop has been also found in an out-of-pile titanium bomb (H-15) in addition to the rutile phase of TiO_2.

Examination of two out-of-pile bombs (H-15 and H-16) has shown that the vapor phase of both stainless steel and titanium bombs can be corroded significantly, and therefore conclusive corrosion data on the solution phase alone cannot be obtained from pressure data without modifying the technique. Metallographic studies show that the metal used in some of the bombs (H-16 and H-15) has abnormal physical structure and therefore is not suitable for use in conclusive tests.

The solution analyses that have been carried out to date show inconsistencies. It is believed necessary to alter the experimental methods of carrying out the tests and also to improve the reliability of the existing experimental techniques of analysis before precise material balances on the various constituents of the solutions can be calculated.

Future Plans

Plans for all future tests, both in-pile and out-of-pile, involve modification of the pressure-measuring technique to eliminate having vapor-phase corrosion. Two methods are being tried; one involves the use of a platinum liner to eliminate any stainless steel in the vapor phase (the stainless steel being under solution in the form of corrosion pins), and the other method is to rock a bomb continuously so that the whole internal surface of the bomb is covered by a film of the solution at all times. Both methods will be tried, as each requires some study to prove that it will work satisfactorily.

All metal used for corrosion work is now being ordered through E. C. Miller, who is in charge of the metallurgy work of this project. The metal will be analyzed chemically and will be examined microscopically before use in the corrosion tests.

Preparations are finished for a new series of out-of-pile tests. The first tests will be oriented toward evaluating the proposed modifications of the pressure method of measuring corrosion.

BLANKET SYSTEMS

THORIUM OXIDE CHEMISTRY

D. E. Ferguson[1] R. G. Mansfield
J. P. McBride M. E. Whatley[1]
L. E. Morse W. L. Pattison

The development of an aqueous thorium oxide slurry for use in the blanket of a thermal power breeder reactor has continued.[2,3] Effort has been concentrated on methods of preparing the oxide, with thorium nitrate as the source material for all preparations. The conversion of thorium nitrate to oxide via the oxalate, formate, and oxycarbonate has been investigated.

The desirability of a particular preparation method is, of course, determined by the ultimate use of the oxide in an aqueous slurry at 250 to 300°C. Therefore the product should have the physical characteristics of small particle size and minimum abrasiveness, it should be attainable in slurry form in excess of 1000 g of thorium per liter and should be sufficiently pure chemically, and its slurry properties should not become impaired when it is subjected to prolonged heating in water at 250 to 300°C.

Previous work has shown the abrasiveness of the oxide to vary considerably with the method of preparation and treatment, the most striking example being the increase in abrasiveness that results from an increase in calcination temperature in the thermal decomposition of thorium oxalate.[3] Particular attention has therefore been given to the abrasiveness of the product oxide by use of a laboratory abrasion test described in earlier reports.[4]

The use of thorium nitrate as a source material prampted special concern as to the nitrate content of the product oxide. In addition, the effect of nitrate on pH, corrosion, particle growth, and general slurry properties has not yet been fully evaluated in the laboratory and engineering testing. However, in view of the high solubility of thorium nitrate even at 250°C and its significant hydrolysis at this temperature, a high nitrate impurity could be expected to have deleterious effects; thus the nitrate content of the product oxides has been of special interest.

An additional criterion for a desirable method of preparation, prompted by the ultimate utility of the oxide, is that the method should be adaptable to large-scale preparation, preferably by remote operation, with a maximum of wet handling to reduce the hazards associated with slurry refabrication from oxide which has already been irradiated. The work on the hydrolysis of thorium formate will be of particular interest in this regard.

Preparation of Thorium Oxide From Thorium Oxalate

Thermal Decomposition. During the past quarter the preparation of ThO_2 having a minimum nitrate content has been emphasized. Thorium oxide produced at Ames by thermal decomposition of the oxalate at 650°C usually contains less than 10 ppm of nitrate. Previous work has shown that the abrasiveness of thorium oxide prepared from thorium oxalate could be decreased by lowering the temperature at which the oxalate is decomposed[3] but has not fully clarified the effect of "low burning" on subsequent slurry properties and has not been comprehensive enough to demonstrate the efficiency with which nitrate impurities could be removed by the "low burning" procedure.

More detailed examination of the calcination procedure showed that decomposing the oxalate initially at 375 to 400°C and then at 475 to 500°C gave a product of much finer particle size (0.1 μ) and gave better bed-temperature control than was possible with a direct decomposition of the oxalate at the higher temperature. Subsequent autoclaving of a portion of the oxide product in water yielded a slurry with a pronounced tendency to pack. Reheating the rest of the material at 575 to 600°C removed all tendency to pack and reduced the nitrate content from 4000 ppm to less than 200 ppm. Hence the subsequent studies on the nitrate content of thorium oxalate and the oxide product of its thermal decomposition were carried out by utilizing a two-temperature calcination procedure that consisted in an initial heating at 370°C and a final heating at not less than 600°C.

[1] Part time.

[2] F. R. Bruce *et al.*, *HRP Quar. Prog. Rep. July 31, 1953*, ORNL-1605, pp 135-146.

[3] J. P. McBride, L. E. Morse, and W. L. Pattison, *HRP Fuel and Blanket Studies Quarterly Report*, ORNL CF-54-1-34 (Oct. 31, 1953).

[4] J. P. McBride and W. L. Pattison, *HRP Quar. Prog. Rep. July 31, 1953*, ORNL-1605, p 139.

Simple washing with hot water of the thorium oxalate precipitated from an acid thorium nitrate solution at 70 to 80°C was not efficacious in removing nitrate below a few tenths per cent. In a typical preparation (cf. Table 20, method 4) the oxalate was washed with five complete changes of water, each wash consisting of a digestion for 1 hr at 70°C followed by a filtration step. The resulting thorium oxalate contained 44.47% thorium and 0.38% nitrate.

Experiments were carried out to determine the effect of the oxalate precipitation method and of various washing and/or calcination methods on the nitrate content of the final oxide product. The data obtained are presented in Tables 20 through 23.

Table 20 lists the precipitation methods studied, Table 21 gives the oxalate treatment and decomposition procedures, and Tables 22 and 23 list the nitrate contents of oxide products obtained by various combinations of precipitation and decomposition methods.

Examination of Table 22 indicates that treatment of the oxalate by method A or C resulted in ThO_2 with a lower NO_3^- content than could be obtained by the straightforward calcination of the oxalate and that precipitation by method 4 is the least satisfactory. It is difficult to choose between the remaining precipitation methods on the basis of the results; however, method 1 should be favored because a higher concentration of Th(IV) was used

TABLE 20. METHODS OF PRECIPITATION OF THORIUM OXALATE

METHOD	REAGENT CONCENTRATIONS	PRECIPITATION CONDITIONS	WASHING PROCEDURES
1	1.0 M $Th(NO_3)_4$; 10% excess oxalic acid (solid)	Add solid to solution at 40°C; stir for 2 hr	At room temperature for 1 hr with 1 filtrate volume H_2O
2	0.8 M $Th(NO_3)_4$; 3.2 M HNO_3; 10% excess oxalic acid (solid)	Add solid to solution at room temperature; stir for 2 hr	At room temperature for 1 hr with 1 filtrate volume H_2O
3	0.5 M $Th(NO_3)_4$; 1.0 M HNO_3; 10% excess oxalic acid (solid)	Add solid to solution at 70°C; stir until cooled to room temperature	At 70°C for 1 hr with 1 filtrate volume H_2O
4	0.5 M $Th(NO_3)_4$; 1.0 M HNO_3; 10% excess oxalic acid (solution)	Heat both solutions to 70°C and add oxalic acid solution to thorium solution; stir until cooled to room temperature	At 70°C for 1 hr with 1 filtrate volume H_2O

TABLE 21. METHODS OF TREATMENT OF THORIUM OXALATE

METHOD	PREHEATING	WASH	CALCINATION
A	Heat at 200°C overnight	1 hr in H_2O at 70°C	Heat at 370°C for 16 hr; then ignite at 609°C for 16 hr
B			Heat at 370°C for 16 hr; then ignite at 605°C for 16 hr
C	Heat at 370°C for 16 hr	1 hr in H_2O at 70°C	Ignite at 605°C for 16 hr

TABLE 22. EFFECT OF TREATMENT AND PREPARATION METHODS ON THE NO_3^- CONTENT OF ThO_2

TREATMENT METHOD*	NO_3^- CONTENT OF ThO_2 (ppm)			
	Preparation Method**			
	1	2	3	4
A	<10	21	<10	14
B	64	58	63	79
C	<10	<10	13	33

*Treatment methods given in Table 21.
**Preparation methods given in Table 20.

TABLE 23. EFFECT OF CALCINATION TEMPERATURE AND TREATMENT METHOD ON THE NO_3^- CONTENT OF ThO_2*

FINAL CALCINATION CONDITIONS	NO_3^- CONTENT OF ThO_2 (ppm)		
	Treatment Method**		
	A	B	C
500°C for 18 hr	10	13	39
575°C for 18 hr	40	20	30
650°C for 18 hr	<10	<10	<10

*The thorium oxalate used in these experiments was prepared by method 1, Table 20.
**Treatment methods given in Table 21.

in forming the precipitate and because HNO_3 and heat are not required.

The data in Table 23, which shows the effect of varying the final calcination temperature on the products obtained by the A, B, and C treatments, indicate that calcination at 650°C yields oxide products containing less than 10 ppm of NO_3^- regardless of the treatment method used. Also, from examination of all the data it is apparent that any combination of the precipitation methods and decomposition procedures studied yields a product containing much less than 100 ppm of nitrate, and it is very likely that the product is of sufficient purity to be used as a slurry material.

One experiment was tried in which thorium oxalate was precipitated from hot 0.5 *M* thorium nitrate solution by the addition of hot ammonium oxalate solution. A thick creamy suspension resulted which was extremely difficult to filter. The thorium oxalate was eventually recovered by evaporation and was decomposed at 625°C to give an oxide product containing 57 ppm of nitrate.

Pyrohydrolysis. A thorium oxide preparation of possible utility in the preparation of an aqueous blanket slurry is obtained through the hydrolytic decomposition of thorium oxalate in water at 250°C. The product oxide is obtained as a finely divided powder of uniform particle size (100 to 1000 Å) contaminated with an organic decomposition product which may be removed by calcination at temperatures greater than 250°C. The oxide, which has been purified by calcination, may be readily prepared as an aqueous slurry containing a thorium concentration in excess of 1000 g/liter. Reautoclaving in water at 250°C yields a slow settling, readily dispersible slurry showing no tendency to pack.

Decompositions were carried out in a stainless steel autoclave of 1-liter capacity, containing an aluminum liner. The liner was necessary because decompositions carried out in its absence resulted in considerable corrosive attack and resultant high iron contamination (4.3%) in the product oxide. The result of the first few decomposition experiments gave a very low aluminum contaminant in the product oxide (40 ppm), but later products contained as much as 1700 ppm of aluminum (Table 24), which may be indicative of a progression deterioration of the aluminum liner.

In a typical preparation the liner is charged with 200 g of thorium oxalate and 100 to 120 ml of water, and the autoclave is sealed and then heated at 250°C overnight or longer, although as short a heating time as 5 hr appears to be sufficient for complete decomposition. The total gas pressure, including steam, at the end of the decomposition period is 2100 psi with a free gas space of 600 ml. Decomposition products include a foul-smelling organic substance which may be partially removed by bleeding the autoclave to dryness at 250°C before cooling.

Product oxides have been calcined overnight at 250, 500, and 585°C. The resulting oxides in all cases were readily dispersed in water to yield slurries containing more than 1000 g of thorium

TABLE 24. OXIDES FROM THE PYROHYDROLYSIS* OF THORIUM OXALATE (ANALYTICAL DATA)

PRODUCT	PYROHYDROLYSIS TREATMENT		CALCINATION TREATMENT	ANALYSIS OF PRODUCT			
	Reaction Time (hr)	Temperature of Bleeding Autoclave (°C)		Th (%)	NO_3^- (ppm)	C (%)	Al (ppm)
Original oxalate				52.4	6400	5.4	
Pyrohydrolysis	18	25–30	None	83.6	25		
	56	25–30	None	80.9	28	0.22	250
	18	250	None	85.6	<10		
	64	250	None	86.3	<10	0.35	410
Calcination			18 hr at 250°C	85.2	<10	0.25	
			17 hr at 500°C	86.6	<10	0.12	1700
			18 hr at 585°C	87.2	<10	0.09	1700

*Conditions of pyrohydrolysis: 250°C; H_2O; Al liner.

per liter. The slurry of the material dried at 250°C exhibited slow but uneven sedimentation and some tendency to pack. The slurries prepared from the higher burned oxides were slow to settle and readily made homogeneous by gentle shaking after complete sedimentation had occurred. Reautoclaving the slurries from the higher burned oxides in a stainless steel autoclave at 250°C for 18 hr gave no impairment of slurry properties. Laboratory abrasion tests on the reautoclaved slurries gave penetration of the 1-mil steel test plate in 17 min, indicating them to be somewhat more abrasive than slurries prepared from Ames oxide.[4] Chemical analysis showed the oxide to contain 1700 ppm of aluminum, which may account for some of the abrasive action. Further tests are being considered on the effect of the use of a more chemically resistant liner on the abrasive properties of the product oxide. Abrasive properties may also have been enhanced by permitting the oxides to dry after the decomposition at 250°C, and experiments are planned which will not permit the material to become dry at any time during the transition from oxalate to slurry oxide.

Electron micrographs show the average particle size of the oxide from pyrohydrolysis to be less than 0.1 μ. X-ray diffraction patterns of the materials are typical of ThO_2 and are quite sharp (half-widths of 0.4 to 0.5 deg). Both the pyrohydrolysis and subsequent calcination are efficacious in decreasing the nitrate contamination to less than 10 ppm.

Data from several of the preparations and subsequent calcinations are given in Table 24.

Hydrolytic Decomposition of Thorium Formate

A steam distillation experiment in which a thorium formate slurry was used yielded interesting results in that the thorium formate was completely decomposed to the hydrous oxide, indicating that steam stripping under moderate pressure may be a good method of producing thorium oxide.

Thorium formate for the study was prepared by adding slowly 2 *M* thorium nitrate solution to boiling concentrated formic acid.[5] Some decomposition of nitrate ensued, with copious evolution of nitrogen dioxide fumes and precipitation of a crystalline, easily recovered precipitate. The precipitate was removed by filtration, thoroughly washed, and dried overnight at 132°C. Chemical analysis showed it to contain 54.5% thorium, 39 to 40% formate, and 0.005% nitrate. The dried solid

[5]Suggested by J. E. Savolainen, Chemical Technology Division, ORNL.

was completely soluble in water and had a solubility at room temperature of 52.2 g of thorium per liter.

In the hydrolysis experiment, approximately 10 g of thorium as the formate was dissolved in 200 ml of water and steam-distilled at such a rate as to yield about 250 ml of distillate per hour. Fractions of the distillate were obtained and analyzed for formic acid until a total of 5500 ml of distillate had been collected, at which time 97% of the original formate had been decomposed.

The data are illustrated in Fig. 42, in which the formic acid concentration in the distillate is plotted against the per cent total formate removed. For purposes of comparison, the figure includes the equilibrium curve for the equivalent formic acid of the system; this curve was obtained by extrapolating to low formic acid concentrations

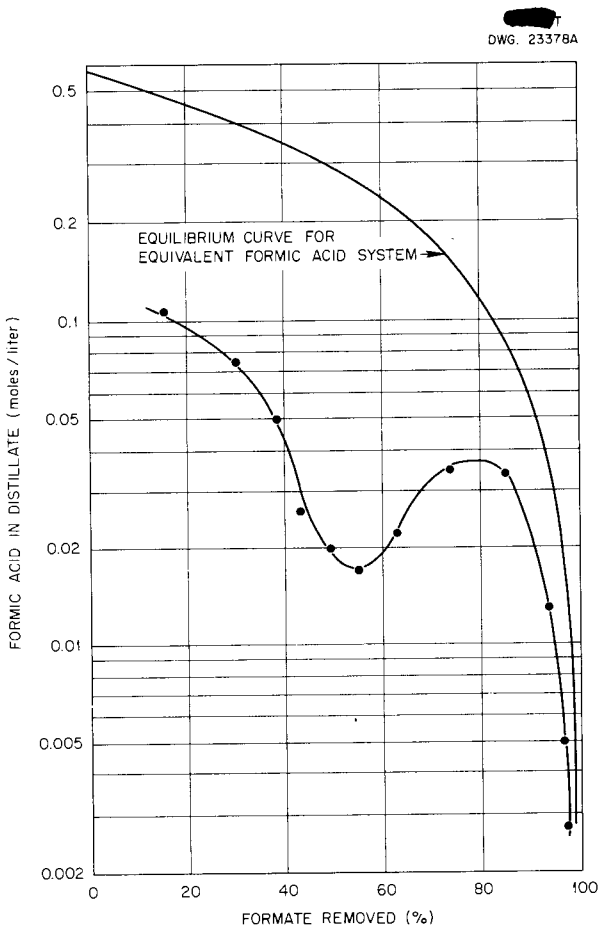

Fig. 42. Hydrolytic Decomposition of Thorium Formate by Steam Distillation.

the published data for the formic acid–water system.[6] The accuracy of the extrapolation is confirmed by the initial results of vapor-liquid equilibrium experiments now in progress in which dilute formic acid solutions are being used.

The formic acid vapor pressure for the formate system is seen to be less than that for the equivalent acid system, reaching a minimum at about 50% formate removal (equivalent to thorium oxyformate) and approaching the vapor pressure of pure formic acid toward the end of the run. The magnitude of the discrepancy between the two curves is, of course, a function of the thorium formate hydrolysis constant and the rate at which thorium passes into the insoluble hydrous oxide form. In subsequent experiments the effect of higher temperatures and pressures on the hydrolysis will be investigated.

In application to production scale, this operation is conceived as introducing the thorium formate into the top of a tower in which it passes countercurrent to steam which strips out the formic acid for subsequent recovery. The thorium oxide is collected in a reboiler which concentrates it for further processing.

Preparation of Thorium Oxide From the Carbonate

The preparation of thorium oxide from the carbonate system of compounds is based on the formation of thorium oxycarbonate and its subsequent thermal decomposition at 500°C to thorium oxide. Two methods of preparing the oxycarbonate were investigated: an ion-exchange method in which thorium was adsorbed on a Dowex-50 cation exchanger and subsequently eluted in an ammonium carbonate solution from which the oxycarbonate was precipitated by heating and a metathesis in which thorium hydroxide was converted to the oxycarbonate through the use of ammonium carbonate. The oxide products from both preparations contained less than 50 ppm of nitrate.

In the ion-exchange process, thorium was adsorbed on a Dowex-50 resin column, and the column was washed free of nitrate with water. The column was then washed with a 0.3 *M* NH_4OH solution until the effluent was alkaline. The thorium was subsequently eluted with a 2.0 *M* ammonium carbonate solution. The eluate was evaporated at 70°C to about one-third its original

[6] J. C. Chu, *Distribution Equilibrium Data*, Reinhold Publishing Co., New York, 1950.

volume to precipitate thorium oxycarbonate, which was recovered by filtration and decomposed to the oxide by heating at 500°C for 16 hr. The oxide products from two runs contained 30 and 50 ppm of nitrate.

Conditioning the column with hydroxide prior to the elution step was found to be necessary to prevent the gassing which occurred in the column in the absence of a hydroxide treatment.

The elution step represents an operational problem in that precipitation of thorium hydroxide occurred in the column, causing the elution band to move down the column in an irregular manner and introducing excessive "tailing out" of thorium. About 90% of the adsorbed thorium was recovered by 4 to 5 column volumes of the eluent. It is possible that the difficulties encountered in the elution step could be minimized by using an upward rather than downward flow of the eluting solution.

In the metathesis procedure, thorium hydroxide was precipitated from a 0.5 *M* thorium nitrate solution at 70 to 80°C by the drop-by-drop addition of 1:1 NH_4OH–H_2O solution and was recovered by filtration. The cake was dissolved in 1 to 2 *M* ammonium carbonate solution, and the thorium was reprecipitated as the oxycarbonate by evaporating the solution at 70°C to about one-third its original volume. After filtration, the carbonate precipitate was heated for 16 hr at 500°C to yield an oxide product containing 86.13% thorium and less than 10 ppm nitrate.

ENGINEERING TESTS

R. N. Lyon, Section Chief
A. S. Kitzes W. Q. Hullings
R. B. Gallaher P. R. Crowley
C. A. Gifford

Thorium Oxide Slurry Tests

Run S-40. A slurry containing 1100 g of thorium per liter (Ames oxide passed through 100-mesh screen) was circulated in loop S at 250°C for 729 hr with flow of water through the back of the pump to lubricate the Graphitar bearings.[7] The run was stopped arbitrarily after 729 hr of operation.

Inspection of the loop confirmed previous observations that the pump and flow restrictor were the areas of severe attack. The straight run of pipe, ells, tees, and reducers did not appear to have been attacked.

Iron, nickel, and chromium increased as constituents of the solid material. The chromium followed the iron in proportion to their ratio in stainless steel, but a substantial deficit of nickel was observed. Approximately 14% of the contaminating metal in the slurry can be accounted for by the loss in weight of the impeller (38 g) and flow restrictor (0.8 g) (Figs. 43 through 46). The remainder of the contamination is probably due to the metal removed from the stainless steel wear rings, which were severely attacked, and from the thrust pads of the pump annulus and thermal spacer (Fig. 47).

As indicated by the chemical data reported in Table 25, the rate of attack on type 347 stainless steel by the ThO_2 slurry, as measured by the iron contamination of the solid material, was 27 g of iron per 100 hr. The pH of the system decreased from its initial value of 6.2 to an average value of 5.5 for the duration of the run.

In the low-velocity regions of the pump and the flow restrictor, and in the circulating system, a black film formed which was not removed by the abrasion by the solids. Analysis of the film by x-ray diffraction and chemical methods gave the following values for the composition: 50% Th, 0.6% Cr, 5.1% Fe, 0.3% Cu, and 12.4% Ni. The x-ray diffraction pattern of the film showed thorium to be present as the oxide and the iron-nickel probably as a spinel. The copper contamination is probably due to pickup during the dry screening of the solids. The relatively high nickel content of the film is a possible explanation of why the nickel content of the circulating solids is lower than would be expected by the abrasion of stainless steel.

To assure that the sample drawn from the loop is representative of the slurry which is being circulated, the sample is drawn into a special 55-ml bomb in which it is submitted to the laboratory for analysis. In sampling from this bomb for analysis, a ±10% error is introduced; so the data in Table 25 are subject to this variation.

Run T-20. Run T-20 was similar to S-40 except that the slurry containing 1000 g of thorium per

[7] R. N. Lyon *et al.*, *HRP Quar. Prog. Rep. Oct. 31, 1953*, ORNL-1658, Fig. 82, p 128.

liter as the oxide was circulated in loop T, in which the pressurizer is isolated from the circulating portion of the loop.[8]

Although the loop was loaded for a circulating concentration of 1000 g/liter, the concentration

[8] *Ibid*, Fig. 81, p 127.

Fig. 43. Front Face of 7-in.-dia Type 347 Stainless Steel Impeller Showing Region of Abrasive Attack by ThO_2 Slurry Containing 1000 g of Thorium per Liter After 729 hr of Circulation at 250°C. Impeller previously used with solutions containing 800 g of UO_2SO_4 per liter at 250°C.

Fig. 44. Back Face of 7-in.-dia Impeller Illustrating Deposit of Black Film. Scratches indicate where film has been removed.

Fig. 45. Upstream Face of Flow Restrictor with 1-in.-dia Opening Showing Abrasive Attack After 729 hr Service at 250°C with ThO_2 Slurries.

Fig. 46. Downstream Face of Flow Restrictor Indicating Black Film Removal.

TABLE 25. CIRCULATION OF ThO_2 SLURRIES AT 250°C WITH WESTINGHOUSE 100A PUMP

SAMPLE NO.*	CIRCULATION TIME (hr)	SOLIDS, BASED ON TOTAL SLURRY						FILTRATE					
		Th (g/liter)	Fe (ppm)	Ni (ppm)	Cr (ppm)	NO_3^- (ppm)	Mg of Fe per g of Th	Th (ppm)	pH	Fe (ppm)	Ni (ppm)	Cr (ppm)	NO_3^- (ppm)
S-40-0	1	1205	165	80	56		0.13	<1	6.2	4	4	<1	
40-1	67	1040	1045	102	445		1.01	<1	6.2	4	2	<1	
40-2	86	788**	982**	110**	225**		1.24	<1	6.2	16	11	<1	
40-3	159	1170	2540	100	600		2.37	<1	5.2	52	25	<1	
40-4	233	1075	2760	78	1162		2.57		5.3	10	15		
40-5	399	1205	4980	150	1132		4.13		4.8	155	17		
40-6	564	1705***	9615***	290***	2050***		5.57		5.6	136	11		
40-7	588	1075	6860	225	1965		6.40		5.2	75	20		
40-8	617	1110	7060	199	1761		6.40		5.5	77	12		
40-9	659	1062	5580	295	1220		6.67		5.4	321	2		
40-10	729	1062	7980	837	1630		7.47		4.9	157	3		
T-20-0	0	580	65	16	8		0.11	<1	4.0	2	<1	<1	
20-1	1	485	93	17	9		0.19	<1	6.1	2	<1	<1	
20-2	17	106	85	18	15		0.13	<6	5.6	1	<1	<1	
20-3	18	268	110	17	14		0.41	<1	5.7	3	<1	<1	
20-4	83	244	854	16	245		3.50	<1	3.5	3	3	<1	
20-5	132	227	1155	24	310		5.08	<1	4.9	47	7	<1	
20-6	180	213	1260	25	385		5.92	<1	5.2	47	4	<1	
20-7	276	230	1450	97	543		6.30	<1	5.5	57	34	<1	
20-8	343	281	1930	143	455		6.87	<1	5.1	15	15	<1	
20-9	416	230	2180	226			9.48	<1	5.5	33	13	<1	
20-10	584	249	3280	333	688		13.20	<1	5.3	19	2		
20-11	688	507	5390	817	135		10.63		5.9	18	13		
20-12	736	325	5880	931	1180		17.72		5.8		3		
20-13	784	247	6540	2760	2180		26.50						
S-41-0	0	150	21	2	<1	1850	0.14	2	8.8	3	41		634
41-1	1	202	690	121	20		3.43	111	1.8	24	102		1420
41-2	4	193				2700		114	1.5				2700
41-3	20	215	850	66	215	1840	3.96	25	1.7	22	45		1440
41-4	21							15	1.8	8	32		88
41-5	24	158	840		206	730	5.33	5	2.0	3	20		24
41-6	95	150	910	55	2	305	6.06	<1	2.6	<1	18		2
41-7	142	162	1565	131	138		9.66	11	2.9	17	8		18
41-8	231	157	1800	200	290		11.45	8	4.6	137	11		2
S-42-0	2	236	72	14	19			3	7.8	<1	1		1
42-1	22		370	50	100			2	8.3	<1	14		
42-2	46	233	1650	120	410			3	5.9	46	5		
42-3	70	210	2200	167				44	6.5	<1			
42-4	145	346	8000	1010	1760								

*S-40, T-20, and S-42 are Ames oxide (particle size of 100 μ or less); S-41 is thorium hydroxide prepared by precipitation from $Th(NO_3)_4$ with NH_4OH.

**Approximate analysis; poor sampling.

***Approximate analysis; chemical analysis faulty.

dropped to 100 g of thorium per liter within the first 18 hr. A survey with a portable scintillation-counter type of meter showed the accumulation of solids in the trap and pressurizer. There is a net vertical flow of about 1 to 2 liters/hr through the $1\frac{1}{2}$-in.-dia trap into the pressurizer due to removal of steam from the top of the pressurizer. The steam is condensed and fed back into the system through the back of the pump to keep the motor and bearings flushed free of solids. The flow of 1 liter/hr corresponds to an average velocity of about 15 mm/min in the $1\frac{1}{2}$-in.-dia trap and 2 mm/min in the 4-in.-dia pressurizer. As was found subsequently, a slurry having an oxide concentration of 1000 g/liter and consisting of 100 to 200 Å particles is essentially nonsettling; so solids were constantly being removed from circulation.

After 18 hr of circulation the run was stopped, and the loop was drained and then reloaded with the same oxide to a concentration of 250 g of thorium per liter. A 4-in.-dia trap was inserted in place of the $1\frac{1}{2}$-in.-dia trap to decrease the vertical upward velocity through it. The loop was in operation for 760 hr before an apparent bearing failure necessitated a shutdown. Inspection revealed that the front stainless steel wear rings were severely abraded, which had caused the pump to lose its thrust balance and had resulted in the bearing failure.

The abrasion attack was similar to that discussed for run S-40. The pump and flow restrictor were abraded, especially in those areas where the particles were forced to undergo a change in direction (Figs. 48 through 54).

Referring to Table 25, the thorium concentrations for samples T-20-11 and 12 are higher than the average concentration for the run. Before these two samples were drawn, the loop was cooled to repair a leak which had developed in one of the pressurizer caps. In the cooling process, solids which had collected in the pressurizer from the first 18 hr of operation and apparently had not been completely removed during the shutdown were washed back into the circulating portion of the

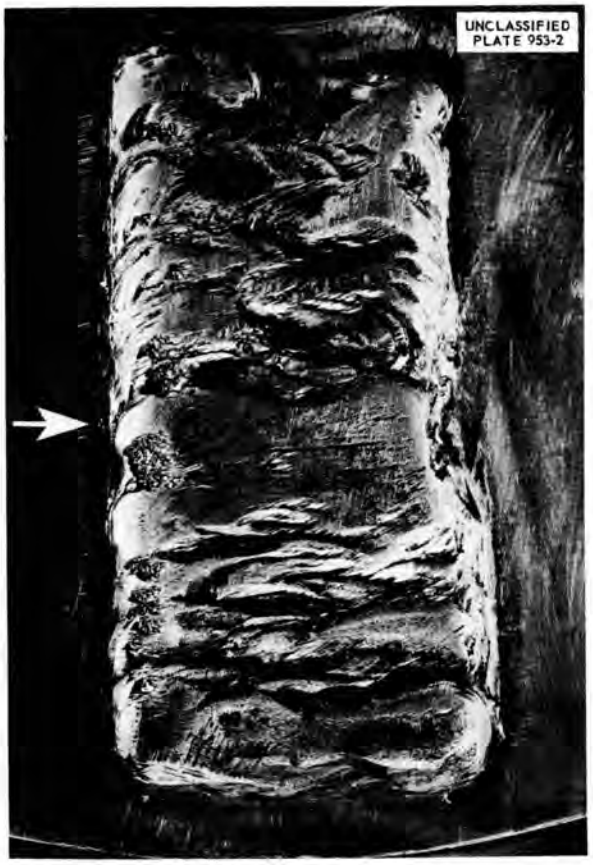

Fig. 47. Weld Pad of Thermal Spacer Showing Abrasive Attack on Leading Edge. Arrow indicates direction of flow past pad.

Fig. 48. Front Face of $8\frac{1}{4}$-in.-dia Type 347 Stainless Steel Impeller Showing Abrasive Attack by Circulating Thorium Oxide Slurry Containing 250 g of Thorium per Liter at 250°C for 784 hr.

Fig. 49. Back Face of 8¼-in.-dia Impeller Showing Black Film Deposit Around Impeller Hub.

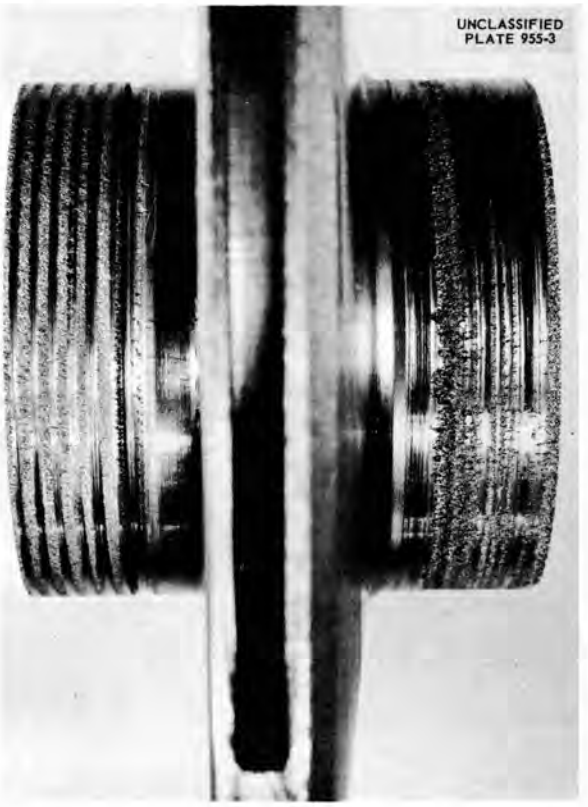

Fig. 50. Front and Back Hubs of Impeller. Front hub is one with most wear.

loop from the pressurizer. The equilibrium concentration was again reached for sample T-20-13.

Again, the chemical results show the increase of the iron and chromium contents of the solids in proportion to their ratio in stainless steel, and a deficit of nickel. X-ray diffraction patterns showed that there was no change in the crystal structure of the oxide being circulated.

The rate of iron buildup was 3.6 g of iron per 100 hr for the first 500 hr of operation and 10.6 g of iron per 100 hr for the last 280 hr.

Thorium Hydroxide Studies

Because of the difficulty encountered by abrasion of stainless steel with Ames thorium oxide, other thorium compounds such as thorium hydroxide are being tested. Slurries prepared from thorium hydroxide are reported to be nonabrasive when tested in a jet-impingement type of tester at room temperature, provided the hydroxide is kept in the wet state at all times.[9]

A slurry containing 150 g of thorium per liter was circulated in loop S at 250°C for 229 hr with

[9] F. R. Bruce *et al.*, *HRP Quar. Prog. Rep. July 31, 1953*, ORNL-1605, p 139.

Fig. 51. Thermal Spacer of Westinghouse 100A Pump. Leading edges of weld pads pitted.

flow of water through the back of the pump to lubricate the bearings. The thorium hydroxide was prepared by precipitation from nitrate solution and subsequent washing of the solids until the wash water contained less than 10 ppm of NO_3^-.

The run was stopped when the solids in the last sample drawn were colored purple, indicating possible corrosion attack on the cobalt-containing Stellite journals, as later confirmed by a qualitative chemical analysis.

Although the metal content of the slurry was high, inspection of the pump parts showed no visible abrasion attack. The impeller lost 7 g in weight which could be due, in part, to the removal of the oxide film which had been deposited from previous uranium runs. The flow restrictor showed evidence of mild abrasion and lost 0.25 g in weight. The titanium wear rings showed no wear when measured with a micrometer after the 229 hr of operation.

Fig. 52. Left Weld Pad of Fig. 51 Showing Pits and Abrasion Track About ½ in. Wide on Downstream Edge of Pad.

Fig. 53. Upstream Face of Flow Restrictor with 1-in. Opening After 784 hr of Service at 250°C with Circulating ThO_2 Slurries.

Fig. 54. Downstream Face of Flow Restrictor.

It will be seen from Table 25, run S-41, that some nitrate ions were still present in the solids and that the pH was unusually low. To reduce the nitrate content, the solids were washed in the loop by circulating for 15 to 20 min, allowing the solids to settle, and replacing the supernate with fresh distilled water. After two washings, the NO_3^- content dropped to less than 100 ppm; however, the pH of the slurry remained low.

X-ray diffraction patterns for the original material showed the solids to be amorphous. However, the x-ray pattern obtained for the material sampled from the loop after 30 min of circulation at 250°C exhibited the characteristic peaks for thorium oxide. The unusually high background in these patterns indicated possibly that amorphous material was still present. A new batch of thorium hydroxide free of NO_3^- ions is being prepared and the circulation test will be repeated.

Alternate Materials of Construction

In order to determine the mechanism of metal removal experienced when thorium oxide slurries are circulated at 250°C, a number of metals which appear to be more resistant than stainless steels are being investigated. With the data available from the limited number of high-temperature circulation runs, it is not clear whether the particles actually gouge out pieces of base metal or whether they merely scrape off the protective oxide film and expose the base metal to corrosive attack by the water and its dissolved oxygen. In addition to the wear rings, titanium was inserted in loop S as the flow restrictor, a $\frac{3}{4}$-in.-orifice, because of its high resistance to corrosion by water, due to a very hard, thin oxide film. To evaluate the wear resistance of chrome plating, which is both very hard itself and protected by an adherent oxide film, a chrome-plated venturi meter was installed downstream from the pump. Through the throat of the venturi meter, a $\frac{3}{8}$-in. stainless steel rod was suspended by means of two spiders so that velocity effects could also be studied. A slurry containing approximately 250 g of thorium per liter (Ames oxide that had been passed through 100-mesh screen) was circulated for 145 hr at 250°C through this combined system.

The run was arbitrarily stopped at 145 hr to determine the damage, if any, to the titanium orifice plate. Inspection showed that all the pump parts (impeller, annulus, and thermal spacer in the high-velocity areas) were apparently "chrome-plated." The upstream face of the orifice around the opening and the stainless steel rod in the high-velocity area of the venturi meter were also "chrome-plated." The plate, except on the stainless steel rod in the venturi, was uniformly laid down, and there was no evidence of selective buildup of chromium. The surface of the rod, in the high-velocity region, was covered with small irregularities or waves, as though the deposited metal or underlying metal had been subjected to a ball-peening operation. The impeller lost 47 g in weight as compared with its weight when installed at the beginning of the run. This loss in weight was greater than was expected and is unaccountable for from the limited data. By removing the plating and examining the orifice plate microscopically, evidence of mild abrasion was observed. In the same length of time, unplated stainless steel would show macroscopic evidence of attack. The deposited film on the stainless steel rod is being studied metallographically to determine, if possible, the method of deposition and thickness so that a comparison can be made with an electrodeposited chrome film. Additional runs are being planned to duplicate this phenomenon and to study the stability of the plate under conditions of reactor operation.

A run has been completed to check further the influence of titanium. The impeller of the Westinghouse 100A pump was the only component of titanium in an otherwise all–stainless steel system. After 20 hr of operation at 250°C in loop T with a slurry containing 150 g of thorium per liter as the oxide, the run was stopped for inspection of the impeller. No damage was found. The chemical data for this 20-hr run are listed in Table 26 as T-21.

The test with the titanium impeller was then continued. Loop T was again loaded with a new batch of oxide to a concentration of 150 g of thorium per liter. After 108 hr of continuous operation at 250°C, the run was stopped for inspection of the impeller. There was no evidence of abrasion. The impeller was not pitted, did not lose weight, and appeared to be highly polished or plated. The bright areas in Fig. 55 illustrate the high luster of the impeller surfaces. The pump annulus and thermal spacer also showed no evidence of attack. Both appeared to be "chrome-plated," except in those areas where the stainless

steel oxide film was not removed.

The flow restrictor, a $\frac{3}{4}$-in. orifice, was also plated. Visual inspection gave evidence that the metal around the opening had been abraded prior to the deposition of the metallic film. Once the film was deposited, abrasion apparently stopped, as there is no indication that the film was attacked. In Fig. 56 the orifice is compared with one removed from run S-40 (ragged opening) in which thorium hydroxide was circulated for 231 hr. Although the orifice with the ragged opening was in service at 250°C twice as long as the plated one, the protective action of the film is clearly indicated. The dark area around the opening is the deposited metal. A run is now in progress to determine the abrasive resistance of the film.

Fig. 55. Front Face of Titanium Impeller Used in Run T-22 to Circulate ThO_2 Slurry at 250°C for 111 hr. No evidence of attack.

The chemical data for this run are reported in Table 26. The iron, chromium, and nickel content of the solid material increased with time, not, however, in proportion with their ratio in stainless steel. The nickel content of the solids is high, whereas the chromium contamination is low, indicating removal of the nickel-rich black oxide film and deposition of chromium.

Homogeneity of Circulating Slurries

In sampling a two-phase system, the question is always raised as to whether or not the sample represents the circulating medium.

At present, the following procedure for sampling the loop is employed. A 50-ml sample from the loop is drawn into a bomb and discarded. A second sample is then drawn, cooled, and transferred to a 60-ml blender used to split the sample into aliquots for chemical analysis. The essential part of the apparatus is a V-shaped chamber formed by welding two stainless steel tubes at the apex. The chamber is rotated with a small electric motor for about 5 min to disperse the solids uniformly. Ten-milliliter samples are then obtained through a quick-opening valve which automatically vents

TABLE 26. CIRCULATION OF THORIUM OXIDE SLURRIES AT 250°C WITH A WESTINGHOUSE 100A PUMP USING A TITANIUM IMPELLER

SAMPLE NO.	TIME (hr)	SOLIDS					LIQUID				
		Th (g/liter)	Fe (ppm)	Ni (ppm)	Cr (ppm)	Ti (ppm)	pH (ppm)	Th (ppm)	Fe (ppm)	Ni (ppm)	Cr (ppm)
T-21-0	1	170	66	17	17		6.58	3	<1	1	<1
21-1	20	161	380	31	82		6.14	<1	<1	7	<1
T-22-0	17	121*	520*	53*	143*	0	6.11	<1	<1	6	<1
22-1	42	171	960	755	306	23**	6.76	<1	<1	13	<1
22-2	108	161	2150	845	445	80**	6.64	<1	<1	26	<1

*Concentration based on specific-gravity measurements is about 146 g of thorium per liter.

**Probable error in determination of titanium is ±15%.

the system. Between each sampling, the blender is rotated to ensure homogeneity of the remaining slurry.

Results of chemical analysis in which known samples were split into aliquot portions indicate that the error introduced by this "splitting" technique is about ±3%, which is well within the accuracy of the various chemical procedures for thorium, chromium, iron, and nickel determinations.

Low-fluidity slurries cannot be split into aliquot portions with this blender; so the error introduced in taking an aliquot of viscous slurries is still high, about ±10%.

To minimize sampling errors, the following three methods to determine concentration changes without sampling the loop are being investigated.

1. The difference between the pressure drop in a vertical pipe and that in a horizontal pipe of the same length indicates the pressure which would be exerted by the slurry in a static vertical column of the same length. From this pressure, the density of the slurry can easily be computed. The sensitivity or the minimum change in density which can be detected by this method will be determined by circulating zinc bromide solutions of different concentrations in a room-temperature loop and by measuring the pressure drops with Foxboro differential pressure cells.

2. The attenuation of gamma rays is dependent upon the density for a given thickness of the absorber. Using the isotope Se^{75}, a 10% change in concentration can be detected reliably by measuring the attenuation in passing the gamma rays through a pipe which contains the slurry. A change in concentration of 1% was detected in a low-radiation-background laboratory. However, this may not be possible in actual use because of the high background.

3. An Ultra-Viscoson, marketed by the Bendix Aviation Corporation, measures the product of density and viscosity. It consists of a flat probe and a high-frequency electronic generator which actuates the probe longitudinally by means of a magnetostrictive transducer. When the probe is immersed in a liquid, the power required to maintain the reciprocation of the probe within a minimum and maximum amplitude is a measure of the product of the viscosity and density of the liquid. This power is registered on a meter which is graduated in centipoise-grams per cubic centimeter.

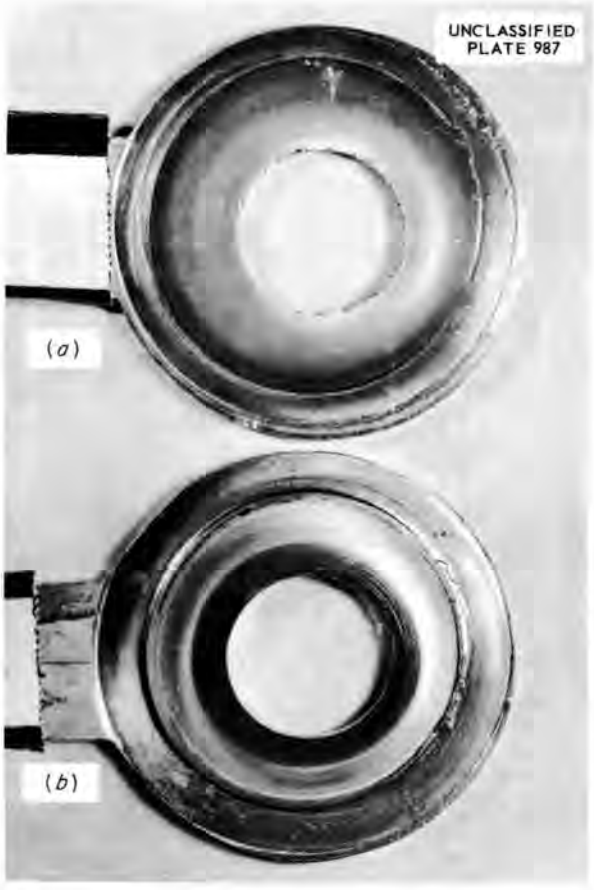

Fig. 56. Comparison of Two ¾-in. Orifices Illustrating Effect of Titanium in the System on the Abrasion of Stainless Steel. (*a*) Abraded orifice was in use for 231 hr with circulating ThO_2 slurry (150 g of Th per liter) at 250°C. Stainless steel impeller. (*b*) Orifice with dark area around opening was exposed 110 hr. Titanium impeller.

Abrasion Tests

Since abrasion by thorium oxide slurries occurs only in high-velocity areas and when the particles change direction suddenly, slower moving, low-pressure-drop axial-flow and mixed-flow pump systems are being studied. A 6⅞-in.-dia stainless steel beaker has been fitted with baffles and a 3-in.-dia three-bladed propeller. The propeller can be placed at varying distances above four sample blocks attached to the bottom of the beaker. The type 316 stainless steel blocks are polished and weighed to the fourth decimal place.

After 500 hr of operation at room temperature, in which a slurry containing 500 g of thorium per

liter (Ames oxide that had been passed through 325-mesh screen) was agitated, there was no evidence of attack on the sample plates or propeller. The blocks were still polished, did not change in weight, and were not pitted.

Operation of the propeller at 1500 rpm gave an estimated fluid velocity of 20 fps downward at the tip of the propeller. Because of the baffles, the fluid is forced to go down past the propeller, makes a U-turn just above the sample blocks, and passes upward between the baffles. The system is now being modified so that tip velocities of the order of 50 to 100 fps can be obtained.

A high-temperature abrasion tester is being fabricated which, if proved satisfactory, can be modified for in-pile studies. The system consists of a close-fitting disk which is moved as a reciprocating piston in a closed cylinder containing the slurry. The bulk of the displaced slurry passes through holes in the disk, and a small amount will pass through the 0.005 clearance between the disk and the cylinder wall. The velocity of the slurry through the openings in the disk can be varied by changing the size of the openings or by varying the rate of displacement. To obtain a velocity of 100 fps through the holes, the disk will be moved approximately 15 cpm by means of a bellows actuated by an external force. A mockup of the apparatus operated by hand worked satisfactorily with a slurry containing 1000 g of thorium per liter.

CHEMICAL PROCESSING

D. E. Ferguson, Section Chief
W. B. Howerton
R. A. McNees
O. K. Tallent
W. E. Tomlin

CALCIUM FLUORIDE PROCESS

The only method that has been found that will lower the fluoride contamination of CaF_2-treated uranyl sulfate solution below 55 ppm is to evaporate the solution to dryness and then to heat the solid UO_2SO_4 at 300°C for 1 hr to effect complete fluoride removal. A residual fluoride concentration of 55 ppm has been obtained by the addition of soluble thorium sulfate to the treated fuel solution to precipitate thorium fluoride.

Based on preliminary data,[1] corrosion of the zirconium core tank by uranyl sulfate solution containing 55 ppm of fluoride may be excessive.

Optimum Temperature for CaF_2 Adsorption

The effect of temperature on the removal of rare earths and on the fluoride content of the effluent from a CaF_2 column was reinvestigated under flow conditions more nearly representative of a full-scale process. More than 99% of the yttrium-tagged rare earths were removed at 20, 40, 60, 80, and 100°C under these conditions (Table 27). The fluoride content of the effluent varied from 380 ppm at 20°C to 335 ppm at 40°C and back up to 380 ppm at 100°C. These data indicate that any temperature between 20 and 100°C is acceptable for the process, with 40°C giving the lowest fluoride contamination of the effluent.

[1] J. L. English, private communication.

ALTERNATE METHODS OF REMOVING RARE EARTHS

Precipitation of $CaSO_4$ at Elevated Temperature

A precipitation method for controlling the concentration of rare-earth fission products in the fuel solution of a two-region thermal breeder reactor has been tested on a laboratory scale. In the experiments a simulated fuel solution of 0.02 *M* UO_2SO_4–0.005 *M* H_2SO_4 containing 0.5 g of mixed rare-earth sulfates per liter tagged with Eu^{155} was saturated with calcium sulfate at 40°C. The solution was then heated to 250 to 270°C in passing through a packed column. Several packing materials were used: granules of hydrated calcium sulfate, anhydrous calcium sulfate, stainless steel gauze, and platinum gauze.

When the column packing was granular hydrated calcium sulfate, a maximum activity removal of 97% was obtained for a short period of time at

TABLE 27. EFFECT OF TEMPERATURE ON CaF_2 ADSORPTION PROCESS

Simulated fuel solution: 0.02 *M* UO_2SO_4–0.005 *M* H_2SO_4, containing 0.5 g/liter of mixed rare-earth sulfates, Y^{91} traced

CaF_2 column: 20 cm long, 1 sq cm in cross section

Residence time of solution in column: 10 min

TEMPERATURE (°C)	RARE-EARTH REMOVAL (%)	CONTAMINATION OF TREATED FUEL SOLUTION (ppm)	
		Calcium	Fluoride
20	99+	260	380
40	99+	290	335
60	99+	310	350
80	99+	330	375
100	99+	330	380

275°C. After the column had been at 275°C for 3 hr, about 50% activity removal was being obtained. This decrease in rare-earth removal was attributed to the dehydration of the calcium sulfate granules in the column. The volume of the column was 10 ml, and the solution was pumped through the column at about 1.3 ml/min.

When the column was packed with calcium sulfate which had been dehydrated by heating at 135°C for 24 hr under a nitrogen atmosphere, a uniform rare-earth activity removal of about 50% was obtained under the conditions described above.

Substitution of a rolled-up piece of stainless steel gauze as a packing material resulted in 95% activity removal, but also resulted in removal of most of the uranium from the solution because of excessive corrosion of the gauze. When platinum gauze was substituted, a uniform activity removal of 65% was obtained without uranium precipitation. In all the above-mentioned experiments at 275°C the calcium content of the effluent was 30 to 40 ppm.

It was found that the soluble anhydrite form of calcium sulfate was rapidly dissolved by 0.02 *M* UO_2SO_4 solution at 40°C. The solution attained 82% of its calcium sulfate saturation value (360 ppm of calcium) in ½ hr. The calcium concentration increased to 470 ppm after 100 hr.

Solubility of Rare-Earth Sulfates in a Simulated Fuel Solution

When a simulated fuel solution containing 0.5 g of mixed rare-earth sulfates per liter and tagged with Eu^{155} was heated to 250°C and passed through a column loosely filled with platinum gauze, the rare-earth sulfate concentration was reduced to 0.08 mg/ml without otherwise affecting the solution.

The mechanism by which this rare-earth removal is effected is not understood and is thought to be complex. However, several experiments have indicated that a large fraction of the rare earths previously precipitated at elevated temperature could be redissolved by passing additional solution through the column at room temperature. Data from one such experiment showed 37% dissolution of the rare earths precipitated from 200 ml of solution by passing an additional 80 ml of fuel solution through the column at room temperature. When 400 ml of the 0.02 *M* UO_2SO_4–0.005 *M* H_2SO_4 solution containing 0.5 g of rare-earth sulfates per liter had been used, the recovery was 53%. At the end of this experiment the rare earths were still being dissolved but at a very slow rate.

Batch experiments have failed to yield consistent solubility data for mixed rare-earth sulfates in 0.02 *M* UO_2SO_4–0.005 *M* H_2SO_4 solutions. In these tests 5-ml portions of this solution containing dissolved mixed rare-earth sulfates were heated in a stainless steel bomb to 200 to 300°C and filtered at the elevated temperature through a sintered-platinum filter disk. The amount of rare-earth sulfate remaining in solution at elevated temperatures decreases with increasing temperature, but also seems to increase as the initial concentration of dissolved rare earths is increased. Additional work with new equipment now available will be necessary to resolve this anomaly and to make possible an evaluation of the effect of the many variables affecting the solutions in question. The preliminary data so far obtained would indicate that mixed rare-earth sulfate solubility may be as high as 0.6 g/liter or as low as 0.2 g/liter at 300°C.

In a 320-Mw core of a two-region homogeneous thermal breeder, 0.24 g of fission-product rare-earth sulfates per liter in the fuel solution corresponds to a poison level of 1.8%. Therefore, if the solubility of rare earths does not greatly exceed 0.2 g/liter, removal of the insoluble material from the fuel solution will adequately control the poison resulting from rare earths.

Alternate Rare-Earth Adsorbents

Several adsorbent materials other than CaF_2 have been tested as adsorbents for rare earths from 0.02 *M* UO_2SO_4–0.005 *M* H_2SO_4 solution. None of those tested show any real promise of being suitable rare-earth adsorbents. Calcium oxalate removed 70% of the yttrium-traced rare earths from solution at 200°C, but the feasibility of using an organic material under such intense radiation conditions is questionable.

An experimental inorganic ion exchanger was tested for separating rare earths from uranium over the temperature range 25 to 250°C. Chemically, this exchanger was zirconium phosphate. The results indicated that no significant separation can be obtained with this material up to the temperature at which it decomposes. At 250°C the exchanger rapidly reacted with the uranyl sulfate in solution.

Several other insoluble phosphates were also tested as adsorbents. Thorium orthophosphate, tribasic calcium phosphate, monobasic calcium phosphate, and dibasic calcium phosphate all

[redacted]

react with the uranium in solution and cause uranium precipitation.

SUMMARY OF CHEMICAL PROCESS DEVELOPMENT BY THE VITRO CORPORATION OF AMERICA[2]

The Homogeneous Reactor Chemical Processing Group at the Vitro Corporation of America has continued the study of the CaF_2 process for removing rare-earth fission products from the fuel solution of an aqueous homogeneous thermal breeder, and scouting experiments have been conducted with the use of titanite as a rare-earth adsorbent. The construction and preliminary testing of the pilot-scale adsorption unit are complete. This equipment is designed for high-temperature, high-pressure adsorption studies and may be used for either CaF_2 process development or development of alternate methods for rare-earth fission-product removal.

Calcium Fluoride Process

Detailed flowsheets have been developed for the following three alternate calcium fluoride adsorption and posttreatment processes. An economic comparison of the following three alternates is being made.

1. The method of no fluoride removal consists of passage of reactor fuel through a column packed with 95% sand–5% CaF_2 at 200°C to remove over 90% of the rare earths. This would produce an effluent containing 0.4 g of calcium per liter and 0.4 g of fluoride per liter. This effluent would then pass through a filter cartridge at 315°C to precipitate the calcium as $CaSO_4$. The fuel solution (treated in this way) would contain 400 ppm of fluoride and 10 to 20 ppm of calcium. Based on corrosion data, such a solution would not be suitable for use in a reactor with a zirconium core tank.

2. The fluoride removal by ThF_4 precipitation would be carried out as in alternate 1; however, a $Th(SO_4)_2$ slurry would be added to the solution before entering the $CaSO_4$ precipitation column to remove fluoride as ThF_4. The fuel treated by this process would contain 55 to 65 ppm of fluoride, 10 to 20 ppm of calcium, and 0.4 g/liter of thorium. Sufficient corrosion data have not yet been obtained to establish that this concentration of fluoride will not cause excessive corrosion of a zirconium core tank.

3. In fluoride removal by evaporation, adsorption of rare earths and subsequent calcium removal would be carried out as indicated in alternate 1. The effluent containing 400 ppm of fluoride would then be evaporated to dryness and heated for 1 hr at 300°C. The UO_2SO_4 could then be redissolved in D_2O and returned to the reactor as a solution containing less than 1 ppm of fluoride. Although producing a water-soluble, fluoride-free cake of UO_2SO_4, the cost of evaporation may make this method impractical.

Fluoride Removal. The results of batch tests at 100°C of precipitation of fluoride as ThF_4 indicate that the minimum concentration of fluoride in solution that can be obtained by this method is 55 ppm. This solubility of fluoride occurs when sufficient $Th(SO_4)_2$ has been added to the fluoride-contaminated fuel solution to leave the solution containing 0.4 g of thorium per liter after the ThF_4 precipitation is complete. Addition of more $Th(SO_4)_2$ increases instead of decreases the solubility of fluoride.

The residual fluoride concentration of 55 ppm after ThF_4 precipitation cannot be significantly decreased by electrolytically reducing 5% of the uranium contained in the solution.

Data obtained on the behavior of fluoride during evaporation of fluoride-contaminated 0.02 *M* UO_2SO_4–0.005 *M* H_2SO_4 indicate that water, free of fluoride, can be evaporated from the solution to leave a solid cake. Heating this cake at 300°C then drives off fluoride along with sulfuric acid and the water of hydration, leaving fluoride-free UO_2SO_4. This cake can then be completely redissolved in the original water.

A cost estimate of this procedure is being made to determine its feasibility.

Adsorption Tests with Titanite

A ¼-in. column built inside a pressure bomb was filled with 6.4 ml of 40- to 80-mesh calcium titano silicate, and 0.02 *M* UO_2SO_4–0.005 *M* H_2SO_4 solution containing 0.2 g of mixed rare-earth sulfates per liter was passed through the bed at 250°C. The titanite removed essentially all the rare earths and uranium from the first 30 ml of solution put through it. Removal of rare earths remained greater than 98% for the next 200 ml, and uranium adsorption dropped to zero. The titanite continued to remove about 50% of the rare earths, as traced by yttrium, from the next 300 ml of solution; however, it also removed about 15% of the uranium. Selective elution data for this bed are now being obtained.

[2] Vitro Corporation of America, *Quarterly Progress Report October 1–December 31, 1953: Homogeneous Reactor Fuel Reprocessing*, Job 87, KLX-1711 (Jan. 18, 1954).

[redacted]